CHAPTER 5

ACCUMULATOR RING

5.1 Accumulator - Functional Summary

The first function of the Accumulator is to accept a pulse of $\bar{p}$'s every 2 seconds. In order to make room for this pulse, the $\bar{p}$'s must be compressed (cooled) into a smaller area of phase space. A technique to accomplish the continuous $\bar{p}$ accumulation and compression has been developed at CERN and is the basis of this design. The technique consists of establishing a stack of $\bar{p}$'s with an energy density that rises approximately exponentially from the injection density (the low-density end is referred to as the "stack tail") and then culminates in a roughly Gaussian high-density region (the "core"). Betatron amplitudes are also cooled during the stacking process. The design criteria for the accumulation process are given in Table 5-1, and the parameters of the Accumulator are given in Table 5-II.

TABLE 5-I ANTIPROTON STACK PARAMETERS

Injected Pulse	
Number of $\bar{p}$'s	8×10^7
$\Delta p/p$	0.2%
Horizontal and vertical emittance	$<10\pi$ mm-mrad
Time between injections	2 sec
Fraction of beam accepted	>85% of injected pulse
Flux	4×10^7 $\bar{p}$/sec
Final Stack	
Number of $\bar{p}$'s	5×10^{11}
$\Delta p/p$	0.05%
Horizontal and vertical emittance	2π mm-mrad
Peak density	1×10^5 eV^{-1}
Core width (Gaussian part)	1.7 MeV (rms)
Total stacking time	5 hours

TABLE 5-II ACCUMULATOR RING PARAMETERS

Kinetic energy	7.9 GeV
γ_t, transition energy	5.43
$\eta = 1/\gamma_t^2 - 1/\gamma^2$	0.023
Average radius	75.45 m
RF frequency	52.812 MHz

Maximum rf voltage	120 kV
Harmonic number	84
Beam gap for injection kicker	115 nsec
Momentum aperture, $\Delta p/p$	2.5%
Betatron acceptance, h and v	10π mm-mrad
Betatron tunes, ν_H	6.611
ν_V	8.611
Natural chromaticities ζ_H	-8.48
ζ_V	-12.88
Periodicity	3, each with mirror symmetry
Maximum amplitude function, β	33 m
Maximum dispersion value, α_p	8.9 m

5.2 Design Requirements

The lattice of the Accumulator has been designed to accept the injection of antiprotons every few seconds at an energy of 8 GeV, momentum stack and stochastically cool the antiprotons, accumulate over a period of several hours a very dense core of antiprotons, and, finally extract a high-intensity beam to re-inject into the Main Ring and Tevatron. The requirements on the lattice are twofold. The Accumulator must be a high-class storage ring capable of reliable operation, and it must accommodate all the conditions imposed by the stochastic-cooling systems. The second set of requirements has led to the design of this ring and its somewhat unusual appearance, while those of the first set have also been incorporated. These conditions are:

(i) The momentum mixing factor must be correct.

$$\left|1/\gamma_t^2 - 1/\gamma^2\right| = 0.023$$

where γ_t is the transition gamma of the ring and γ is the relativistic factor of the particle. Thus for 8-GeV kinetic energy the ring must have

$$\gamma_t = 5.41$$

ii) There must be several long straight sections, some 16 m long, with very small transverse beam sizes. Some of these must have zero dispersion, and the rest dispersion of approximately 9 m. This requirement leads to the choice of transition gamma below rather than above the γ of the particles.

(iii) Betatron-cooling straight sections must be an odd multiple of $\pi/2$ apart in betatron phase. Pickup and kicker straight sections must be far enough apart physically so that a chord will be at least 75 nsec shorter than the arc for signal-transfer purpose.

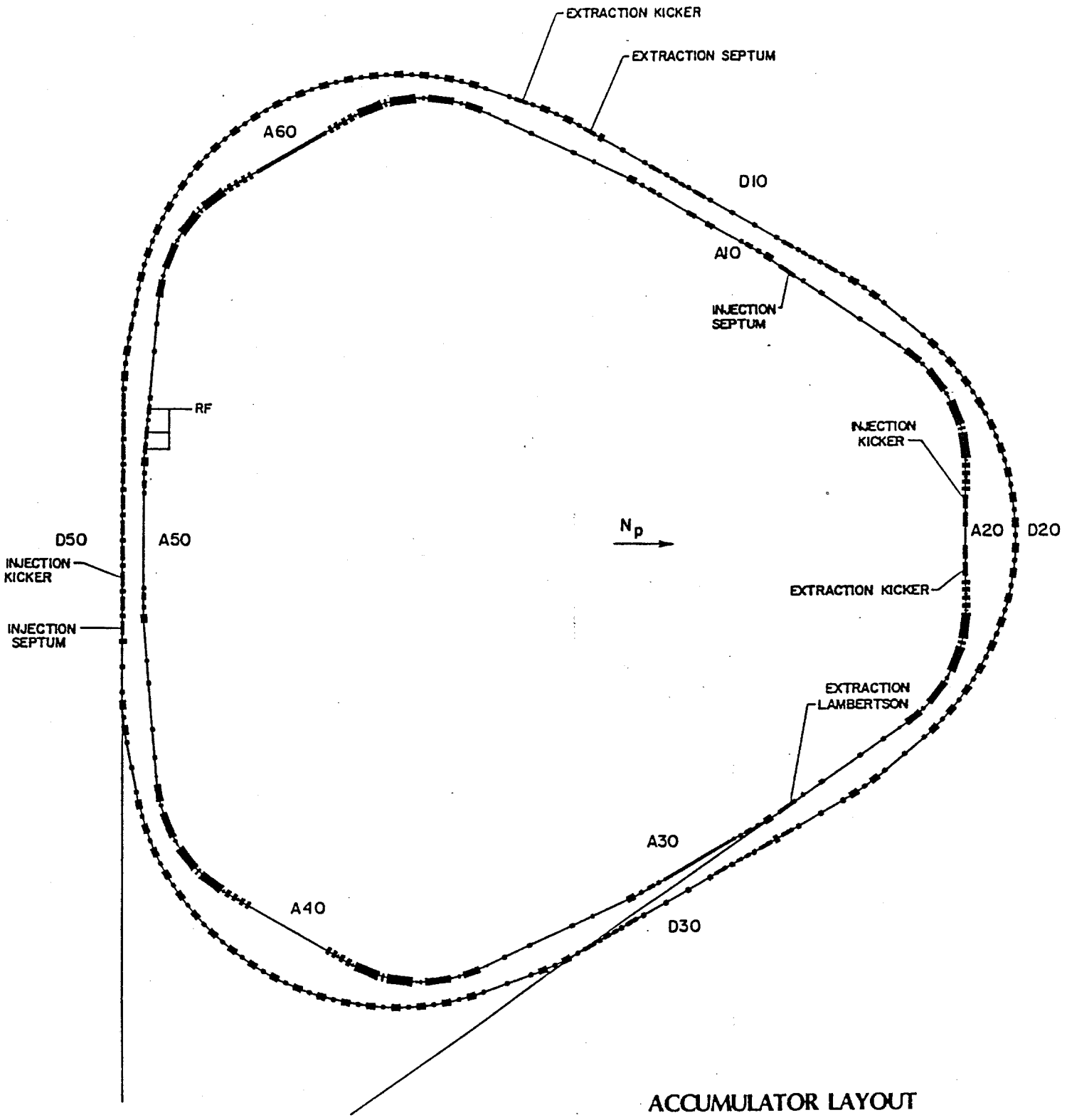
EXTRACTION KICKER
EXTRACTION SEPTUM
A60
D10
A10
INJECTION SEPTUM
RF
INJECTION KICKER
D50
A50
N_p
A20
D20
INJECTION KICKER
INJECTION SEPTUM
EXTRACTION KICKER
EXTRACTION LAMBERTSON
A30
A40
D30
ACCUMULATOR LAYOUT

Figure 5-1

(iv) The β values of the lattice should be about the same for the horizontal and vertical planes in the straight sections.

(v) The ring should match the Booster circumference.

(vi) There should be easy injection and extraction schemes.

(vii) The beam everywhere should be as small as possible, consistent with the large-dispersion straight sections.

(viii) The ring must have very good chromaticity corrections, be situated far from any resonances, have tuning flexibility, and generally be a good storage ring.

5.3 Accumulator Lattice

The lattice chosen is a six-sided ring with six 16-m long straight sections placed between optical triplets. The dispersions of the straight sections alternate between zero and 9 meters. The lattice has mirror symmetry about the straight sections and periodicity three. The middle quadrupole of the triplets near the high dispersion straight sections has been split in order to allow space for orthogonal chromaticity correction and to reduce the required sextupole fields. A plan view of the ring is shown in Fig. 5-1. The triangular shape was chosen as the most efficient in terms of the stochastic-cooling requirements. A ring with four straight sections and periodicity two will not allow a signal to be propagated from a high-dispersion to a zero-dispersion region fast enough relative to the beam. Lattices with eight and ten straight sections were considered, but had several drawbacks, including the fact that they severely limited the amount of non-straight section free space in which to put trim and correction elements.

Table 5-III lists the lattice structure and parameters for the Accumulator. The lattice functions for one sixth of the ring are plotted in Fig. 5-2.

TABLE 5-III DETAILED ACCUMULATOR PARAMETERS

1. General

Kinetic Energy (central orbit)	7.94779 GeV
Bend field	16.84 kG
Magnetic bend radius (ρ)	17.46 m
Circumference	474.07 m
Revolution time	1.59 μsec
Superperiodicity	3
Focusing structure	Separated function FODO normal cell
Nominal working point	

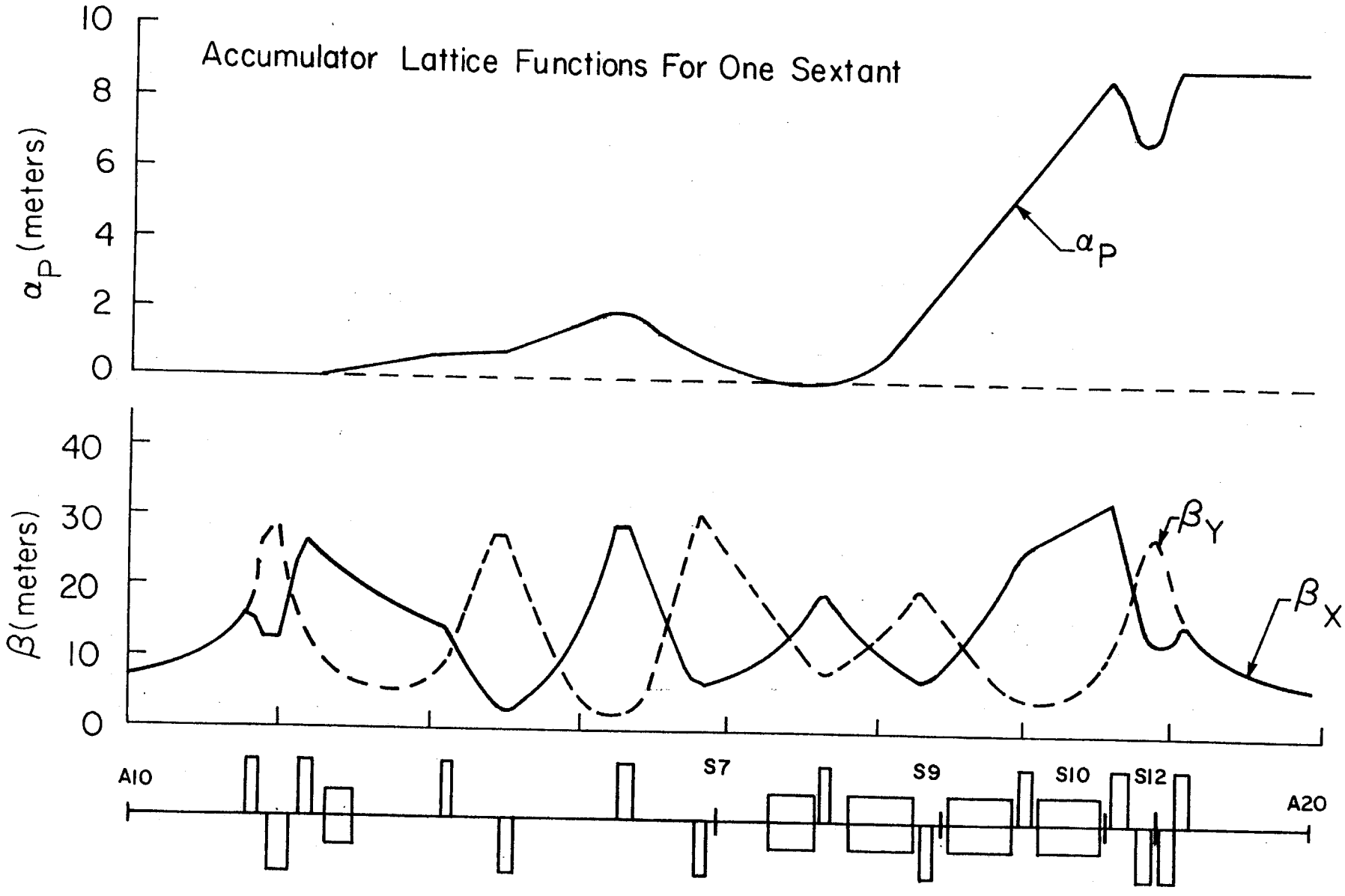
Accumulator Lattice Functions For One Sextant
α_P (meters)
10
8
6
4
2
0
α_P
β (meters)
40
30
20
10
0
β_Y
β_X
A10
S7
S9
S10
S12
A20

Figure 5-2

ν_x	6.61
ν_y	8.61

Nominal chromaticity

ξ_x	-8.52
ξ_y	-12.93

Chromaticity-Corrected Parameters

	Injection Orbit	Stacking Orbit	Core Orbit	Central Orbit
Kinetic Energy (GeV)	8.02951	7.96229	7.89068	7.94779
$\Delta p/p$ (%)	+0.930	+0.165	-0.690	
ν_x	6.616	6.611	6.614	
ν_y	8.611	8.611	8.611	
ξ_x	2.05	1.13	-0.22	
ξ_y	0.21	0.32	0.33	
γ_t	5.37	5.42	5.50	
$1/\gamma_t^2 - 1/\gamma^2$	0.023	0.023	0.022	

2. Magnets

Number of dipoles 30
Number of quadrupoles 84
Number of sextupoles 24

A. Small-aperture dipoles

	Length	Field	Number
(B3)	5.0 ft.	16.84 kG	6
(B7)	10.0 ft.	16.84 kG	6
(B8)	15.0 ft	16.84 kG	6

B. Large-aperture dipoles

(B9)	15.0 ft.	16.84 kG	6
(B10)	15.0 ft.	16.84 kG	6

C. Small-aperture quadrupoles

(Q1)	25.2 in	103.81 kG/m	6
(Q2)	51.6 in	-103.81 kG/m	6

(Q3)	27.6 in	103.81 kG/m	6
(Q4)	18.0 in	96.63 kG/m	6
(Q5)	32.6 in	-97.41 kG/m	6
(Q6)	27.6 in	96.63 kG/m	6
(Q7)	27.6 in	-97.41 kG/m	6
(Q8)	18.0 in	96.63 kG/m	6
(Q9)	18.0 in	-97.41 kG/m	6

D. Large-aperture quadrupole

(Q10)	18.0 in	40.88 kG/m*	6
(Q11)	34.4 in	89.40	6
(Q12)	30.4	-89.40	6
(Q13)	30.4 in.	-89.40	6
(Q14)	25.3 in.	89.40	6

*Q10 will be built with missing turns to run in series with the other large aperture quadrupoles.

E. Sextupoles

(S7)	8.0 in.	53.58	kG/m^2
(S9)	8.0 in.	-329.28	
(S10)	10.0 in.	162.16	
(S12)	10.0 in.	-205.01	

F. Octupoles

(O10)	10.0 in.	-390.33	kG/m^3
(O12)	10.0 in.	325.12	kG/m^3

3. Structure

A. Drift Lengths

LS	7.9465 m
LS*	7.8449
01	0.5124
02	0.9606
03	0.9042
0B3	6.4237
04	3.2610
05	7.3478
06	4.1872
07	0.3556
0S7	3.8866
0B7	0.5080
08	1.2192
0B8	0.5080
09	0.3556
0S9	0.6604

0B9	0.5080
010	0.5080
0B10	0.3173
0S10	0.3173
011	0.5210
012	0.2432
0S12	0.2432
013	0.4972

B. Sextant Structure (S)

LS	(Q1)	01	(Q2)	02	(Q3)	03	(B3)		
0B3	(Q4)	04	(Q5)	05	(Q6)	06	(Q7)		
07	(S7)	0S7	(B7)	0B7	(Q8)	08	(B8)		
0B8	(Q9)	09	(S9)	09	(B9)	0B9	(Q10)		
010	(B10)	0B10		(S10)		0S10	(Q11)	011	(Q12)
012	(S12)	0S12		(Q13)		013	(Q14)	LS*	

C. Ring Structure

$\bar{S}(\bar{S})\bar{S}(\bar{S})\bar{S}(\bar{S})$

Length of central orbit 474.0702 m
1555.348 ft

4. Aperture and Acceptance

Maximum Lattice functions (central orbit)

	β_x	β_y	α_p
Center of LS1	7.565 m	7.268 m	0.000 m
End of LS1	15.912	15.956	0.000
Center of LS2	7.577	7.520	8.946
End of LS2	15.699	15.704	8.946

Required beam
Emittance $\varepsilon_x = \varepsilon_y < 10\pi$ mm-mrad
Momentum aperture $\Delta p/p = \pm 1.25\%$

Beam Size	A_x	A_y
Small-aperture dipole	52.4 mm	29.2 mm
Large-aperture dipole	219.6	17.3
Small-aperture quadrupole	68.3	36.9
Large-aperture quadrupole	246.3	33.1
Small-aperture sextupole	54.9	34.1
Large-aperture sextupole	245.4	33.2

Injection into and extraction from this ring are done in a similar manner. The injection orbit is displaced radially outward by approximately 0.9% in $\Delta p/p$. The shuttered kicker in the high-dispersion straight section is closed just before the $\bar{p}$'s are injected. The momentum displacement is enough to allow the injected beam to clear the shutter. Beam is transferred from the Debuncher ring via two 2 m long, 6-kG current septum magnets located near the upstream end of a zero-dispersion straight section. It arrives at the kicker and is kicked onto the injection orbit. The kicker is 2 m long and has a field of 500 G. The shutter is then opened and the beam is rf stacked. A drawing of the injected, stacked and accumulated beams at the position of the shuttered kicker is shown in Fig. 5-3. The injection and extraction positions are shown on Fig. 5-4.

The beam envelope for one half of a superperiod is shown in Fig. 5-5. Four orbits have been superposed, corresponding to the rf-displaced injection orbit, the stacking orbit, the accumulated antiprotons, and the very dense core.

5.4 Tuning

The Accelerator ring is designed to have a nominal tune of 6.61 horizontally and 8.61 vertically for the central orbit. This puts the working point in a region clear of all resonances up to 15th order. It is easily tunable over a large range using the four existing quadrupole buses - QF, QD in the "regular" part of the lattice and QT, QL, the triplet buses for the zero and high dispersion straight sections, respectively. the tuning properties of the Accumulator are totally linear over a large range of values. While the beta and dispersion values vary as a function of tune in the straight sections, the variation is very small and causes no problems up unitil the structural stop band $\nu_y = 9.0$. A list of the tuning parameters is given in Table 5-III and is plotted in Fig. 5-6. The natural chromaticity vs. tune is shown in Fig. 5-7 and the zero-dispersion straight section lattice functions vs. tune are plotted in Fig. 5-8.

5.5 Chromaticity Corrections

The Accumulator has a momentum aperture of about 2%, 1% for stochastic accumulation and 1% for rf stacking. The largest part of the beam stays near the edge of the aperture for several hours. It must be noted that the equilbrium orbit for an off-momentum beam is changed so drastically in the curved section that the octupole tune shift coming from edge effects of the quadrupole magnets becomes very signficiant in the vertical plane. In principle, we can reduce this octupole tune shift by a suitable configuration of sextupoles, which gives large second-order sextupole fields. We avoid such a configuration for the stability of betatron oscillations. We take care to minimize the distortion of transverse emittance coming from nonlinear kicks in sextupoles, because the geometry of the pickups and kickers is very tight. We use four families of sextupoles and two families of octupoles, where each two families of sextupoles and octupoles correct the chromaticity and the additional two

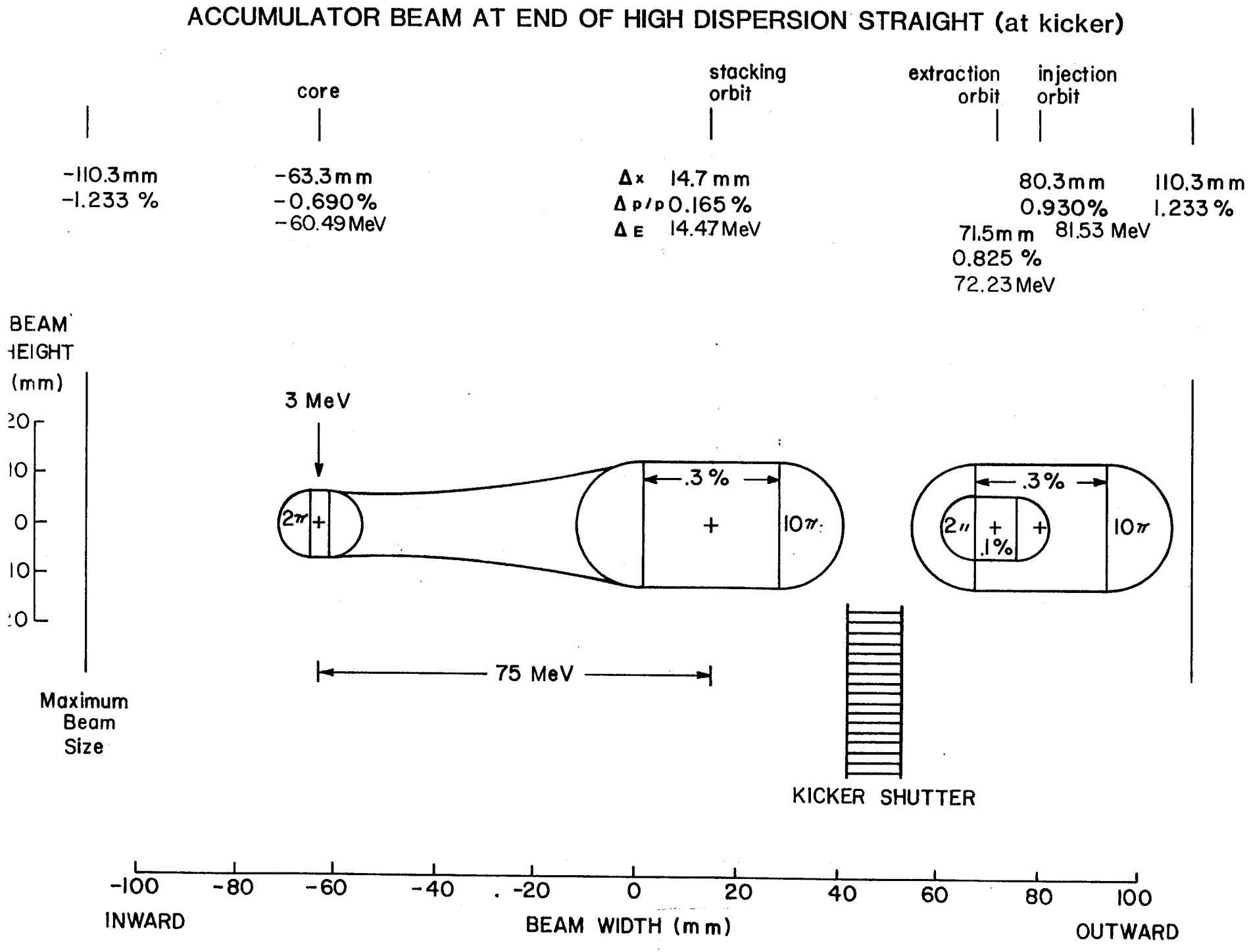
ACCUMULATOR BEAM AT END OF HIGH DISPERSION STRAIGHT (at kicker)
core
stacking orbit
extraction orbit
injection orbit
-110.3mm
-1.233 %
-63.3mm
-0.690%
-60.49MeV
Δx 14.7mm
Δp/p 0.165 %
ΔE 14.47MeV
80.3mm
0.930%
110.3mm
1.233 %
71.5mm
0.825 %
72.23MeV
81.53 MeV
BEAM HEIGHT (mm)
20
10
0
10
20
Maximum Beam Size
3 MeV
2π
.3 %
10π
2π
.1%
10π
75 MeV
KICKER SHUTTER
-100
-80
-60
-40
-20
0
20
40
60
80
100
INWARD
BEAM WIDTH (mm)
OUTWARD

Figure 5-3

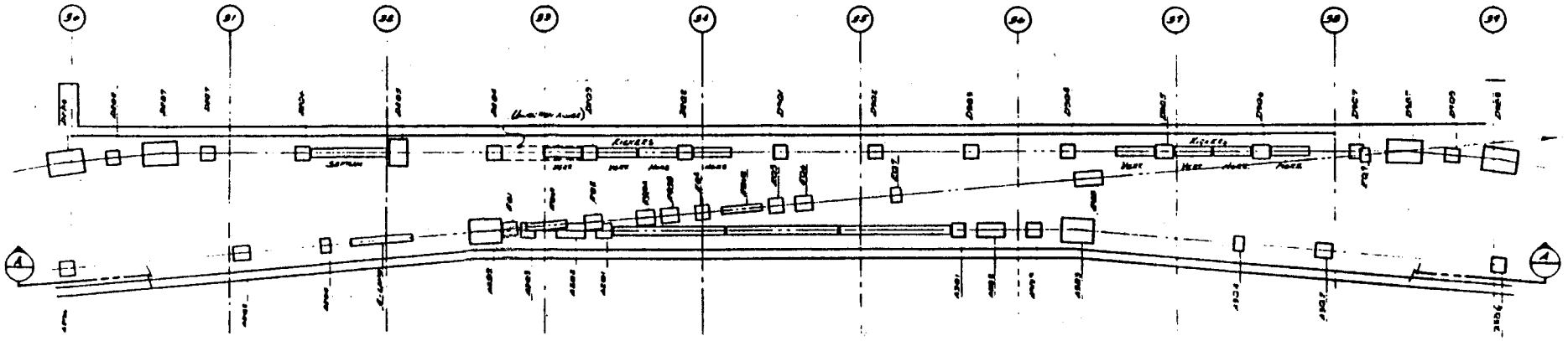

Extraction Straight Section
Plan View

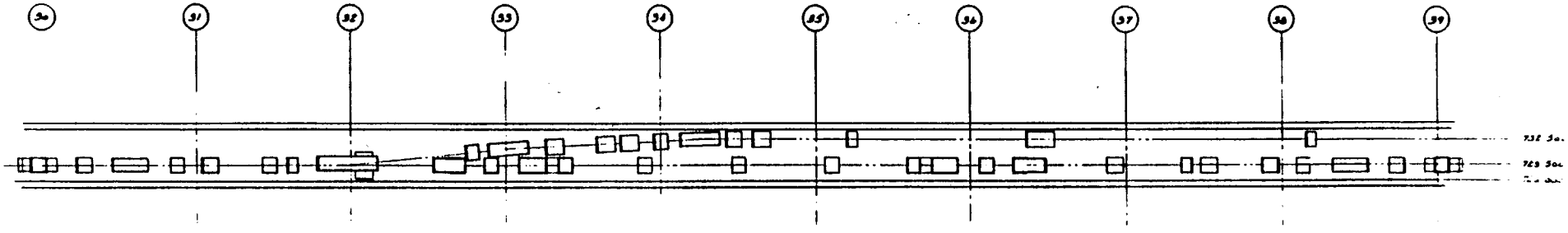

Extraction Straight Section
Elevation View

Figure 5-4

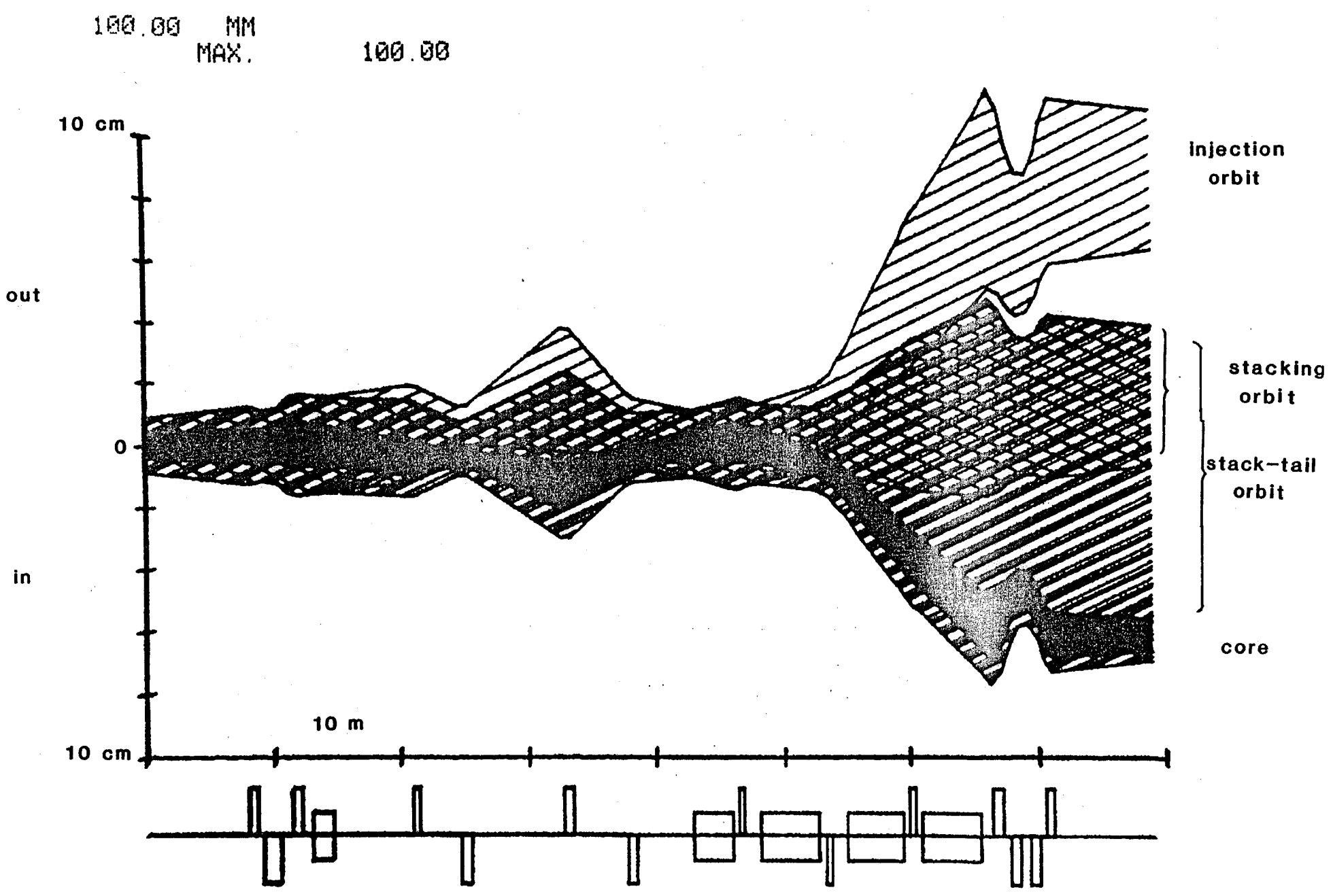
100.00 MM
MAX. 100.00
10 cm
out
0
in
10 cm
10 m
injection orbit
stacking orbit
stack-tail orbit
core

Figure 5-5

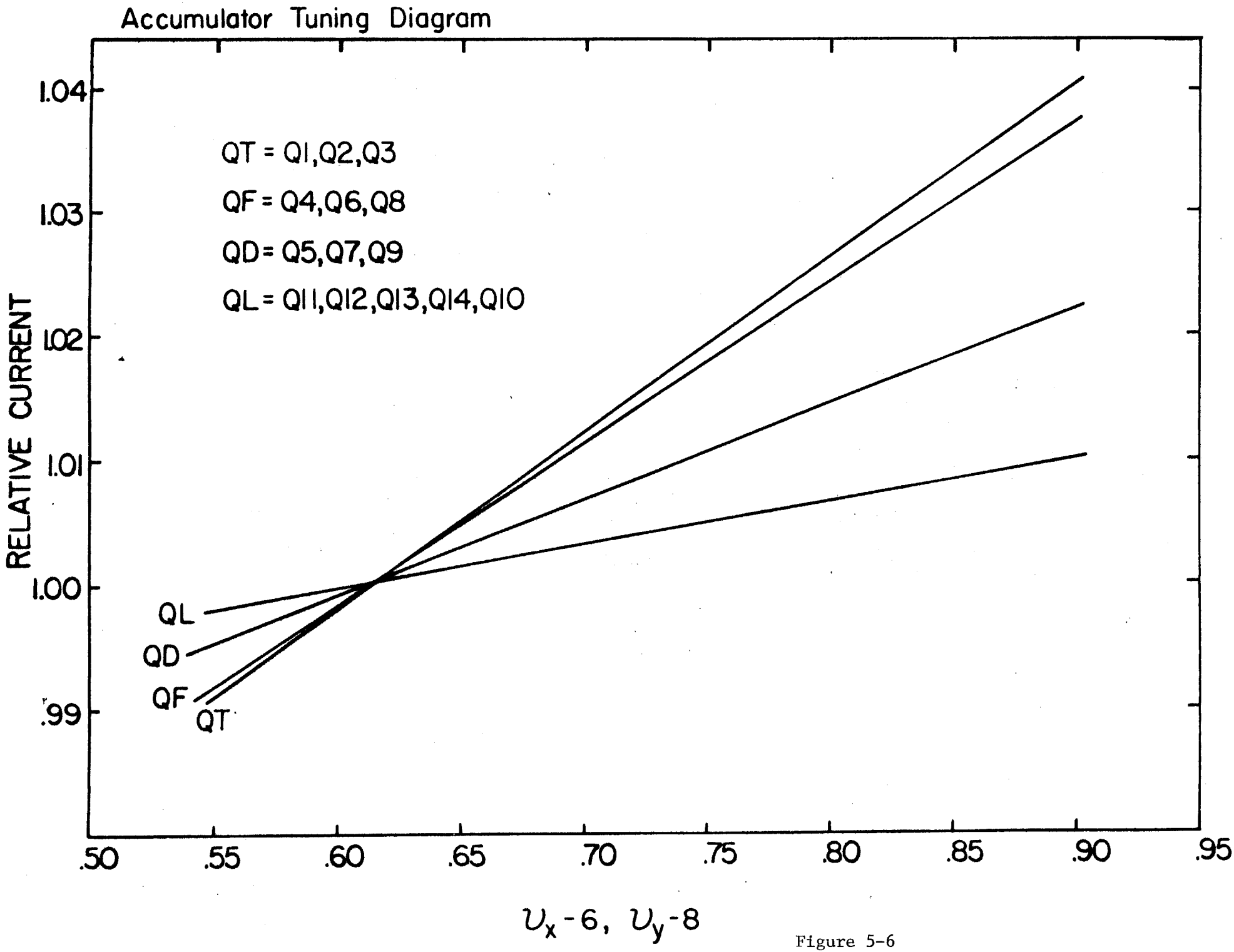
Accumulator Tuning Diagram
QT = Q1,Q2,Q3
QF = Q4,Q6,Q8
QD = Q5,Q7,Q9
QL = Q11,Q12,Q13,Q14,Q10
RELATIVE CURRENT
1.04
1.03
1.02
1.01
1.00
.99
QL
QD
QF
QT
.50
.55
.60
.65
.70
.75
.80
.85
.90
.95
$\upsilon_x - 6,\ \upsilon_y - 8$

Figure 5-6

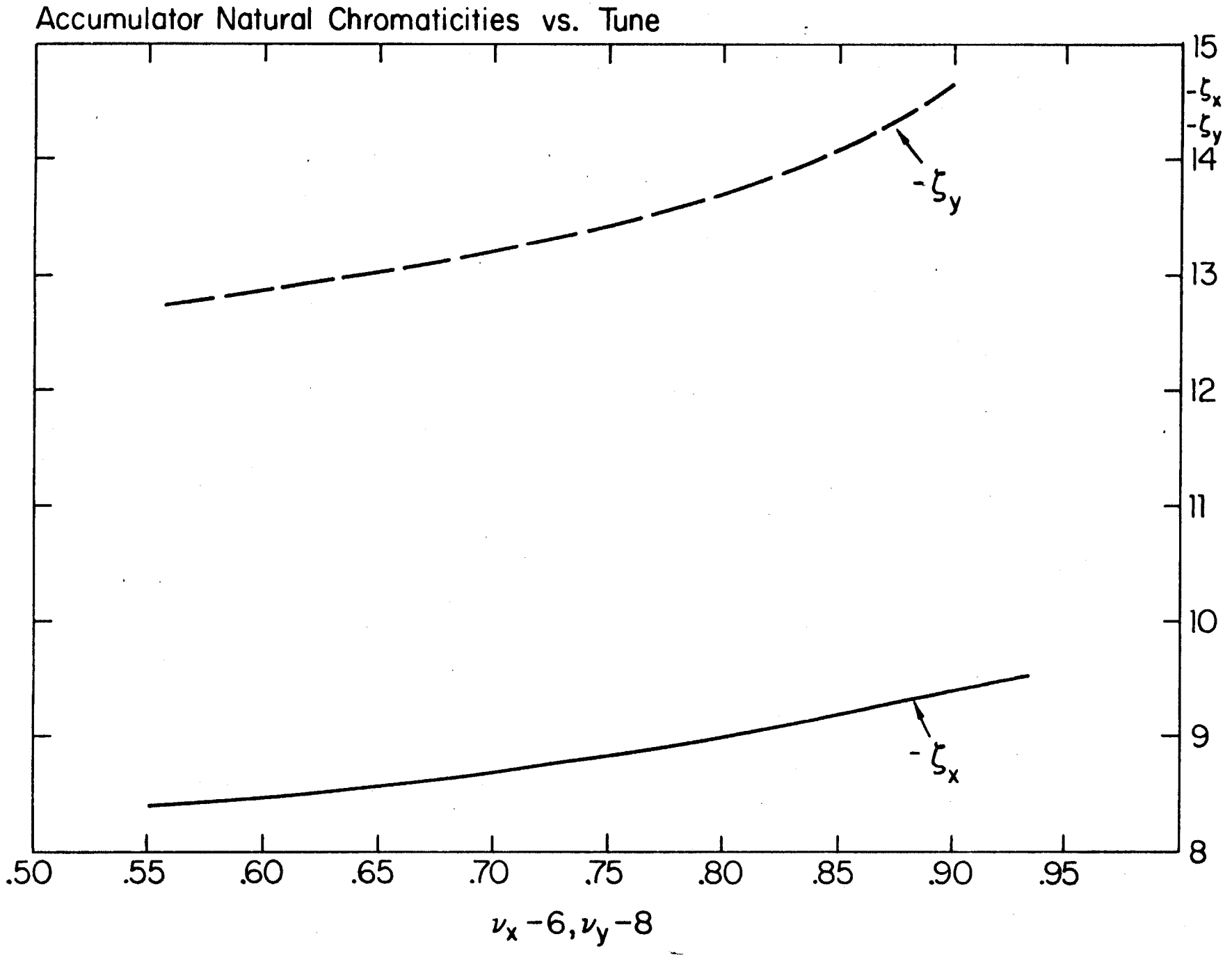
Accumulator Natural Chromaticities vs. Tune
15
14
13
12
11
10
9
8
$-\zeta_x$
$-\zeta_y$
$-\zeta_y$
$-\zeta_x$
.50
.55
.60
.65
.70
.75
.80
.85
.90
.95
$\nu_x - 6, \nu_y - 8$

Figure 5-7

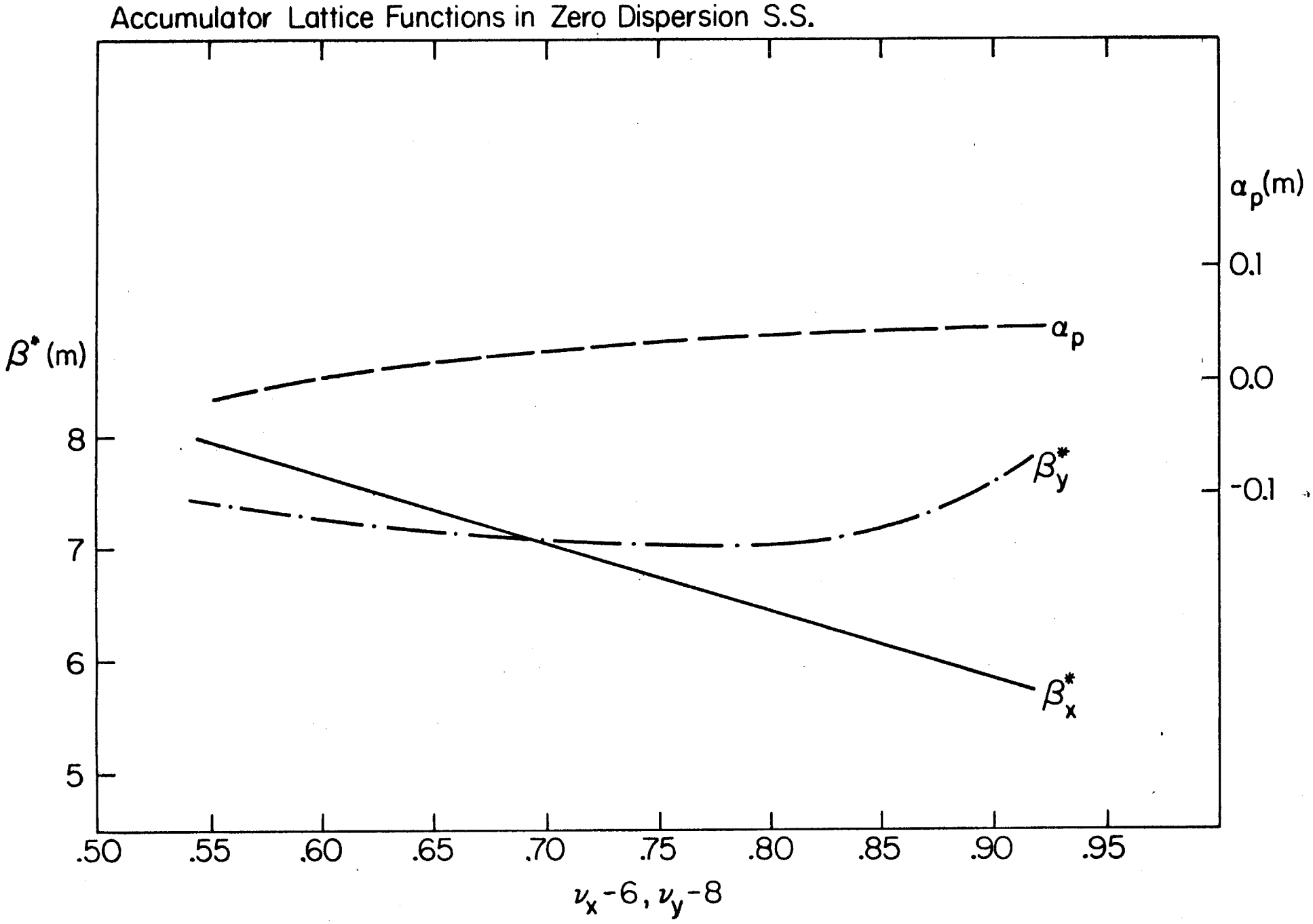
Accumulator Lattice Functions in Zero Dispersion S.S.
β* (m)
8
7
6
5
α_p(m)
0.1
0.0
-0.1
α_p
β*_y
β*_x
.50
.55
.60
.65
.70
.75
.80
.85
.90
.95
ν_x-6, ν_y-8

Figure 5-8

families of sextupoles compensate the emittance distortion. The locations and strengths of these multipoles are given in Table 5-III. The lattice also has enough space to install more sextupoles or any multiples if they are necessary for more correction.

5.6 RF Stacking System

With the injection shutter closed, antiprotons are injected from the Debuncher with a total momentum spread of about 0.2%. The energy spread (18 MeV) and Accumulator revolution period (1.5 μsec) result in an injected longitudinal emittance of about 29 eV-sec. This beam is bunched adiabatically and then decelerated by 0.7% to the edge of the stack of previously injected antiprotons by an h = 84 (53 MHz) rf system. Finally the beam is released and debunched by reducing the rf voltage adiabatically.

The phase-oscillation period is 0.9 msec; the capture can be accomplished in about 5 msec. The deceleration time at $\phi_s = -2°$ is 30 msec. Thus, about 40 msec is required for the entire stacking operation.

At frequencies well below the GHz cooling band, the cooled core may be subject to longitudinal instabilities induced by the shunt impedance of the stacking rf cavity. Additional 53 MHz rf at nearly the required voltage will be installed for bunching of the antiprotons for extraction (see Sec. 6.1). It appears that this system should be used for stacking to economize on the number of high-impedance gaps in the ring. A criterion $Z_n/n < 500\ \Omega$ requires a shunt impedance $< 42\ k\Omega$. The rf power required during the deceleration is about 135 kW. The parameters for the stacking system are summarized in Table 5-IV.

TABLE 5-IV RF STACKING PARAMETERS

Injected Longitudinal Emittance	30 eV-sec
Stacking rf Total Bucket Area	32.3 eV-sec
Stationary Bucket RF Voltage	91 kV
Stationary Bucket Phase Oscillation Period	0.88 msec
Δp/p Required for Stacking	0.77%
Δ (cp)	69.2 MeV
Deceleration Synchronous Phase Angle	2 degrees
$\Gamma = \sin \phi_s$ =	0.035
Moving Bucket Factor $\alpha(\Gamma)$	0.918
RF Voltage During Deceleration	106 kV
Time Required for Deceleration	29.4 msec
Number of Cavities (similar to Debuncher cavity with ceramic gap in beam tube and broad-band swamping applied to reduce shunt impedance)	2
Cavity Small-Signal Shunt Impedance	42 kΩ
Peak RF Power Requirement	135 kW
Average RF Power Requirement	2.7 kW

Harmonic Number (h)	84
RF Starting Frequency	52.8104 MHz
$\eta = \gamma_t^{-2} - \gamma^{-2}$	0.023
$\beta = v/c$	0.99447
Injection Orbit Circumference	474.202 m
Stacking Efficiency*	98%

*Based on computer simulation

5.7 Accumulator Magnets

The main magnet system consists of 30 dipoles and 84 quadrupoles. In Table 5-III is shown a list of magnets, lengths, strengths and required apertures. The required apertures were calculated assuming construction tolerances of 2.5×10^{-4} (relative standard deviation) for dipole strengths, dipole level angles (radians), and quadrupole random position errors (meters). Sufficient space is allowed for at least 4σ, where σ is the standard deviation of the expected orbit position error, or the beam emittance plus momentum spread plus 10 mm whichever is larger. In addition, space is left for 4-mm (thickness plus deflection) vacuum chamber thickness and 5-mm insulation thickness. Several mm must be included also for heating tapes to bake the chamber (dipoles). The specification of these magnets are listed in the tables of Chapter 12.

There are three lengths of dipoles, all with field strengths of 1.689 T. There are 2 different apertures, 3 different lengths in the smaller aperture, in the larger. Because of the large sagitta, these magnets will be curved. The coils will be made of four pancakes plus two single-layer saddle coils.

There are 13 different quadrupoles, of two different profiles. Q1-Q9 have poletip radii of 1.75 mm and 5 different lengths. Q10-Q14 have poletip radii of 3.312 in and four different lengths. Each quadrupole will have a shunt with capability of about 10% of the quadrupole strength. The coils are fabricated in individual layers and assembled on the quad half cores, which are then assembled as a complete magnet.

There are 24 sextupoles of two types. S7 and S9 have a poletip radius of 71.4 mm and a length of 20.3 cm. The (maximum required strength is $33.0 T/m^2$. These sextupoles will be the same as those used in the Debuncher and will be constructed with parallel-sided poles and a single-layer 6-turn winding. S10 and S12 are located in the high dispersion region and require an aperture of 96.5 mm x 300.0 mm (vertical and horizontal). These magnets will have a rectangular aperture with a variable current density across the upper and lower poles to produce the desired field. Octupole and vertical (correction) dipole windings will also be incorporated. The maximum required strengths are 20.5 T/m^2 (s), 39.0 T/m^3 (O), and .064 T (D). The

sextupoles are divided into four families each with its own power bus. There are two families of octupoles. These magnets are described in Tables 5-V and 5-VI.

TABLE 5-V ACCUMULATOR SEXTUPOLES

Max. B"	205	330 T/m^2
ℓ eff	0.25	0.20 m
poletip radius	96.5x300.	71.4 mm
NI	6420	1550 AT/pole
Max. I.	430	2560 A
N	15	6 Turns/pole
Conductor		
Current density	5.2	5.0 A/mm^2
R	8.6	5.6 mΩ
Max. voltage drop	3.7	1.5 V
Max. ohmic loss	1575	375 W
Weight, cu	63	16 lbs
Fe	590	200 lbs

TABLE 5-VI ACCUMULATOR OCTUPOLES

Max. B"	39.0	T/m^3
Length	0.25	m
Aperture	96.5x300	mm
Current	15	A
Current Density	2.3	A/mm^2
Turns	120	
R	0.22	Ω
Voltage	3.2	V
Power	47.0	W
Number of magnets	12	

5.8 Accumulator Vacuum System

5.8.1 Vacuum Requirements. The base pressure is determined by the effects of the residual gas on the accumulated antiproton beam. These effects include particle loss by single Coulomb scattering and nuclear interactions, beam heating by multiple Coulomb scattering, energy loss by ionization, and effects of neutralization by positive ions attracted to the negative beam.

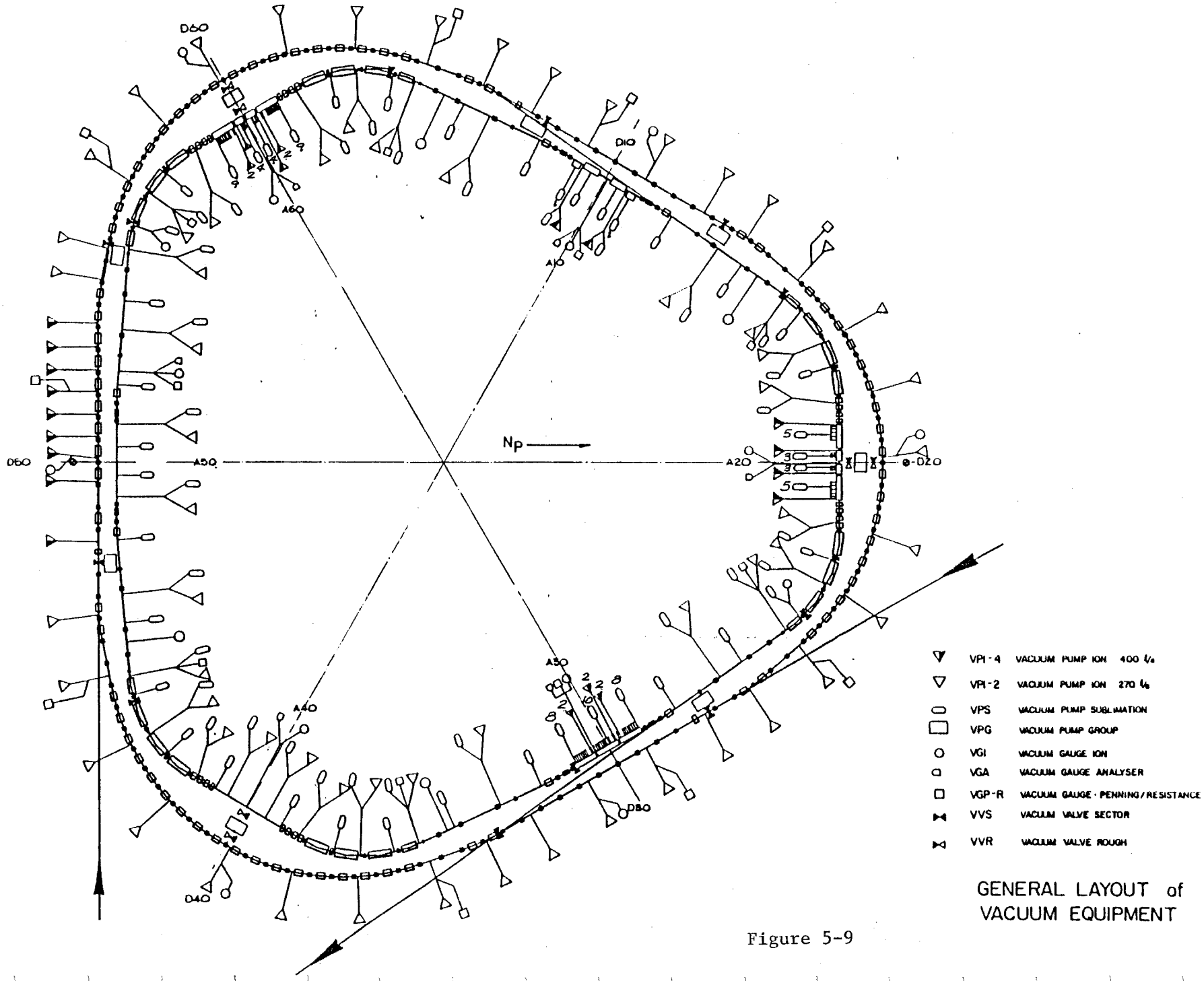
D60
D10
A60
A10
D50
A50
Np
A20
D20
A40
D40
D30
VPI-4 VACUUM PUMP ION 400 l/s
VPI-2 VACUUM PUMP ION 270 l/s
VPS VACUUM PUMP SUBLIMATION
VPG VACUUM PUMP GROUP
VGI VACUUM GAUGE ION
VGA VACUUM GAUGE ANALYSER
VGP-R VACUUM GAUGE - PENNING/RESISTANCE
VVS VACUUM VALVE SECTOR
VVR VACUUM VALVE ROUGH
GENERAL LAYOUT of
VACUUM EQUIPMENT

Figure 5-9

A detailed analysis has been made[1] of these effects. As a result, the system is designed for a nominal pressure of 3×10^{-10} Torr (nitrogen equivalent). At this pressure, the single-scattering lifetime will be 240 hr and the nuclear-interaction lifetime will be 2000 hr. Thus these effects are negligible. The heating rate for the final stack from multiple scattering will be 2×10^{-5}/sec, 10 times less than the cooling rate. (Here a gas composition of 50% H_2, 50% N_2 or CO is assumed). The energy loss per antiproton will be 20 keV/hr. Both the heating and energy loss can be easily compensated by the stochastic-cooling systems. We will keep the nominal design value of the neutralization factor H 0.03. With this value, the scattering by positive ions trapped in the beam will be increased less than 2%. The vertical space-charge tune shift will be reduced by 10^{-3}. Thus these neutralization effects are negligible.

5.8.2 Vacuum System Layout and Characteristics. The pressure requirement can be met with a combination of sublimation sputter ion-pumps. Furthermore, vacuum-annealed austenitic high-tensile stainless steel will be used for the chambers so that specific degassing rates of better than 1×10^{-12} Torr-ℓ/cm^{-2}-sec can be attained. The maximum design bakeout temperature is 300°C.

Figure 5-9 shows the vacuum-system layout over one-sixth of the Accumulator ring. The sputter ion pumps should have a speed of 200 ℓ/sec. The stochastic-cooling pickups and kickers will be isolated with all metal valves, during the bakeout to prevent any vacuum contamination. These valves will divide the ring into approximately 5 irregular vacuum sectors.

The baking equipment (heaters, controls, thermal insulation) will be installed in a permanent fashion to allow bakeout to proceed without major preparations. Exceptions are areas that cannot tolerate the high temperature e.g. pump magnets, cable feedthrus and special devices.

Pump-down during bakeout will be carried out using mobile turbopump carts. This will allow the use of a large number of pumps in any given section being baked. These carts will be connected to metal valves distributed for that purpose throughout the system. Tests indicate that the pressure during bakeout has little effect on the success of the bake.

Vacuum gauges include 6 Pirani gauges to monitor pumpdown, 36 Bayard-Alpert ionization gauges, and 6 mass-analyzer heads, located near areas of complex equipment to monitor leaks and contamination.

The stochastic-cooling equipment will be capable of being baked at a maximum temperature of 150°C and materials compatible with the high-vacuum requirements will be used. Sublimation and ion pumping will be used to provide a pumping speed of up to 2000 ℓ/sec/m.

Clearing electrodes will be installed to remove low-energy positive ions and thus keep the neutralization factor H 0.03. There will be a pair of electrodes at the downstream end of each magnet. Ions move

longitudinally to the electrodes by E x B drifting caused by the beam electric field and the ring guide field. This kind of system has been used successfully in the ISR.

The straight sections between magnets will also need clearing electrodes to avoid trapping ions in the cool-beam potential of 5 V. We plan to apply a dc potential of more than 5 V to the clearing electrodes and to the beam-position detector electrodes whenever these are in a suitable location.

All devices and ring sections will undergo a preliminary bake and low-pressure test before being installed. Their design will conform with strict rules of choice of material and will be subject to approval by the vacuum coordinator.

The vacuum control system will be constructed along the design evolved for the Tevatron. It is highly modular and economical. Many of the required modules and device controls have already been developed, including ion-pump supplies and ion-gauge controllers. A card cage containing all control modules will interface to the host computer through a CAMAC module. Much of the necessary software can be used or adapted.

5.9 Momentum Cooling

5.9.1 Introduction to Stochastic Stacking. The stochastic stacking system consists of pickup electrodes, an amplifier system with electronic filters and phase-compensation networks, and kicker electrodes. Each particle produces an electronic signal that, when applied to the kicker, changes its momentum in the direction of the core. The signal of each given particle thus produces a kick that tends to cool the beam into a small momentum width around the core. Other particles in the beam with approximately the same revolution frequency produce random kicks on the given particles and cause diffusion or heating. The interesting systems, of course, are those in which cooling dominates over heating.

Momentum cooling is usually described in terms of the Fokker-Planck equation

$$\frac{\partial \psi}{\partial t} = \frac{\partial}{\partial E} \left[-F\psi + (D_0 + D_1 + D_2\psi) \frac{\partial \psi}{\partial E} \right] \qquad (5.1)$$

where $\psi = \partial N/\partial E$ is the particle density, F is the coefficient of the cooling term, D_0 is the coefficient of the heating term due to intrabeam scattering (described later), D_1 is the coefficient of the heating term due to thermal noise, and D_2 is the coefficient of the heating due to other particles. A derivation and discussion of this equation are given by Mohl et al.[2]

A simplified version of the Fokker-Planck equation has been used by van der Meer[3] to describe the stacking process. It is assumed that the voltage on the kicker is exactly in phase with the particles that created it, that there is no amplifier thermal noise or intrabeam scattering, the feedback gain is independent of harmonic number, and that there are no beam-feedback effects. A more general approach, including thermal noise, is possible.[4] While none of these assumptions is justified in the proposed system, the simplified discussion yields semi-quantitative results that can form the basis of a design. Following van der Meer, the flux can be written as

$$\Phi = \underbrace{-\frac{V}{T}\psi}_{\substack{\text{cooling}\\ \text{term}}} \underbrace{- A V^{2} \psi \frac{\partial \psi}{\partial E}}_{\substack{\text{heating}\\ \text{term}}} , \tag{5.2}$$

where $N(E,t)$ is the number of particles with energy less than E and

$$\Phi = \frac{\partial N}{\partial t}$$

$$\psi = \frac{\partial N}{\partial E} ,$$

from which the Fokker-Planck equation

$$\frac{\partial \psi}{\partial t} = \frac{\partial \Phi}{\partial E} \tag{5.3}$$

follows. Here $V = V(E)$ is the average energy loss per turn and T is the revolution period. The constant A describes the strength of the heating term and is given by

$$A = \frac{\beta p \Lambda}{4T^3 W^2 |\eta|} \quad , \tag{5.4}$$

where $\beta = v/c$, p is the momentum, T is the revolution period, W is the bandwidth $= f_{max} - f_{min}$, $\Lambda = \ln (f_{max}/f_{min})$, and $\eta = \gamma_t^{-2} - \gamma^{-2}$. If the amplifier gain is not independent of frequency, Λ is modified. The ideal gain profile, in fact, rises linearly with frequency, but the exact value of Λ is not important for this discussion.

The Fokker-Planck equation is nonlinear in ψ and it is therefore usually solved numerically. Stationary solutions, $\Phi(E,t) = \Phi_0 =$ constant, can often be found by elementary methods. These solutions are useful because in the stack tail between the core region and the injection region, the actual time-dependent solution is normally very close to the steady-state solution.

Consider $\Phi_0 =$ constant and $\psi(E,t) = \psi(E)$, and ask what the shape of the voltage profile $V(E)$ should be. The answer, as given by van der Meer, is to maximize $d\psi/dE$ everywhere and thus minimize the energy aperture which is required. This choice also minimizes the total Schottky power in the amplifier. The solution is

$$V(E) = -\frac{2\Phi_0 T}{\Psi(E)} = -\frac{2\Phi_0 T}{\Psi_1} e^{-(E_1 - E)/E_d} \quad , \tag{5.5}$$

where Ψ_1 is the initial stack-tail density at E_1 and E_d is the characteristic energy

$$E_d = -4A\Phi_0 T^2 = -\frac{4p\Lambda\Phi_0}{TW^2|\eta|} \quad . \tag{5.6}$$

This equation exhibits the major design consideration. We know that $d\psi/dE$ is maximized by a gain profile $V(E)$ that is exponential in energy. The exponential slope $d\psi/dE$ is maximized by minimizing E_d. In the stack tail, we want a density increase of 1000, so we require a minimum momentum aperture of $\Delta p/p = \ln(1000)\ E_d/p = 6.9\ E_d/p$. If we want to limit the aperture $(\Delta p/p)$ required for the stack tail to 0.75%, then E_d 0.001 p ≈ 10 MeV for $p = 8.9$ GeV/c. Since we want to have Φ_0 as large as possible, we must make E_d small by choosing $TW^2|\eta|$ to be as large as possible. The density profile is shown in Fig. 5-10.

We have chosen to work with a maximum frequency of 4 GHz for the purposes of this report, but we intend to use frequencies up to 8 GHz for core cooling if our research program indicates that 8 GHz cooling systems are practical. The stack-tail system was chosen to have a maximum frequency of 2 GHz. As described below, the choice of frequency dictates the choice of η. By limiting the stack-tail system to 2 GHz, we are able to use a relatively high η ($\eta = 0.02$). The high value of η is useful for the core-cooling systems, where the core cooling times are inversely proportional to η.

The maximum value of η is limited once we choose f_{max}. For a number of reasons, it is required that $\eta(\Delta p/p) f_{max} T < \delta$, where δ is some number of order unity. The reasons that determine the value of δ are:

(i) The Schottky bands must not overlap in a system that uses electronic filters for gain shaping. In such a system, the particle energy is sensed in the electronics by the connection between energy and the harmonics of the revolution frequency. If the relationship is not unique, it is difficult and probably impossible to design appropriate filters. In this case, $\delta = 1$ and $\Delta p/p = 1\%$ so η 0.03 with $T = 1.6$ μsec.

(ii) The phase shift between PU and kicker must not vary across the momentum band more than about ±45°. If PU and kicker are exactly opposite in the Accumulator Ring, then $\delta = 0.5$. If the stack-tail system is divided into subsystems with $\Delta p/p = 1/3\%$, then this constraint applies to each system individually, so η 0.05.

(iii) For reasons described below, the filters must have the peak of their response at the tail end and a notch in the core. Between Schottky bands, of course, the response must rise from the notch in the core back to the peak value. Since the rise back to the peak value cannot be done infinitely sharply, at least without undesirable phase characteristics, this requirement is more severe than 1) above. We have found that $\eta = 0.02$ is a suitable value for a maximum frequency of 2 GHz.

We have chosen a Booster-sized ring ($T = 1.6$ μsec) because it is large enough to accommodate the cooling-system hardware and can run at 8 GeV, a good energy for production of $\bar{p}$'s and their injection into the Main Ring.

5.9.2 Summary of Design Considerations. We have chosen $E_d = 0.001p = 10$ MeV to keep the required momentum aperture sufficiently small. The product $Tf_{max}\eta$ is fixed by the requirement of a minimum spacing between Schottky bands. We have chosen $W = 1$ GHz with $f_{max} = 2$ GHz to yield a somewhat higher value of η (0.02) than would be the case if we chose a higher frequency. Higher frequencies also have the disadvantage that it is somewhat more difficult to build the quality of hardware that is required.

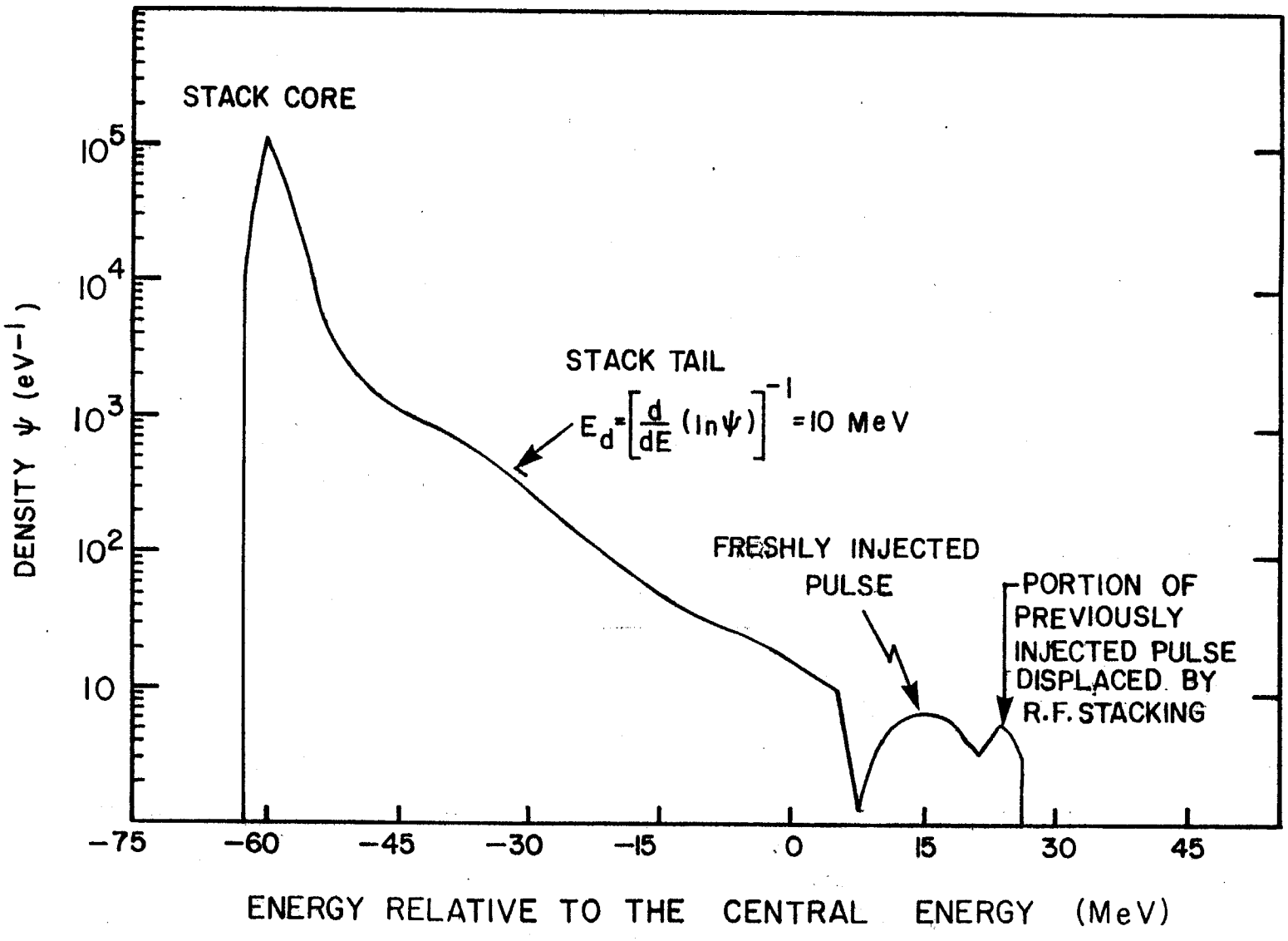
STACK CORE
STACK TAIL
$E_d = \left[\frac{d}{dE}(\ln\psi)\right]^{-1} = 10$ MeV
FRESHLY INJECTED PULSE
PORTION OF PREVIOUSLY INJECTED PULSE DISPLACED BY R.F. STACKING
DENSITY ψ (eV^{-1})
10^5
10^4
10^3
10^2
10
−75
−60
−45
−30
−15
0
15
30
45
ENERGY RELATIVE TO THE CENTRAL ENERGY (MeV)

Figure 5-10

5.9.3 Building the Exponential Gain Profile. Once the parameters of the stack tail have been chosen, the next step is to build the required gain profile. We use a combination of two techniques. The first technique is to sense the particle momentum by sensing its position in a region of high momentum dispersion. The position sensitivity of the strip-line pickups we plan to use is given in Section 5.11.1. For large horizontal displacement x the sensitivity of these pickups becomes

$$s(x,0) \quad e^{-\pi x/h}, \tag{5.7}$$

where h is the gap between plates. In our case, the momentum dispersion is α_p = 9 m and we have chosen h = 3 cm. Thus for large ΔE,

$$V(E) \quad e^{-|\Delta E|/E^*}, \tag{5.8}$$

$$\text{where } E^* = \frac{\beta^2 E h}{\pi \alpha_p}$$

where V(E) is the average (coherent) particle voltage gain per second, ΔE is the difference between energy E and the energy where the pickup response is centered, and E^* = 10 Mev. In our system we use the pickups in the region where the falloff is not truly exponential, but the system can be characterized roughly by an E^* of approximately 15 MeV for the pickup response.

The second method of gain shaping is with filters. However, the main purpose of the filters is to reduce the thermal noise in the core. In order to maintain a flux of 3×10^7 sec^{-1} into the stack tail, an amplifier system with very high gain (150dB) is required. Even with preamplifiers with low noise temperatures (80°K), the thermal noise produces an rms voltage of approximately 1500 V/turn. This noise voltage is (perhaps surprisingly) tolerable in the tail where the average (cooling) voltage gain is about 10 V/turn. In the core region, where the cooling voltage is a few mV/turn, this noise voltage must be reduced to a tolerable level. The filter does this by making a notch at all harmonics of the revolution frequency of the particles in the core. The filter also does some gain shaping in the tail region. The filters used are composed of a series of notch filters similar in concept to those used at CERN. A schematic diagram of the individual component filters is given in Fig. 5-11. The response of these filters is given by[5]

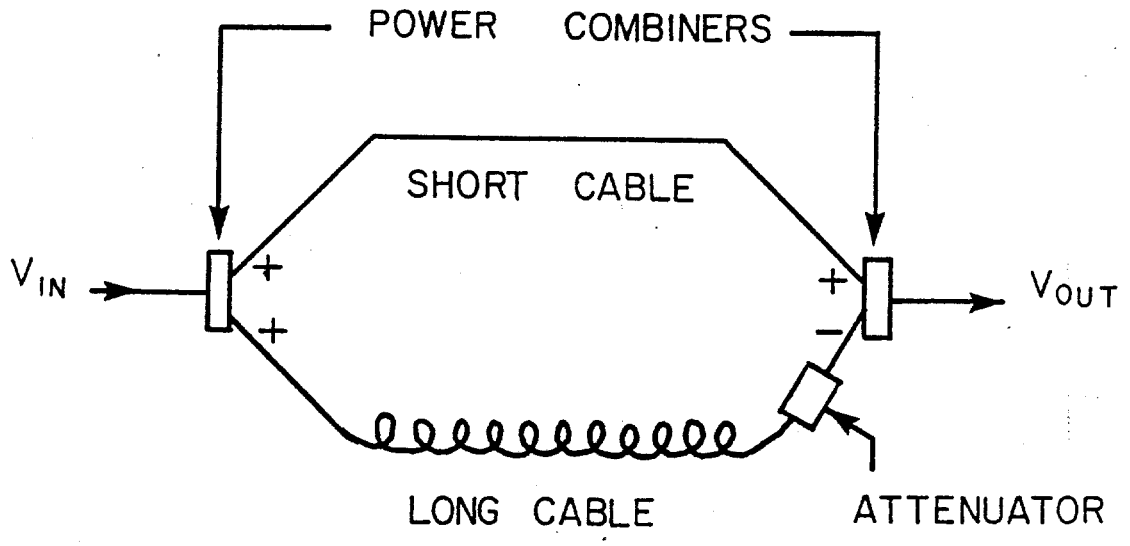
POWER COMBINERS
SHORT CABLE
V_{IN}
+
+
+
−
V_{OUT}
LONG CABLE
ATTENUATOR

Figure 5-11

$$\frac{V_{out}}{V_{in}} = (e^{-i\gamma_1 \ell_1} - \xi e^{-i\gamma_2 \ell_2})/2 \ , \qquad (5.9)$$

where γ_1, γ_2 and ℓ_1, ℓ_2 are the propagation constants and lengths of cables and ξ is a variable attenuation of order unity. To get a clearer picture of the operation of this filter, consider the approximation $\xi = 1$, $\ell_1 = 0$, $\gamma_2 = \omega T_c/\ell_2$, where ω is the applied frequency electrical length of the cable. In this case,

$$\left|\frac{V_{out}}{V_{in}}\right|^2 = (1 - \cos \omega T_c)/2 \ , \qquad (5.10)$$

and the phase changes linearly with frequency except at the transmission zero, where it takes a discontinuous jump of 180°.

The absence of amplifier noise would not necessarily eliminate the need for filters. Nonlinearities in the pickups, amplifiers and other components cause frequency mixing, as is well known to rf engineers. The input power at frequencies corresponding to the stack tail, where the power density is high, will mix in a nonlinear device and produce output power at frequencies corresponding to the core where the power density must be low. The filters suppress the most dangerous part of the unwanted distortion because of the notch at the frequency of the core particles. (These particles are cooled by a separate system without filters, as will be described later.) It will be advantageous to place some of the filtering after the final amplifier to reduce the sensitivity to the nonlinear distortions from that source.

The shape of the gain curve at the injection end is purposely different from the ideal exponential curve, becoming flat in the injection region because of several practical considerations:

(i) It is desirable to keep the electronic gain between Schottky bands as low as possible. The gain between Schottky bands does not affect the cooling process, but the thermal power between Schottky bands is significant.

(ii) To maximize the ratio of Schottky signal to thermal noise, it is desirable to place the pickups so they have maximum sensitivity to the freshly injected beam, i.e., so they operate in the non-exponential region.

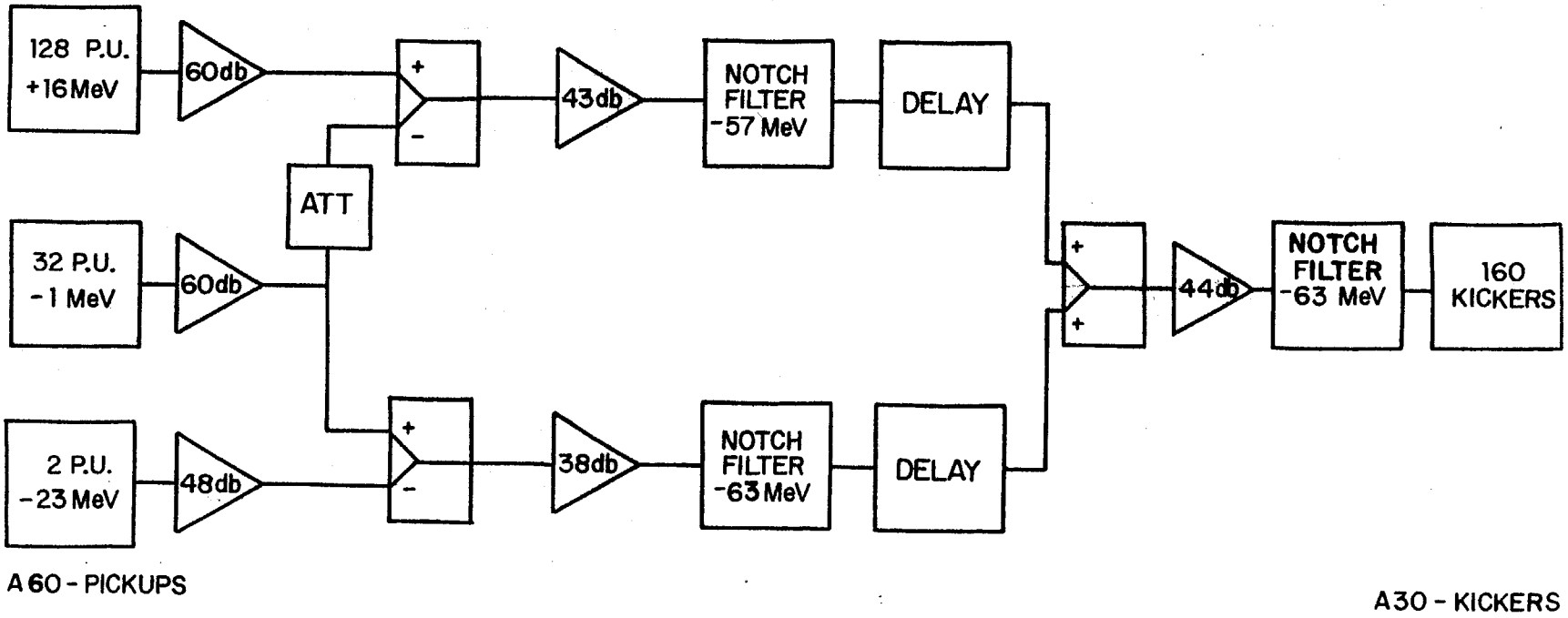

STACK TAIL MOMENTUM COOLING SYSTEM 1-2 GHz

Figure 5-12

(iii) The exponential gain profile minimizes Schottky power only in the approximation that beam is injected in a steady state manner. In fact, each newly injected pulse substantially alters this picture since the density of particles will differ by factors of 2 or 3 from the steady state situation. By making the gain profile flatter in the injection region, we can reduce the required Schottky power immediately after a new pulse is injected.

The stack-tail system we have designed consists of two sections of pickups and associated amplifiers and filters. The two sections make it possible to control undesirable phase shifts and thermal noise in the tail. A block diagram of the system is shown in Fig. 5-12. The number of pickups was chosen to be a large as possible to minimize the thermal-noise to Schottky-signal ratio and to minimize the total thermal power. In order to keep the betatron oscillations from substantially affecting the momentum cooling, the betatron amplitudes must be limited. To achieve the desired gain profile, the pickups have a plate separation of 3 cm. Calculations indicate that the beam size should be less than 2.4 cm to avoid trouble with betatron motion. For an emittance of 10π mm-mrad, the β function at the pickup must be 15 m or less. This requirement limits the pickup straight section to 15 m in length and a total of 200 pickups. The function of the subtracting pickups is discussed in the next section. The number of kickers was chosen to fill the straight section across from the pickups to minimize total power (inversely proportional to the number of kickers). The gain profile achieved with this system is shown in Fig. 5-13 abc for the Schottky bands at 1.1, 1.5 and 1.9 GHz.

5.9.4 Signal Suppression and Stability. An important aspect of the cooling process, when using high-gain cooling systems, is signal feedback via the beam. A signal of frequency ω will modulate the beam at frequency ω, and this modulation will be sensed at the pickup. Thus the cooling system forms a closed-loop feedback system. This feedback system is analogous to amplifier systems with conventional electronic feedback. An expression for the beam feedback has been given by van der Meer[6] and independently by Ruggiero.[7] An approximate expression is

$$F = \frac{I_p}{V} = jef_0^2\,\bar{p}\int \frac{CP}{nk(E-E')}\,\frac{d\psi}{dE'}\,dE' \quad - \frac{\pi e f_0^2}{n|k|}\,CP\,\frac{d\psi}{dE}\,, \tag{5.11}$$

where $\bar{p}$ denotes the principal value of the integral, I_p = induced current at the frequency $f = nf_0$ in the pickup due to modulation caused by voltage V on the kicker, f_0 is the revolution frequency corresponding to energy E, n is the harmonic number, e is the unit charge, $j = \sqrt{-1}$, $k = 2\pi\, df_0/dE$, C is the phase factor due to transit time differences between pickup and

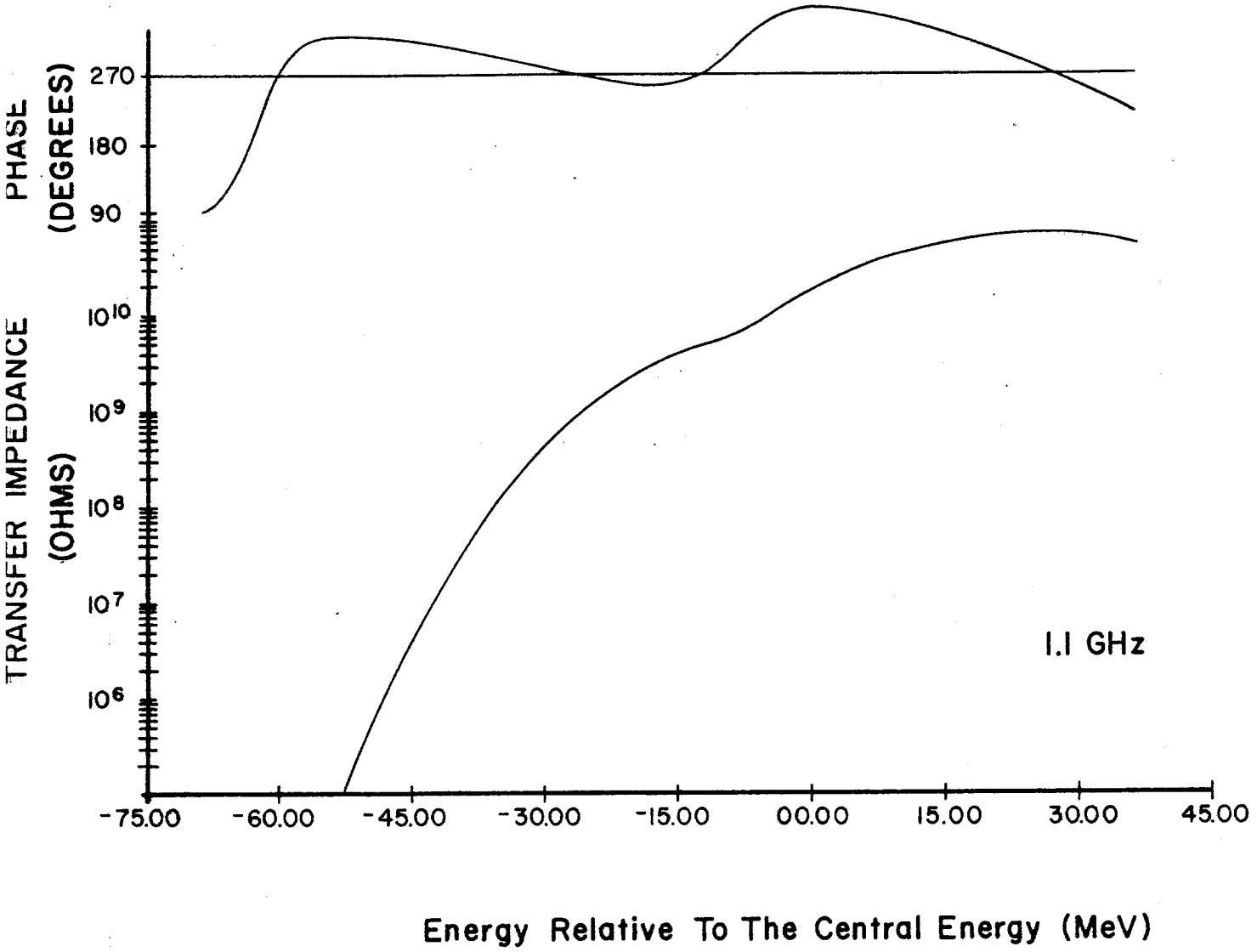
TRANSFER IMPEDANCE (OHMS)
PHASE (DEGREES)
270
180
90
10^{10}
10^{9}
10^{8}
10^{7}
10^{6}
1.1 GHz
-75.00
-60.00
-45.00
-30.00
-15.00
00.00
15.00
30.00
45.00
Energy Relative To The Central Energy (MeV)

Figure 5-13a

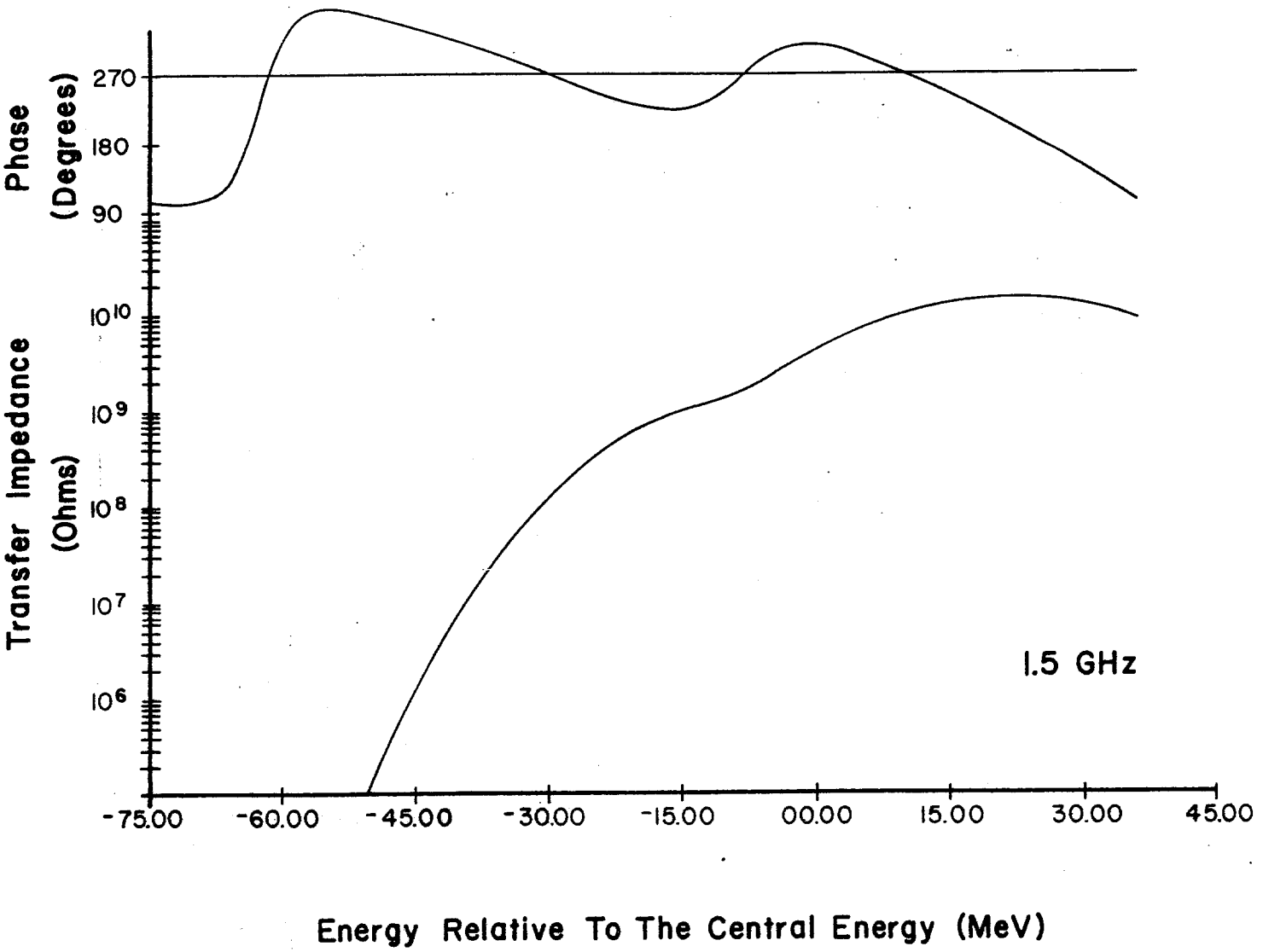
Phase (Degrees)
270
180
90
Transfer Impedance (Ohms)
10^{10}
10^{9}
10^{8}
10^{7}
10^{6}
1.5 GHz
-75.00
-60.00
-45.00
-30.00
-15.00
00.00
15.00
30.00
45.00
Energy Relative To The Central Energy (MeV)

Figure 5-13b

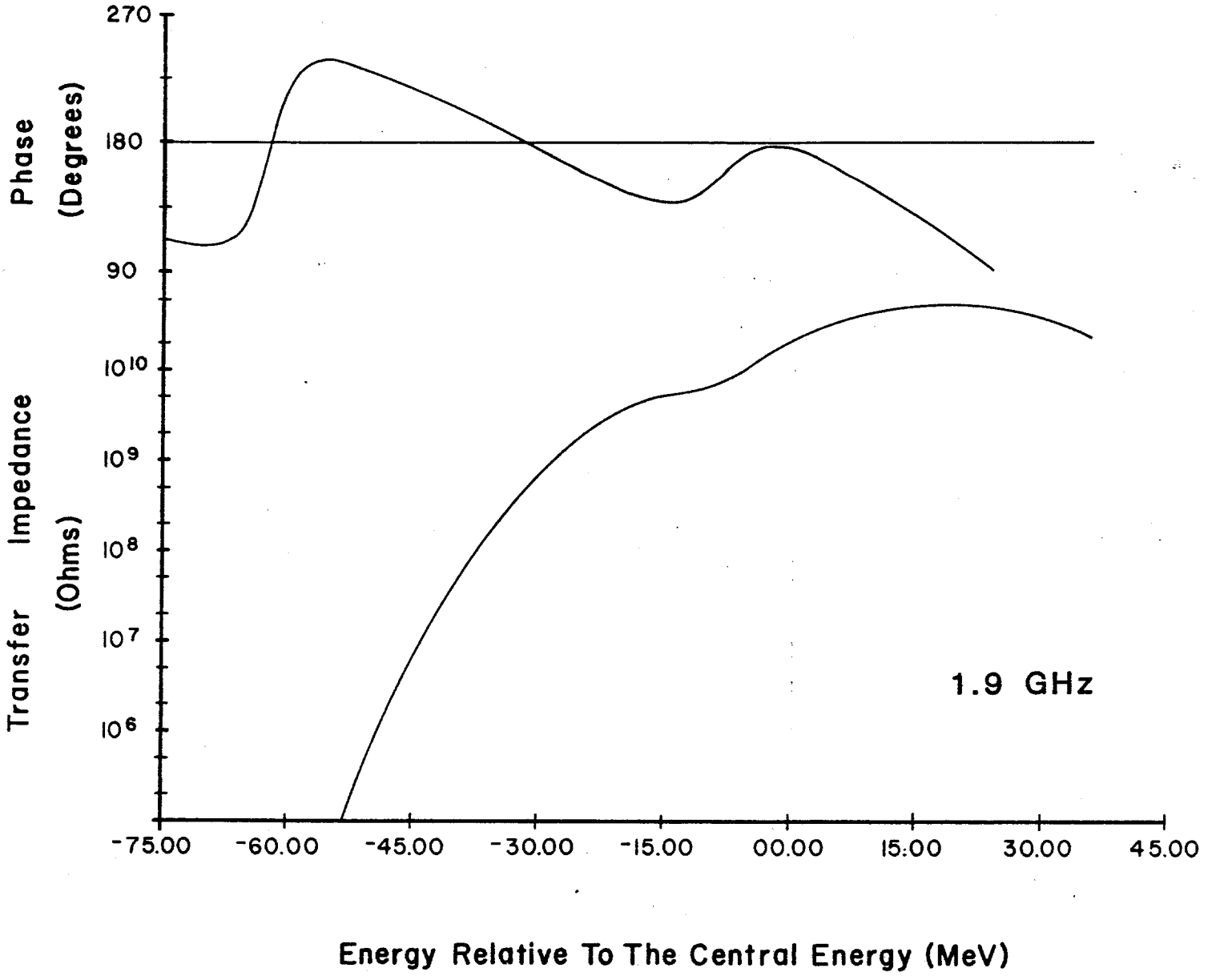
270
180
90
Phase
(Degrees)
10^{10}
10^{9}
10^{8}
10^{7}
10^{6}
Transfer Impedance
(Ohms)
1.9 GHz
-75.00
-60.00
-45.00
-30.00
-15.00
00.00
15.00
30.00
45.00
Energy Relative To The Central Energy (MeV)

Figure 5-13c

kicker, and P = P(f,E') is the pickup sensitivity. P depends on E' because P depends on particle position, which depends on E' (usually exponentially). The dependence of P on f comes from electrical properties and is usually weak.

This approximation is valid when the Schottky bands are well separated, but is a poor approximation for quantitative results for the system described here. Nonetheless, it is sufficient to show the main features of the physical process.

The closed-loop gain of the system is given by $G' = G/(1-FG)$, where G is the open-loop gain ($G = V/I_p$) of the electronics going from pickup to kicker. If the real part of FG is less than zero, then $G' < G$ and the cooling signal is suppressed. If the real part is greater than zero, the signal may be enhanced. If the real part of $FG > 1$, when the imaginary part is zero, the system is unstable. (This situation is completely analogous to the case of conventional electronic circuits with feedback).

In the approximate expression for F, one sees that there is a resistive (energy-absorbing) component of the beam response proportional to the gradient of the density at the driving frequency and a reactive component that depends on the asymmetry of the gradient about the driving frequency. It would be wrong to conclude, however, that the resistive term is the more important when looking at system stability. Both terms must be considered because the open-loop gain function G is a complex quantity; it unavoidably contains phase shifts from the filters and differences in time delays between pickup and kicker.

In fact, in the stack tail, the feedback can be dominated by the contribution from the particles in the core where $d\psi/dE$ is very large - 10^4 times larger than in the tail. Fortunately, $d\psi/dE$, which is increasing exponentially, is multiplied by the pickup response, which is decreasing exponentially. The rate of exponential increase of $d\psi/dE$ depends on the total gain profile, i.e., the product of pickup and filter response. The damping of $d\psi/dE$ in the feedback integral, however, depends only on the pickup response. Thus, it is important that the filter gain profile not be too sharp compared with the pickup in order to avoid severe problems with stability and signal suppression. The importance of the relative amounts of the gain profile derived from filters and pickups has been pointed out previously by Sacherer.[8]

An additional suppression of signal from particles in the core is provided by the subtracting pickups in each section. These pickups are placed closer to the core and normalized so that their sensitivity to the core region is equal and opposite to the sensitivity of the main pickups. In the stack tail, however, they subtract less than 10% of the signal. Several subtracting pickups followed by substantial attenuation are required to avoid having the subtracting pickups appreciably affect the amount of thermal noise in the pickups. Immediately after injection, the signal suppression is substantially larger because of the large values of

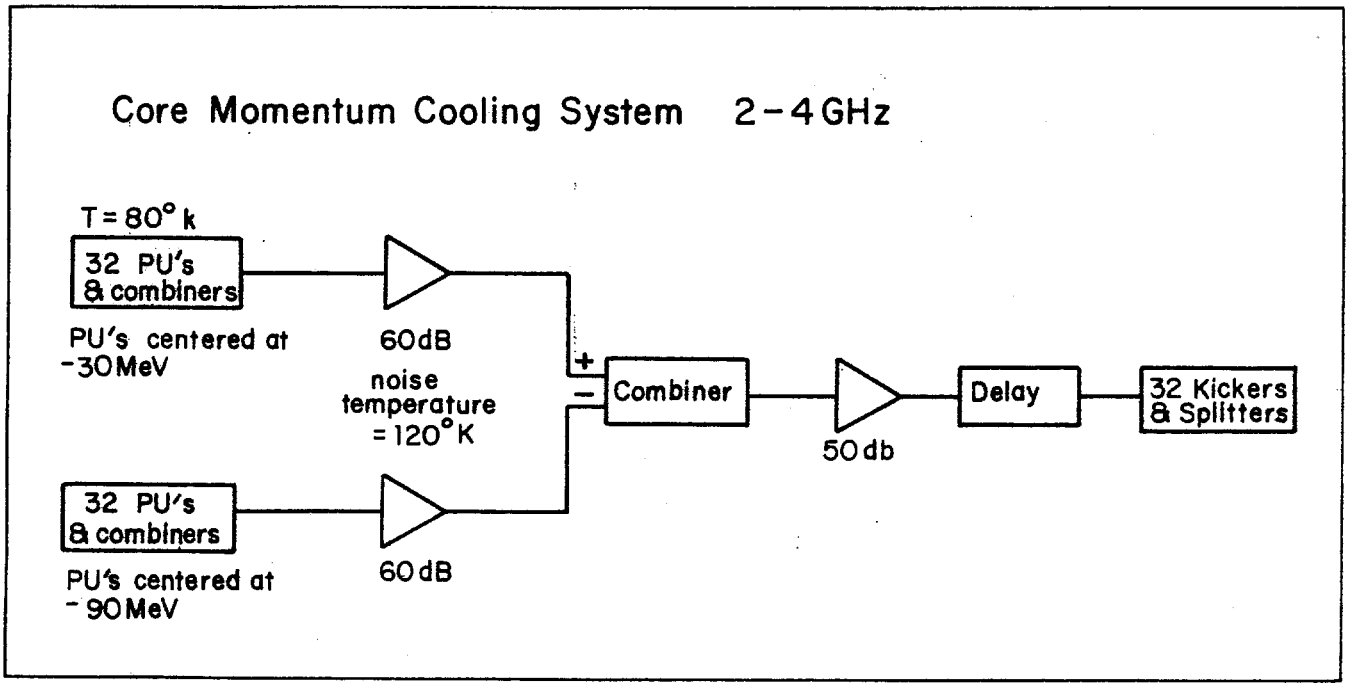
Core Momentum Cooling System 2-4 GHz
T = 80° k
32 PU's & combiners
PU's centered at -30 MeV
60 dB
noise temperature = 120° K
+
−
Combiner
50 db
Delay
32 Kickers & Splitters
32 PU's & combiners
PU's centered at -90 MeV
60 dB

Figure 5-14

$d\psi/dE$ created by the RF stacking process. The gradients quickly (after 200 msec) smooth out because of the diffusion terms in the Fokker-Planck equation. It appears that during the first 200 msec of the injection cycle, it may be necessary to reduce the amplifier gain in order to maintain beam stability. This gain reduction has been taken into account in computer simulations and, in any event, is only of minor importance.

5.9.5 Core Cooling. The same Fokker-Planck equation that describes the stack-tail system also describes the core system. In fact, the distinction between core and tail cooling systems is somewhat arbitrary. The asymptotic distribution is given by

$$\Phi = F\Psi + (D_0 + D_1 + D_2\Psi)\ \frac{\partial \Psi}{\partial E} = 0 \qquad (5.12)$$

The cooling coefficient F has a zero at the peak of the core and a slope proportional to $g_2(E-E_c)$ where g is the electronic gain and E_c is the energy at the peak of the core. The other terms are heating terms. D_0 is the contribution of intrabeam scattering (via the Coulomb force) to the diffusion and has been calculated by Ruggiero[9] to be $D_0 = 0.0015\ N_{\bar{p}}$ $(eV)^2/sec$, where $N_{\bar{p}}$ is the total number of antiprotons in the Accumulator. This value of D_0 corresponds to a momentum heating time of 2 hr. D_0 is independent of both g and E. D_1 is the contribution of thermal noise and is proportional to g^2. D_2 is the Schottky heating term and is proportional to $g^2\ (E-E_c)^2$. In our system D_1 is small compared with D_0. Optimum performance occurs when g is adjusted so that intrabeam scattering dominates in the central part of the core and the Schottky heating term dominates at the edges of the core. Smaller values of g leave the cooling term F less than optimum (g = 0 means no cooling) and larger values of g mean that Schottky heating is larger than the cooling. Computer calculations show that densities in excess of 1×10^5/eV can be reached.

The choice of 1 - 2 GHz bandwidth (and $\eta = 0.02$) for the tail system was made because of the desire to optimize core cooling. Since D_2 is proportional to $1/\eta$, a larger gain can be used to counteract intrabeam scattering in the core. Choosing a higher maximum frequency and the same momentum width for the stack tail system would have required a lower η for the lattice. This would have reduced the core cooling effectiveness.

A block diagram of the core cooling system is shown in Fig. 5-14. The zero in gain is obtained by subtracting the signals from two sets of pickups placed in a region of high momentum dispersion. One set of pickups is centered above the core energy and one is centered below. The signal is then applied to a kicker placed in a region of zero momentum dispersion. The gain profile for the core system Schottky bands at 2.2, 3.0, and 3.8 GHz is shown in Fig. 5-15 abc.

5.9.6 Numerical Calculations of Momentum Cooling. A computer simulation of the combined core and stack-tail momentum cooling systems has been made. These calculations use the full theory developed by van der Meer et al and not the simplified models given here. It has been found that a core density of 1×10^5/eV can be obtained after 4 hours of stacking with an average flux of 4×10^7 sec^{-1}. Figure 5-16 shows the stack profile as a function of time. Figure 5-17 shows the cooling term (F) including the effects of beam feedback after 3 hours. Figures 5-18 and 5-19 show the heating term coefficients $D_0 + D_1$ and D_2. Figures 5-20 and 5-21 are stability plots: the real versus the imaginary part of the cooling system gain G times the beam feedback F. In this plot the system is stable if the curve does not enclose the point (1,0).

5.10 Betatron Cooling

5.10.1 Introduction. Betatron cooling is accomplished by using a pickup sensitive to the transverse displacement of the particles. In going from pickup to kicker the particle oscillates in betatron phase by an odd multiple of $\pi/2$, converting the position displacement to an angle displacement. Each given particle creates a signal in the pickup which, when applied to the kicker, decreases the angle displacement. Other particles with similar revolution frequencies contribute noise that tends to increase the betatron amplitude. This situation is similar to the momentum-cooling discussed earlier.

Betatron cooling is conventionally described in terms of the time decrease of the betatron emittance[10]

$$\frac{d\bar{\varepsilon}}{dt} = \frac{W}{N}\left(2g - g^2(M+U)\right)\bar{\varepsilon} \quad , \tag{5.13}$$

where W is the system bandWidth, N is the number of particles being cooled, g is the system gain, M is the mixing factor, and U is the ratio of noise to signal power. The rms beam size is the square root of the beta function times $\bar{\varepsilon}$. Equation (5.13) can be an exact result if the definition of g is given by a sum over Schottky bands of a gain function including signal suppression. Some algebraic license is also required to define g^2 as something different than g times g. However, the approach taken here will be that the gain function is constant, independent of frequency. The sum over Schottky bands is therefore trivial.

For the loop pickups and kickers that we plan to use, g is defined by

$$g = N\,\beta_p \beta_k n_p n_k \left(\frac{d}{h}\right)^2 \frac{e f_o Z_{pu}}{(\beta^2 E/e)} \frac{g_A}{k} \quad , \tag{5.14}$$

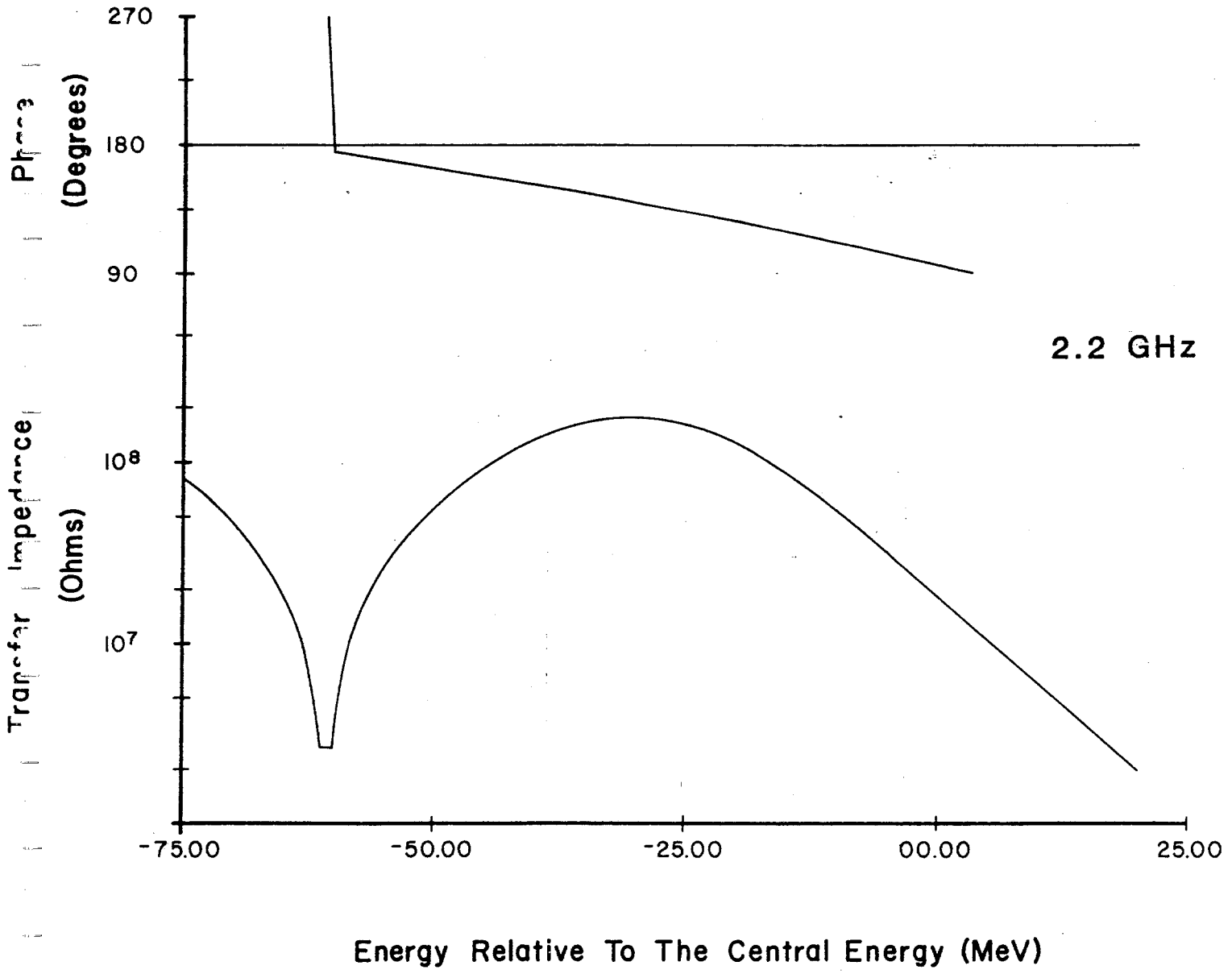
270
180
90
(Degrees)
2.2 GHz
10^8
10^7
(Ohms)
-75.00
-50.00
-25.00
00.00
25.00
Energy Relative To The Central Energy (MeV)

Figure 5-15a

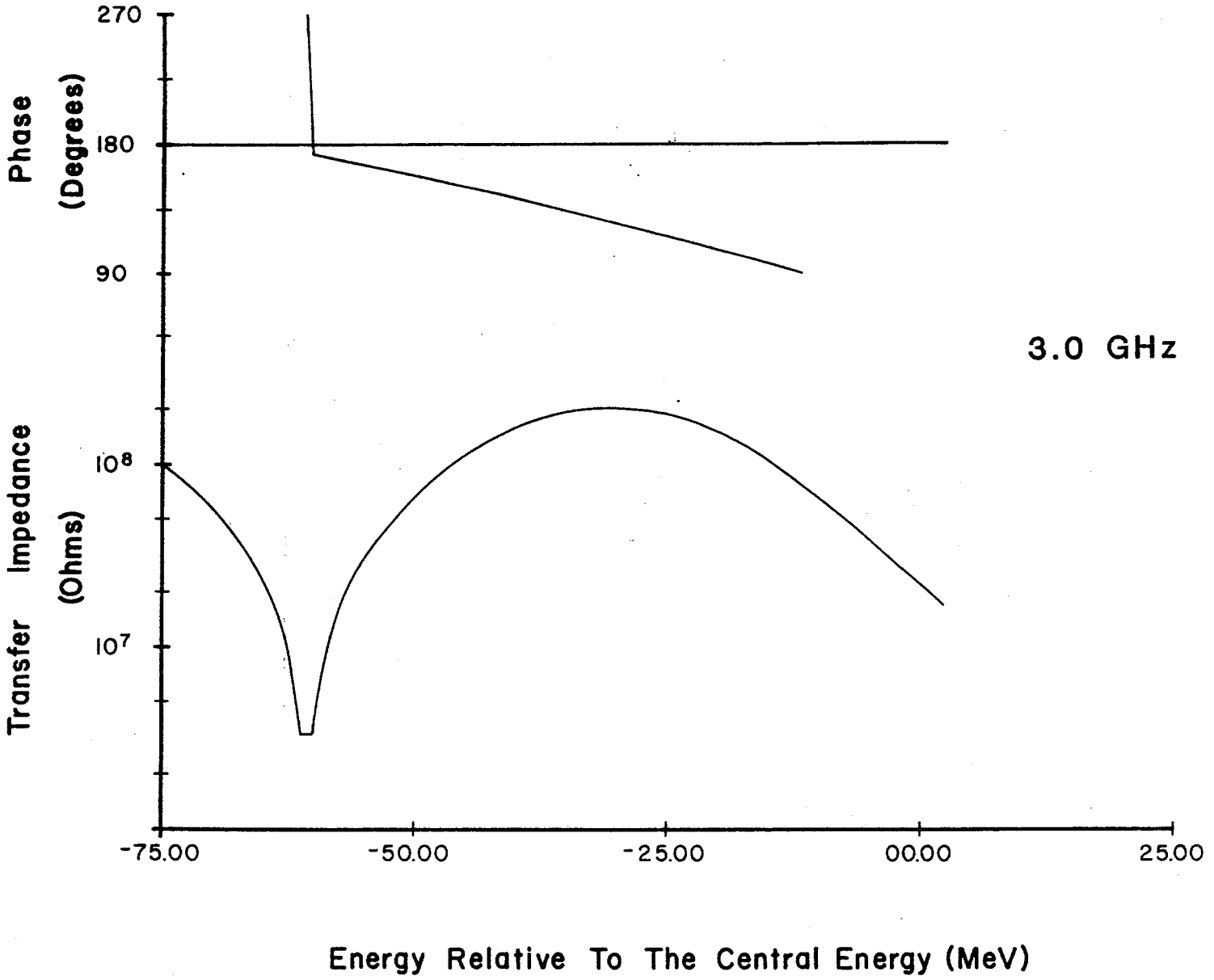
270
180
90
Phase
(Degrees)
3.0 GHz
10^8
10^7
Transfer Impedance
(Ohms)
-75.00
-50.00
-25.00
00.00
25.00
Energy Relative To The Central Energy (MeV)

Figure 5-15b

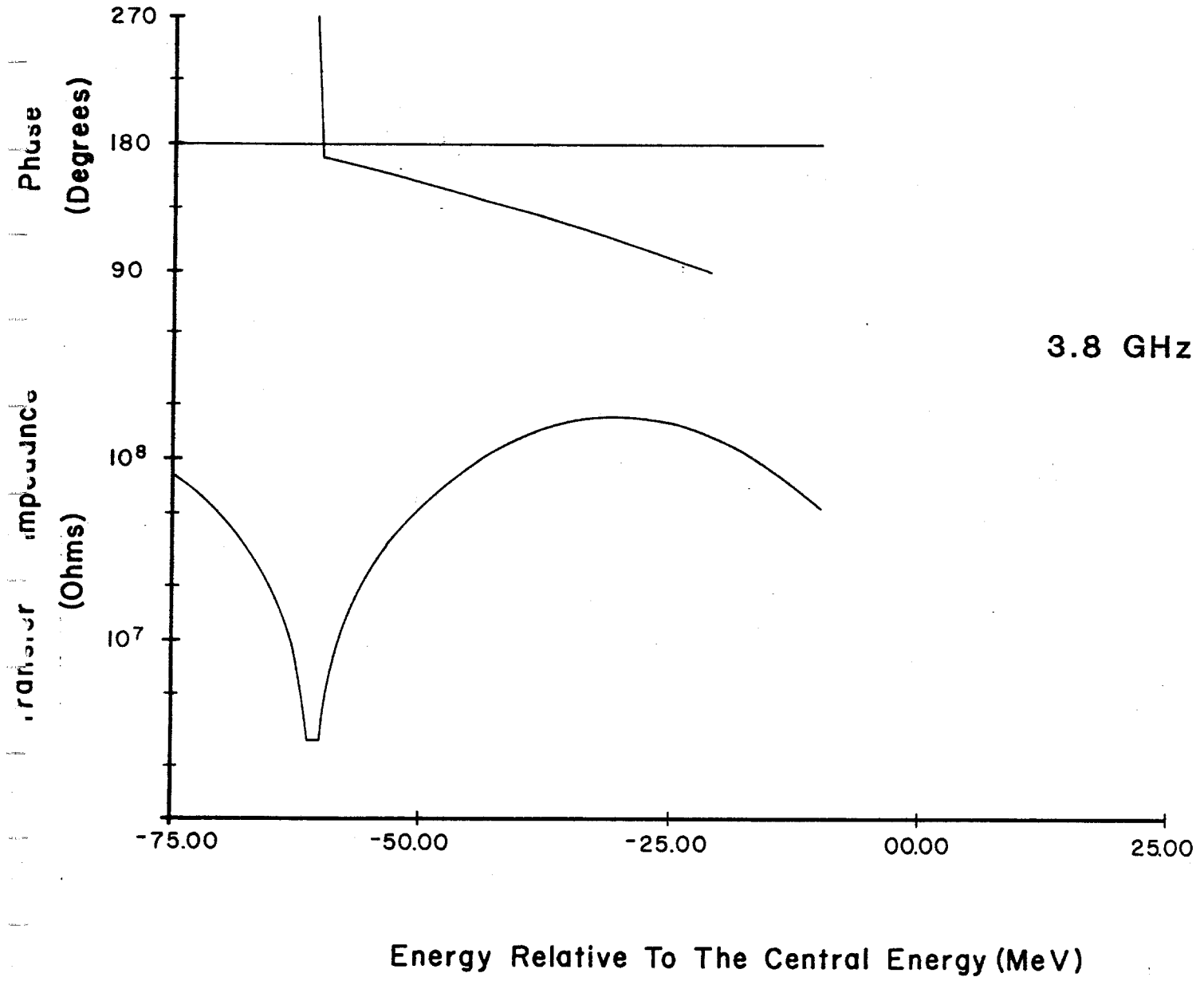
270
180
90
Phase
(Degrees)
10^8
10^7
(Ohms)
3.8 GHz
-75.00
-50.00
-25.00
00.00
25.00
Energy Relative To The Central Energy (MeV)

Figure 5-15c

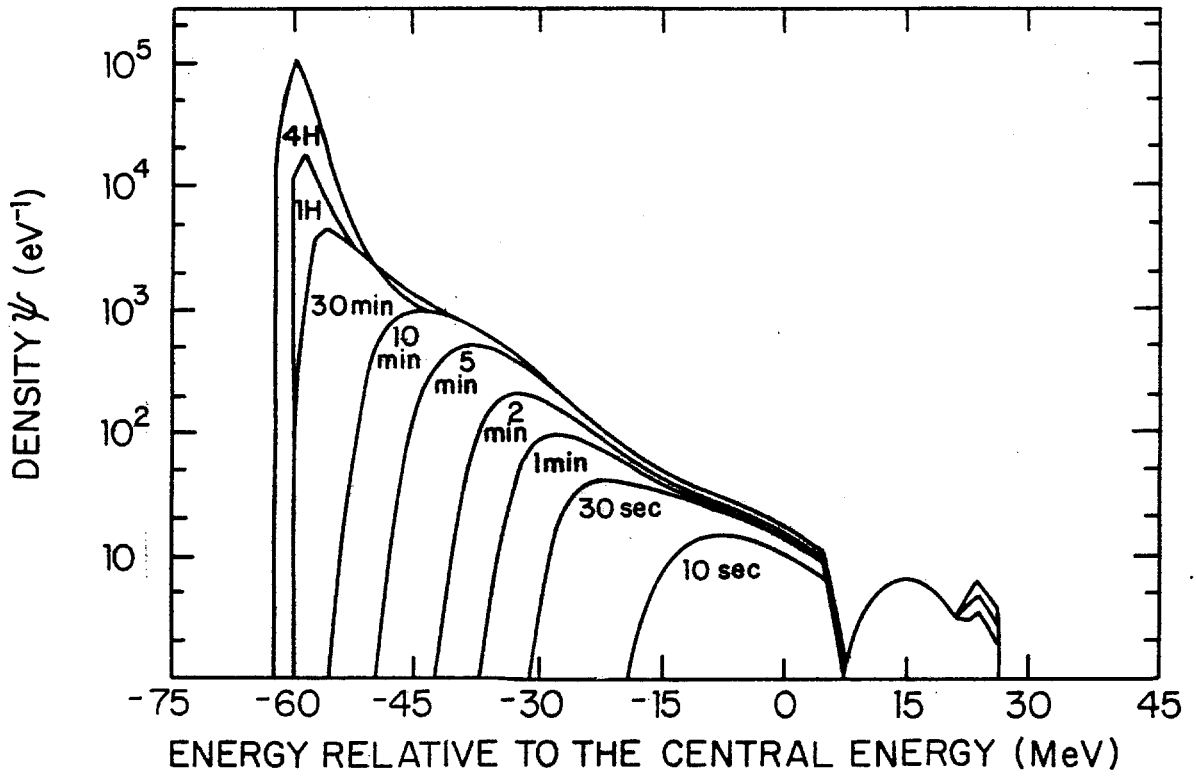
DENSITY ψ (eV⁻¹)
10⁵
10⁴
10³
10²
10
4H
1H
30min
10 min
5 min
2 min
1min
30 sec
10 sec
-75
-60
-45
-30
-15
0
15
30
45
ENERGY RELATIVE TO THE CENTRAL ENERGY (MeV)

Figure 5-16

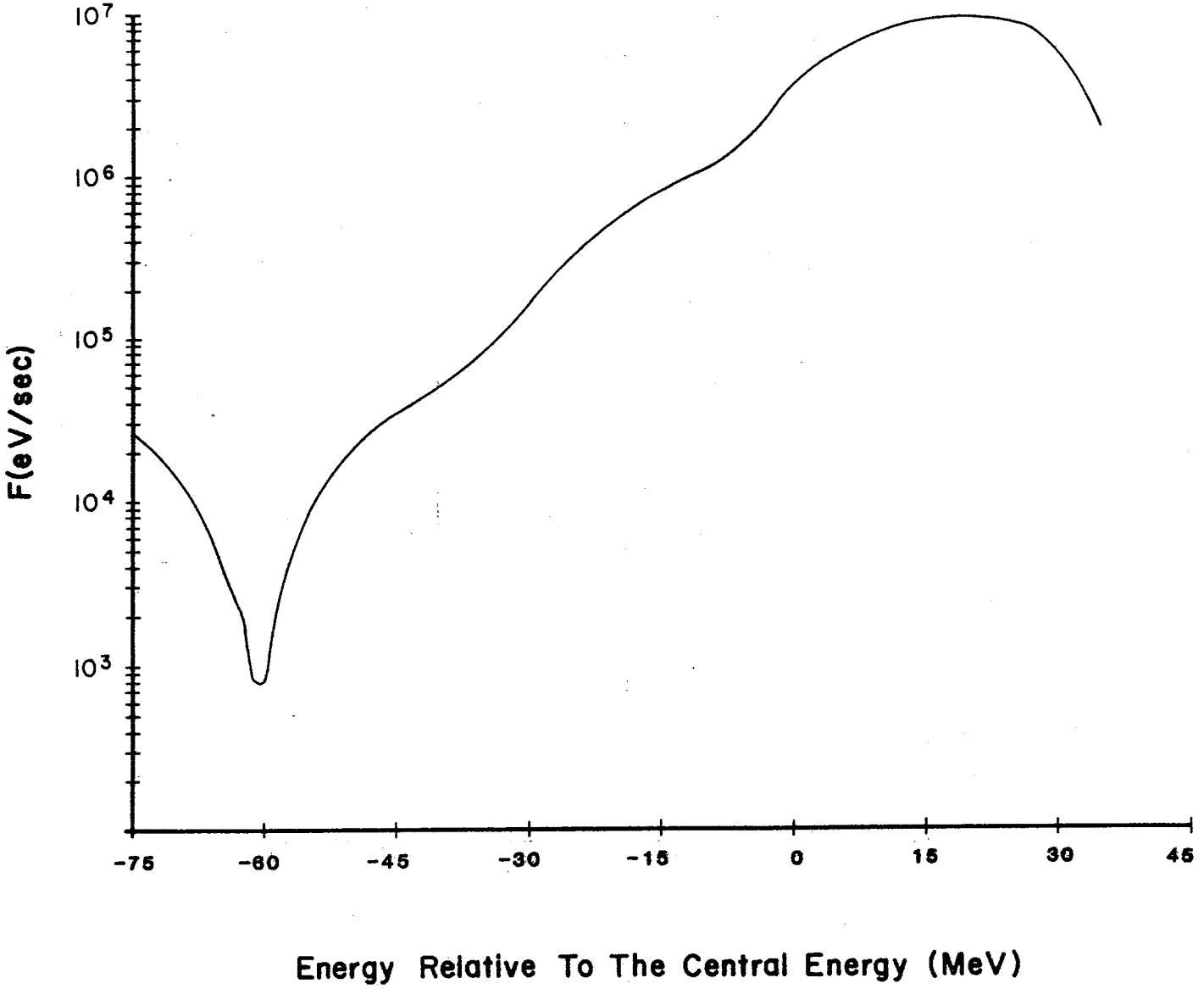
10^7
10^6
10^5
10^4
10^3
F(eV/sec)
-75
-60
-45
-30
-15
0
15
30
45
Energy Relative To The Central Energy (MeV)

Figure 5-17

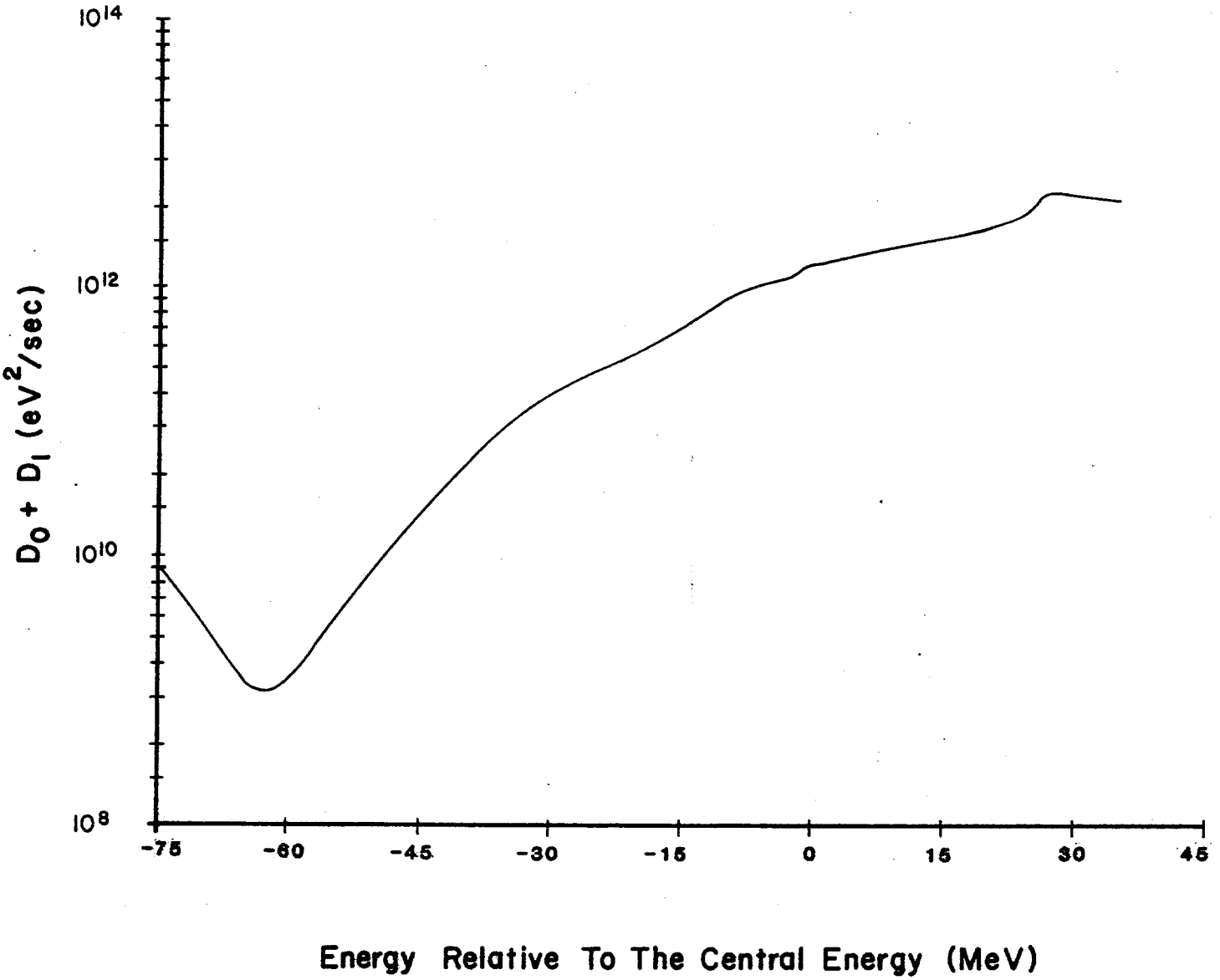
10^{14}
10^{12}
10^{10}
10^{8}
$D_0 + D_1$ (eV^2/sec)
-75
-60
-45
-30
-15
0
15
30
45
Energy Relative To The Central Energy (MeV)

Figure 5-18

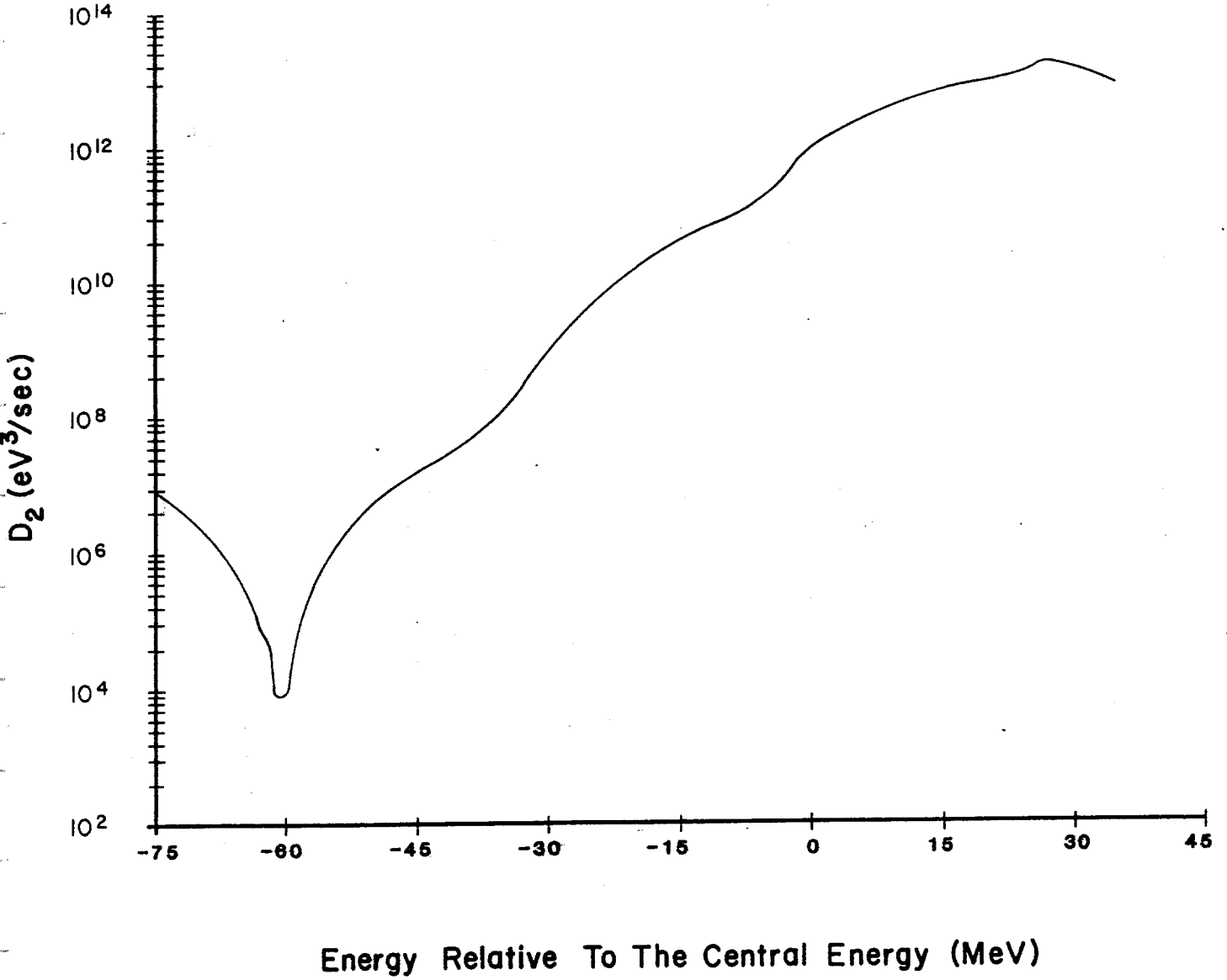
10^{14}
10^{12}
10^{10}
10^{8}
10^{6}
10^{4}
10^{2}
D_2 (eV^3/sec)
-75
-60
-45
-30
-15
0
15
30
45
Energy Relative To The Central Energy (MeV)

Figure 5-19

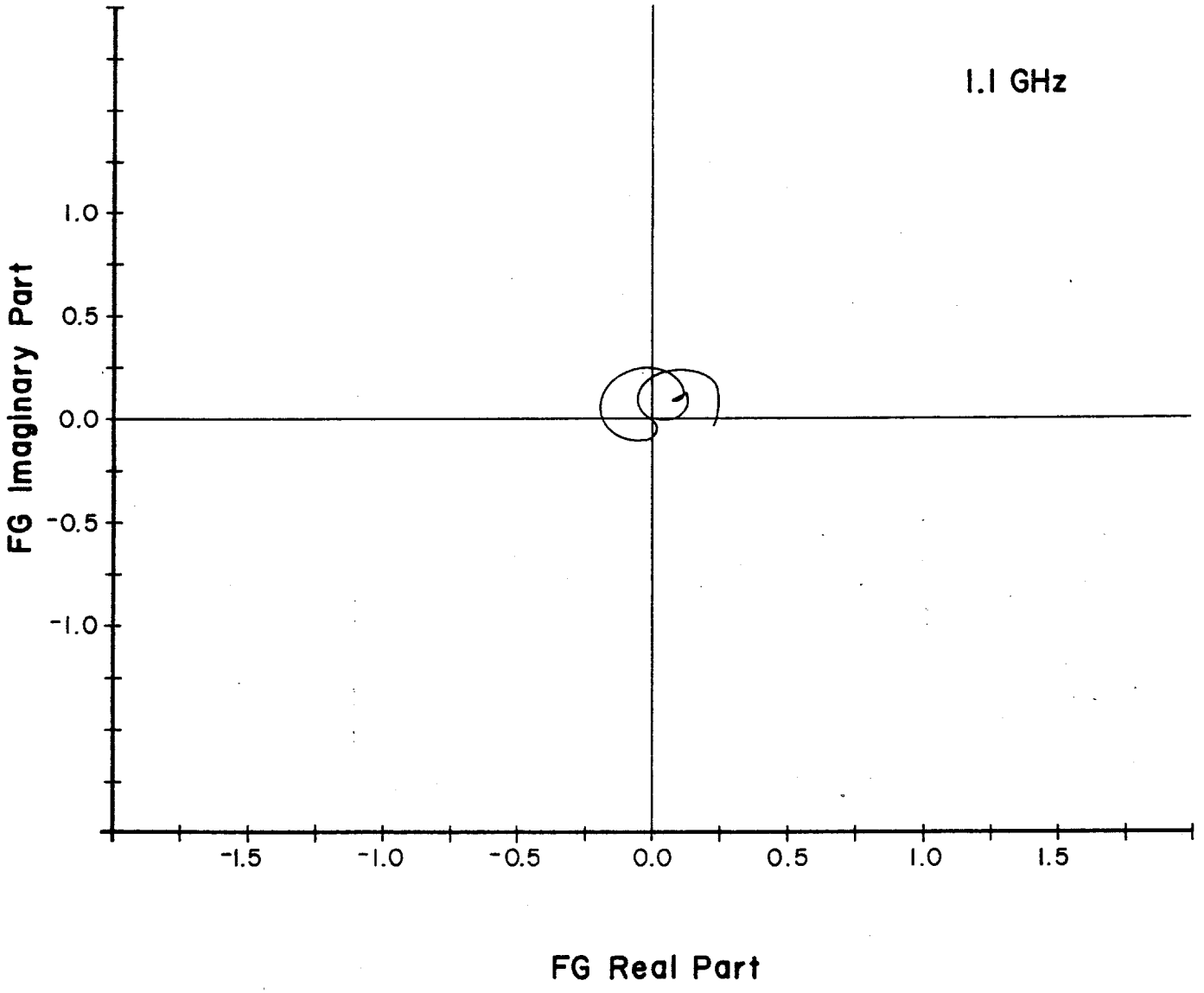
1.1 GHz
FG Imaginary Part
1.0
0.5
0.0
-0.5
-1.0
-1.5
-1.0
-0.5
0.0
0.5
1.0
1.5
FG Real Part

Figure 5-20a

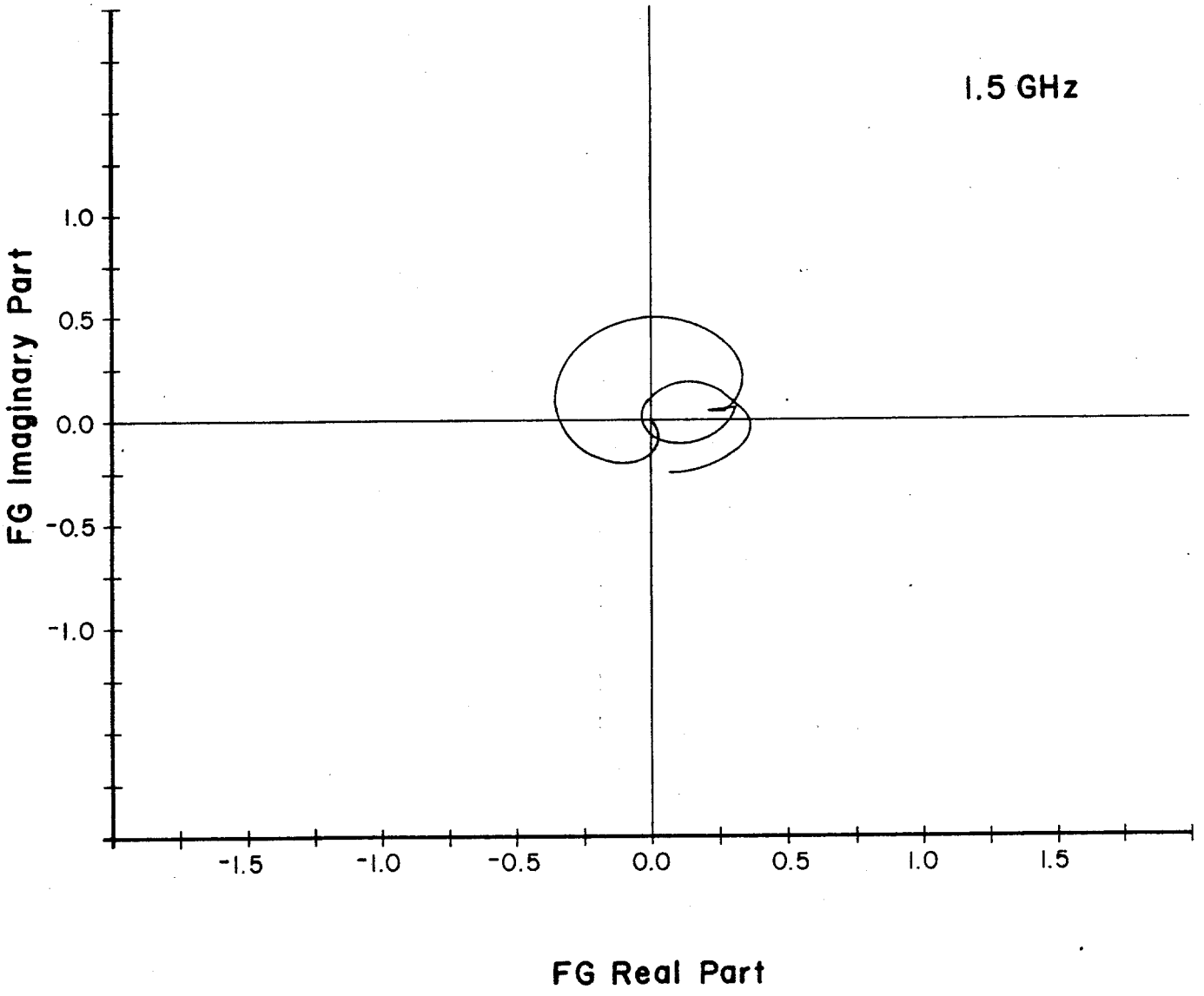
1.5 GHz
FG Imaginary Part
1.0
0.5
0.0
-0.5
-1.0
-1.5
-1.0
-0.5
0.0
0.5
1.0
1.5
FG Real Part

Figure 5-20b

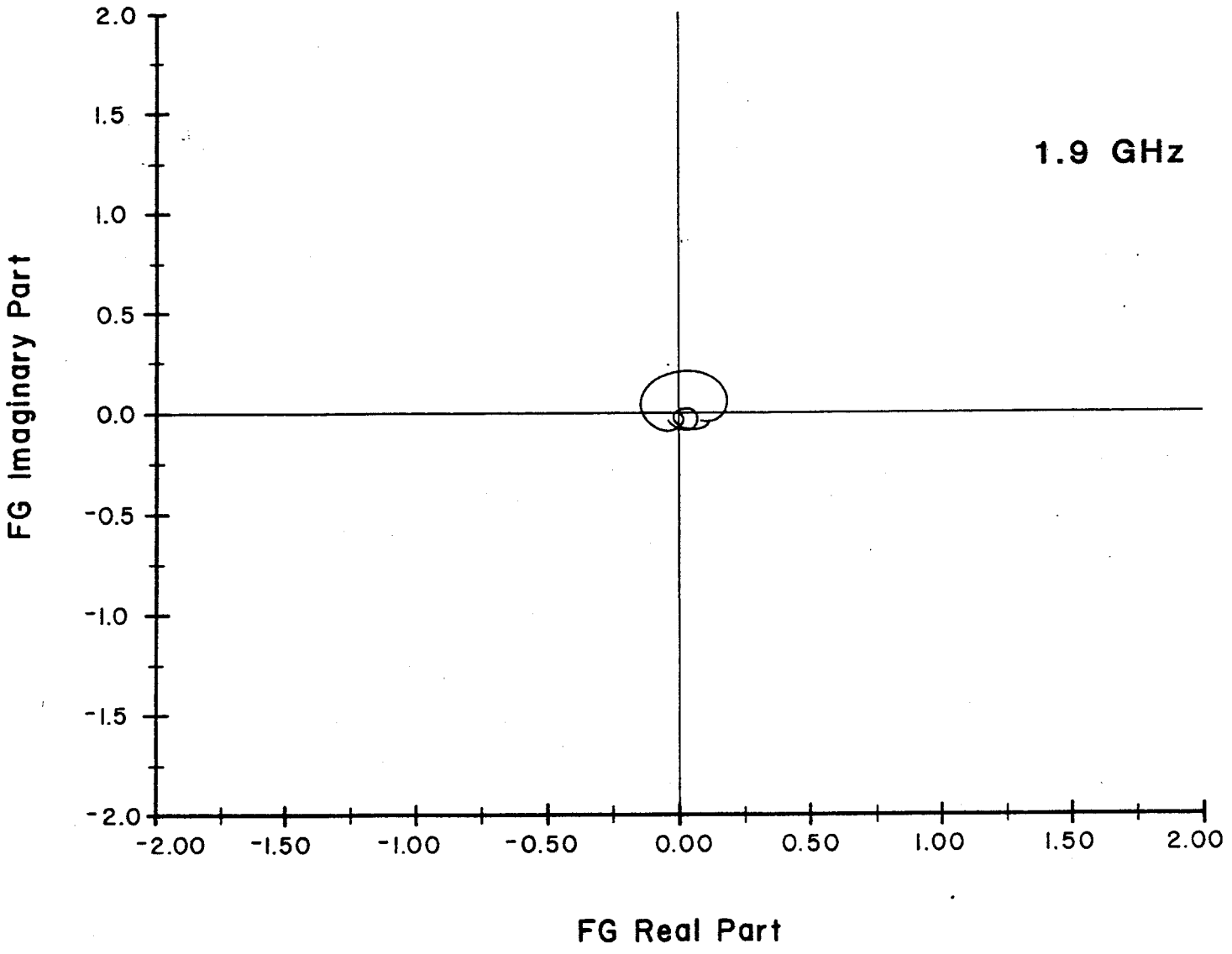
1.9 GHz
FG Imaginary Part
FG Real Part
2.0
1.5
1.0
0.5
0.0
-0.5
-1.0
-1.5
-2.0
-2.00
-1.50
-1.00
-0.50
0.00
0.50
1.00
1.50
2.00

Figure 5-20c

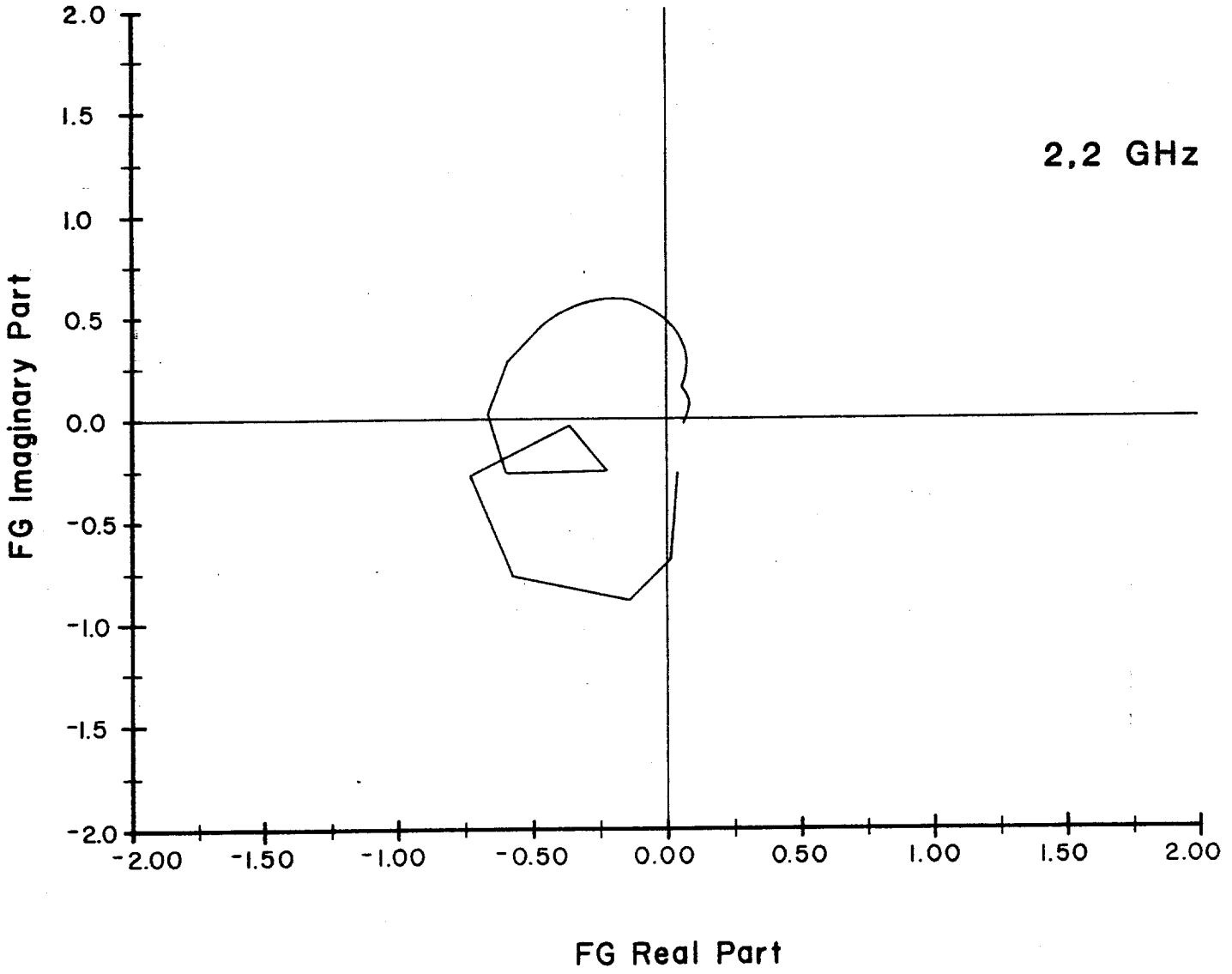
2.0
1.5
1.0
0.5
0.0
-0.5
-1.0
-1.5
-2.0
FG Imaginary Part
2,2 GHz
-2.00
-1.50
-1.00
-0.50
0.00
0.50
1.00
1.50
2.00
FG Real Part

Figure 5-21a

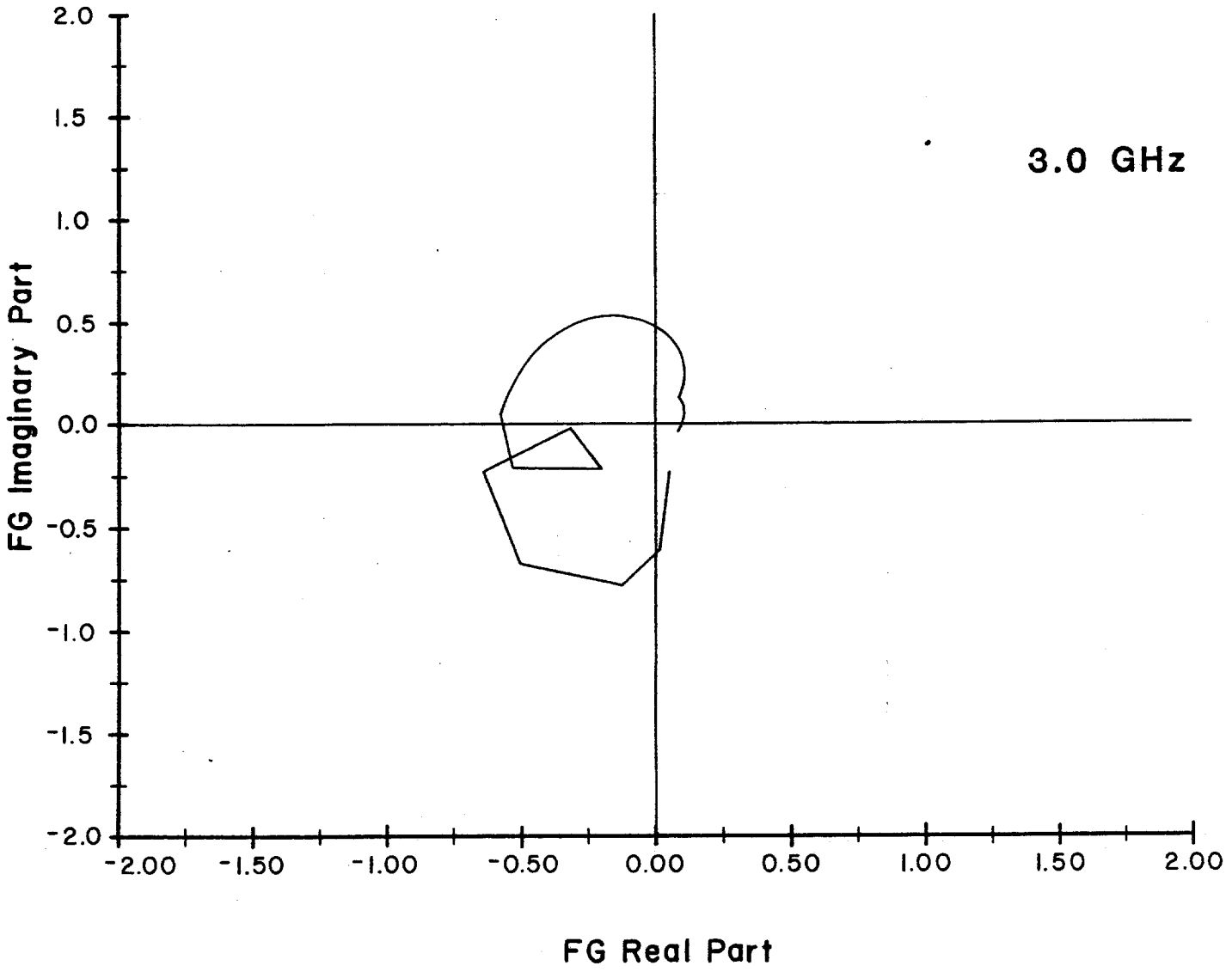
3.0 GHz
FG Imaginary Part
FG Real Part
2.0
1.5
1.0
0.5
0.0
-0.5
-1.0
-1.5
-2.0
-2.00
-1.50
-1.00
-0.50
0.00
0.50
1.00
1.50
2.00

Figure 5-21b

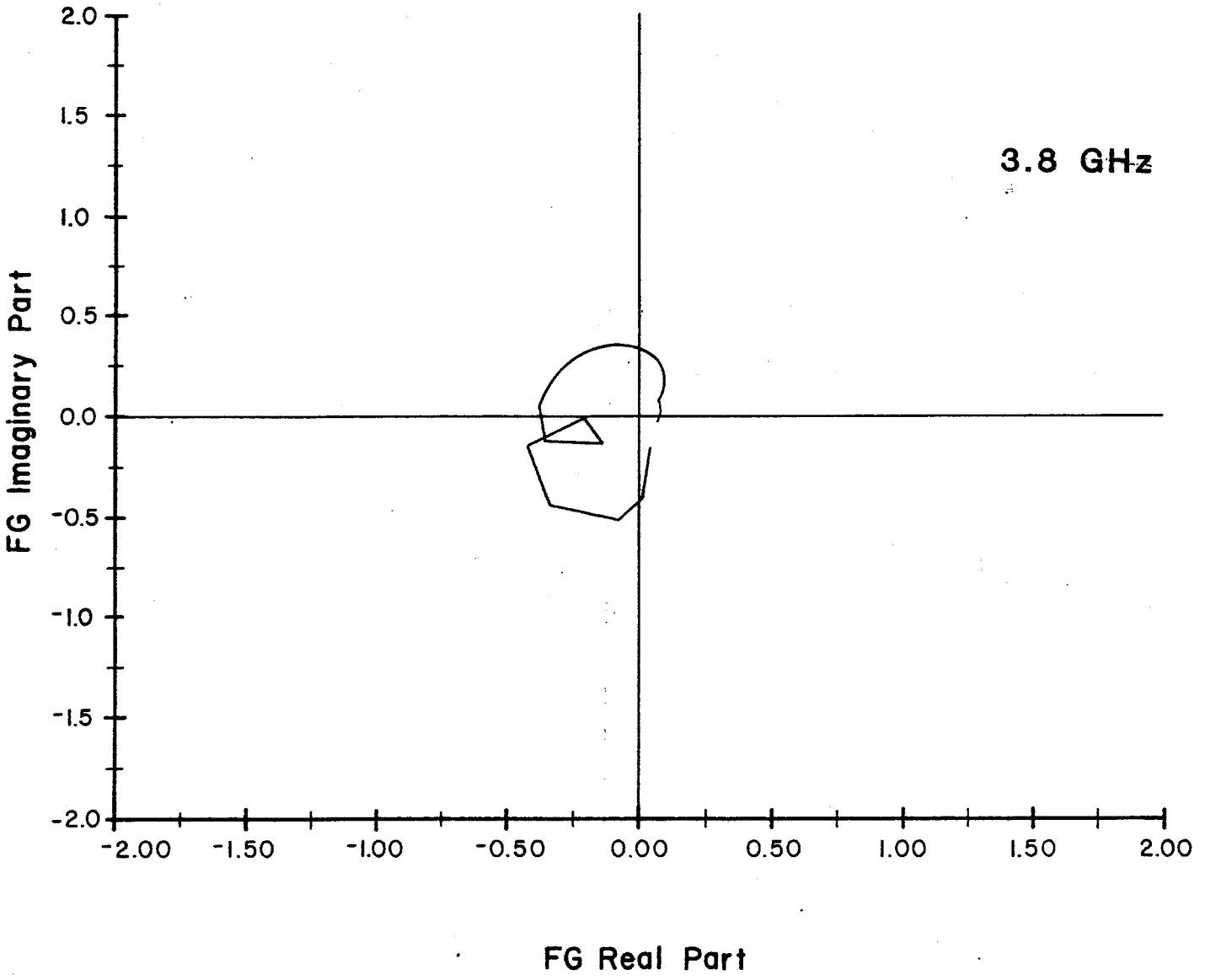
3.8 GHz
FG Imaginary Part
FG Real Part
2.0
1.5
1.0
0.5
0.0
-0.5
-1.0
-1.5
-2.0
-2.00
-1.50
-1.00
-0.50
0.00
0.50
1.00
1.50
2.00

Figure 5-21c

where $\beta_p(\beta_k)$ is the function at the pickup (kicker), $n_p(n_k)$ is the number of pickups (kickers), d is the pickup and kicker sensitivity defined in section 5.11.1, h is the pickup and kicker gap, g_A is the amplifier gain, and $k=\omega/\beta c$. In order for g to be independent of frequency, g_A must increase linearly with frequency. The optimum gain profile would be for g to increase with frequency and therefore for g_A to increase with frequency squared. The effect of signal suppression is to modify 5.2. At small values of amplifier gain, such as exist in the stack tail betatron cooling system, the signal suppression is small and can be ignored. As the gain is increased to obtain the optimum cooling the beam feedback reduces the effective gain of the system by a factor of 2 at the center of a symmetric distribution that is peaked at the center. Off center, the value of the suppression factor depends on the shape of the distribution, but it is generally true that the cooling is slowest at the peak of the distribution. For a system like the core betatron cooling system, it is sufficient to perform calculations ignoring signal suppression, remembering that the actual amplifier gain required is $2\ g_A$.

The mixing factor M is the ratio of the peak power density in the Schottky band to a uniform power density of the same power. For a system with constant gain g,

$$M = \frac{f^2\psi(f)\Lambda}{2WN} = \frac{f\beta^2 E\psi(E)\Lambda}{2WN\ \eta} \quad , \tag{5.15}$$

where f is the revolution frequency, $\psi(f)$ is the particle density (number/Hz), $\psi(E)$ is the particle density (number/eV), $\Lambda=\ln 2$, and $\eta=1/\gamma_t^2 - 1/\gamma^2$.

The total thermal power in the system is

$$P_T = k_B(\theta_R+\theta_A)g_A^2 W \quad , \tag{5.16}$$

where k_B is Boltzman's constant (1.38×10^{-23} Joules/K), θ_R is the temperature of the pickup terminating resistor, θ_A is the equivalent noise temperature of the amplifier. Strictly speaking, g_A^2 should be averaged over the system bandwidth, but it suffices to take the value at midband. The Schottky power is

$$P_S = \frac{1}{2} N e^2 f_o Z_{pu} \left(\frac{d}{h}\right)^2 \beta_p n_p \bar{\varepsilon} g_A^2 W; \tag{5.17}$$

U is the ratio of noise to signal power

$$U = \frac{P_T}{P_S} \tag{5.18}$$

5.10.2 Betatron Cooling in the Core. Betatron cooling in the core is limited by the relatively large density of particles. The cooling is therefore necessarily a slow one, accomplished with low power and a large signal to noise ratio. The core betatron cooling is accomplished with two identical systems. A schematic of one system is given in Fig. 5-22. Both pickups and kickers are located in zero dispersion straight sections. The betatron phase advance between pickup and kicker is $2\text{-}3/4\times2\pi$ in the horizontal and $2\text{-}3/4\times2\pi$ in the vertical. After 4 hours of stacking there are 5×10^{11} particles in the core, with a peak density of 10^5/eV. For W=2 GHz and η=0.02 the mixing factor M is equal to 10. Other relevant parameters are $\beta_p=\beta_k=6$, $n_p=n_k=8$, h=3 cm, d=1.73, $Z_{pu}=75\,\Omega$, $\theta_A=\theta_R=373$ K. With these parameters U=0.5 for the final emittance $\varepsilon=0.5\pi$ mm-mrad. From Eq. (5.13) it can be seen that the maximum cooling rate is obtained when

$$g = \frac{1}{M+U} \quad , \tag{5.19}$$

For this value of g the amplifier gain at midband according to Eq. (5.16) is g_A=100 dB. If the signal suppression effect is included the required gain will become 106 dB. The Schottky power is given approximately by Eq. (5.3) with g_A=100 dB and is about 1 watt. The thermal power is given approximately by Eq. (5.16) with g_A=106 dB (most of the thermal power is between Schottky bands and not greatly affected by the suppression). The thermal power is also about 1 watt.

5.10.3 Stack-Tail Betatron Cooling. The stack tail betatron cooling system uses the same pickups as the second section of the tail momentum-cooling system. The pickup plates are centered at -1 MeV relative to the central energy. For horizontal signals the pickup is most sensitive at its edges at +21 MeV and -19 MeV. Most of the cooling takes place at the -19 MeV edge because the momentum cooling system is pushing particles much more slowly past the -19 MeV edge than the +21 MeV edge. The pickup is most sensitive at its center (-1 MeV) for signals in the vertical direction. The kickers are also placed at -1 MeV in a region with high dispersion. A block diagram of the system is shown in Fig. 5-23.

Approximate calculations of the system performance have been made with Eq. (5.13) except that the time variable has been replaced with the energy variable, using the relationship

$$\frac{dE}{dt} = \frac{\Phi}{\psi(E)} \quad ,$$

where Φ is the flux of particles and $\psi(E)$ is the density of particles. This approximation ignores fluctuations in energy gain in the stacking process. With this approximation, Eq. (5.13) is easily integrated numerically. Figure 5-24 shows the emittance reduction as a function of energy. The thermal power in each system is 10W and the Schottky betatron

CORE BETATRON COOLING SYSTEM 2-4 GHz

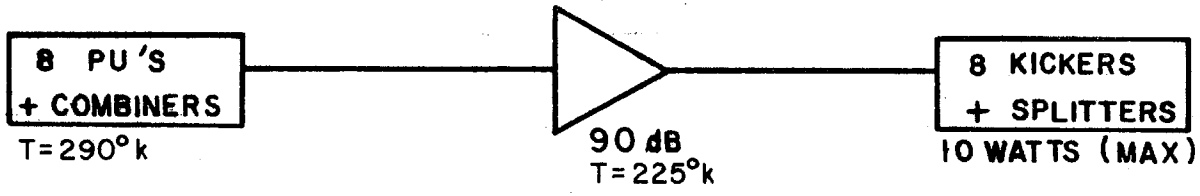

Figure 5-22

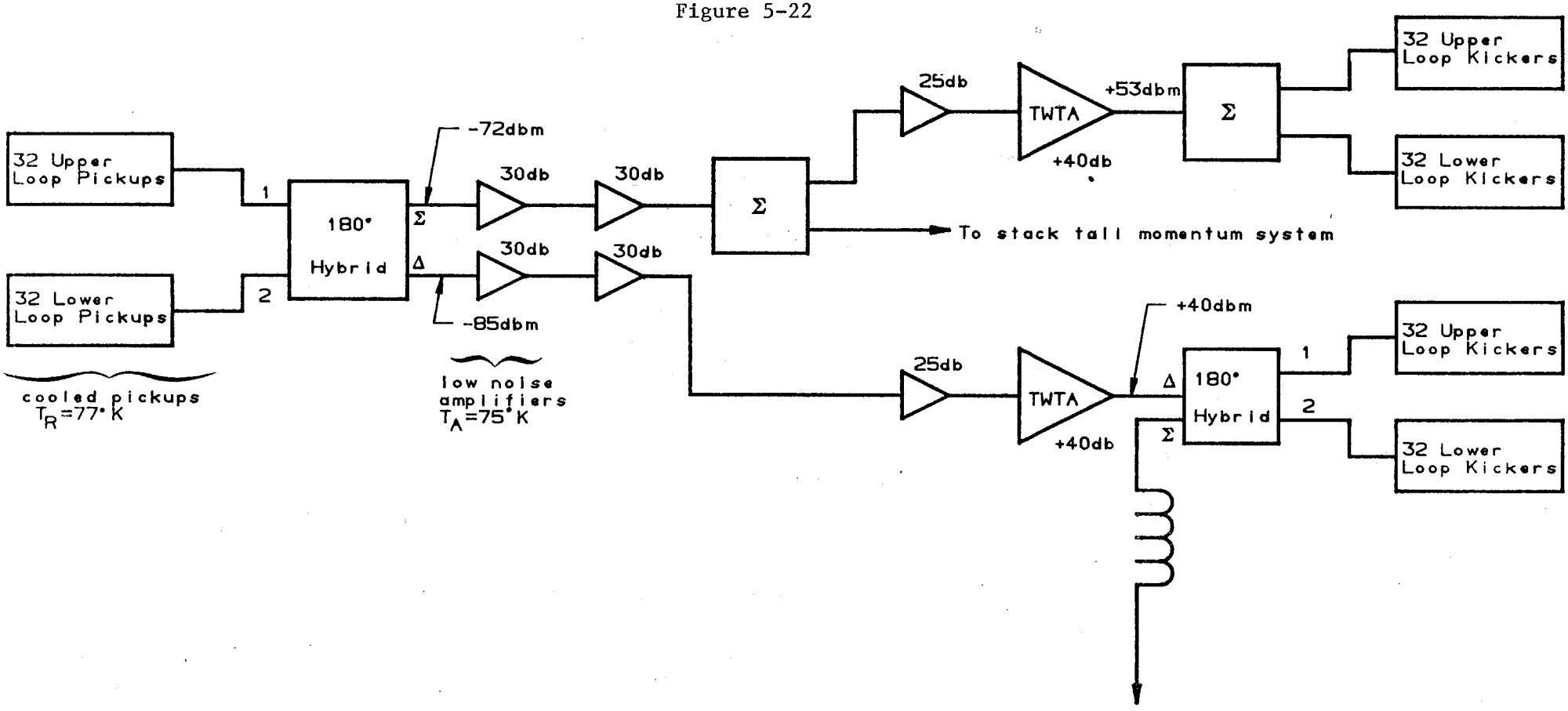

Stack Tail Betatron Cooling System

Figure 5-23

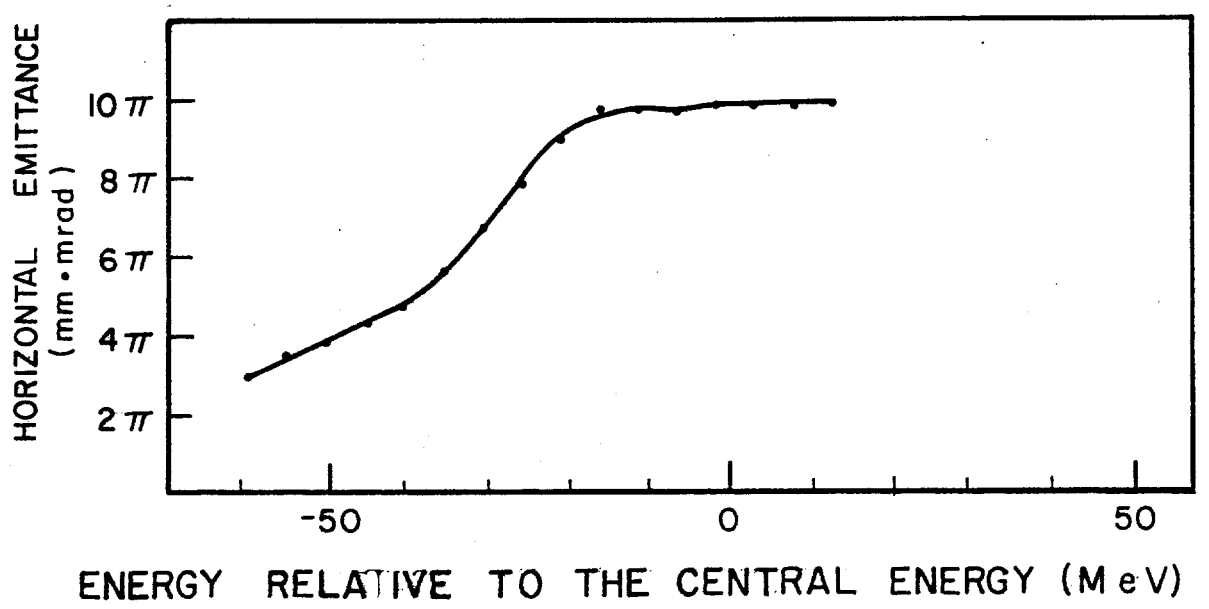
HORIZONTAL EMITTANCE
(mm • mrad)
10π
8π
6π
4π
2π
-50
0
50
ENERGY RELATIVE TO THE CENTRAL ENERGY (MeV)

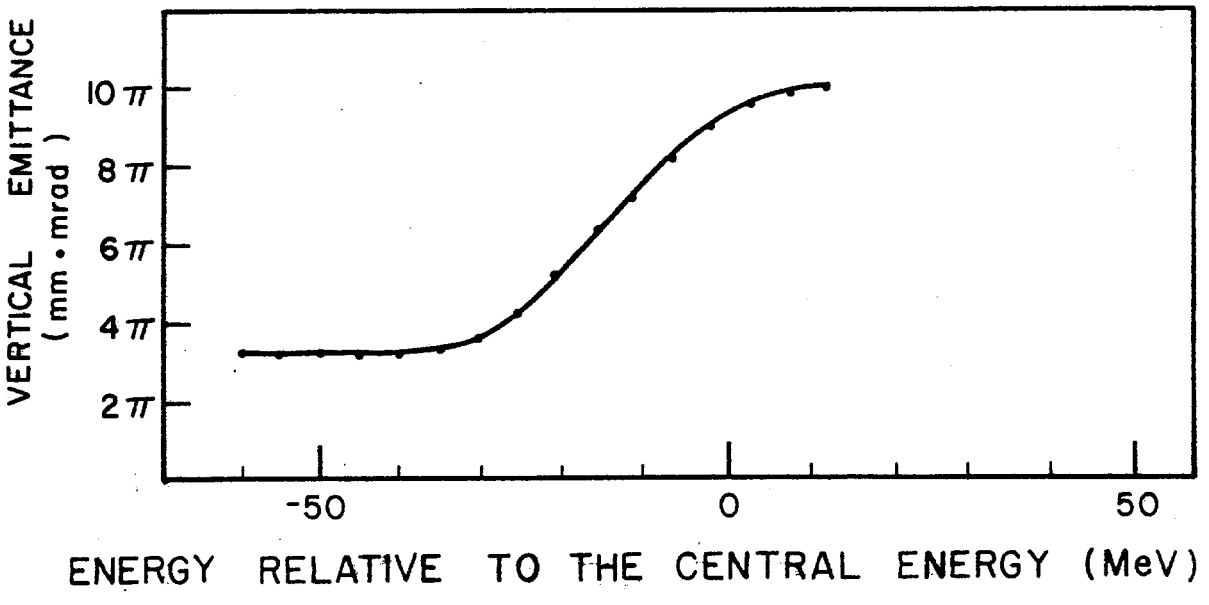
VERTICAL EMITTANCE
(mm • mrad)
10π
8π
6π
4π
2π
-50
0
50
ENERGY RELATIVE TO THE CENTRAL ENERGY (MeV)

Figure 5-24

sideband power is 10W. The horizontal system has a large momentum Schottky signal as well-about 200W.

5.10.4 Operation of Betatron Cooling Systems. In the Accumulator we have available two betatron cooling systems, either of which is capable, or nearly capable, of cooling the beam emittance from 10 to 2π mm-mrad. The core system is clearly required so that a core of $\bar{p}$'s may be held for several hours without diffusion. The tail system serves two functions: 1) to cool the betatron amplitudes in a system with a low particle density (it is not necessary to wait one half to one hour for the core cooling system to do its work) and 2) to counteract possible betatron heating by the momentum-cooling system. The size of the latter effect is difficult to estimate; it depends on how well we are able to build the momentum kickers for the stack-tail system. If the effect is larger than expected, the gain of the stack-tail system can be raised to achieve better cooling, but, of course, the power requirements will be greater. Tentatively, however, we would plan to use the stack-tail system to reduce the beam emittance by about a factor of e and use the core system to reduce it below 2π mm-mrad.

5.11 Stochastic-Cooling Hardware

The purpose of this section is to outline the hardware and techniques we expect to use in order to meet the design requirements presented above. Although the design is not complete, it has been carried out in sufficient detail to make reliable cost estimates. In several instances alternative designs are possible. We present here the design that is most sound technically. Research and development are presently in progress to investigate alternatives that could lead to better system performance, reliability, or cost reduction.

Each stochastic cooling system is composed of 5 basic parts: beam pickup electrodes, low-level electronics (including preamplifiers), medium level electronics (including gain and phase correction circuits, filters etc.), high-level electronics (including traveling-wave tubes), and kicker electrodes. As several of the cooling systems share common elements in their design, and the performance of these elements effects for the proper functioning of the cooling system, they are discussed below.

5.11.1 Pickup Electrodes. The design of the 1 to 2 GHz and the 2 to 4 GHz stochastic cooling systems is based on the known[5,11] and measured[12] performance of quarter-wave loop (directional-coupler) pickups. The loop pickup is a segment of transmission line of well-defined characteristic impedance on which beam-wall (image) currents can be induced. The magnitude of the voltage induced on it depends on its characteristic impedance Z_{pu}, its effective length ℓ, its geometrical coupling $e(x,y)$ (which depends on the transverse beam location as well as the height of the vacuum chamber, and the amplitude of the beam current $i_b(\omega)$.

$$V_{pu}(\omega), = e(x,y)\ Z_{pu}\ \sin(\frac{\ell\omega}{c})\ e^{i\pi/2}\ i_b(\omega), \tag{5.20}$$

where the 90° phase shift at the reference plane (the center of the loop) is due to the inductive nature of the coupling. The geometry of a typical pickup pair is shown in Fig. 5-25. Here h is the full height of the gap between the electrodes and w is their effective width. If the signals are added in a microwave power combiner circuit and the output signal is referenced to a transmission line of impedance Z_o, the output voltage is

$$V_{out}(\omega), = s(x,y)\sqrt{\frac{Z_{pu}Z_o}{2}}\ \sin(\frac{\ell\omega}{c})\ e^{i\pi/2}\ i_b(\omega), \tag{5.21}$$

where $s(x,y) = e(x,y) + e(x,-y)$

$$= \frac{1}{\pi}\left[\tan^{-1}\left(\frac{\sinh\frac{\pi}{h}(x+w/2)}{\cos(\pi y/h)}\right) - \tan^{-1}\left(\frac{\sinh\frac{\pi}{h}(x-w/2)}{\cos(\pi y/h)}\right)\right] \tag{5.22}$$

For $x = y = 0$,

$$s(0,0) = \frac{2}{\pi}\tan^{-1}\{\sinh(\pi w/2h)\}. \tag{5.22a}$$

Transfer impedances of pickup pairs in sum mode are defined with a centered beam at center frequency ($\omega = \pi c/2\ell$) and in a $Z_o = 50$ ohm transmission line,

$$Z_s = s(0,0)\sqrt{25\ Z_{pu}}\ .$$

At large x, $\quad s(x,0) \rightarrow \frac{4}{\pi}\ e^{-\pi x/h}\ \sinh(\pi w/2h)$

A plot s(x,0) vs x is given in Fig. 5-26(a).

If the differences of the signals in the pickup electrode pair are combined into a transmission line of impedance Z_o, the output voltage is

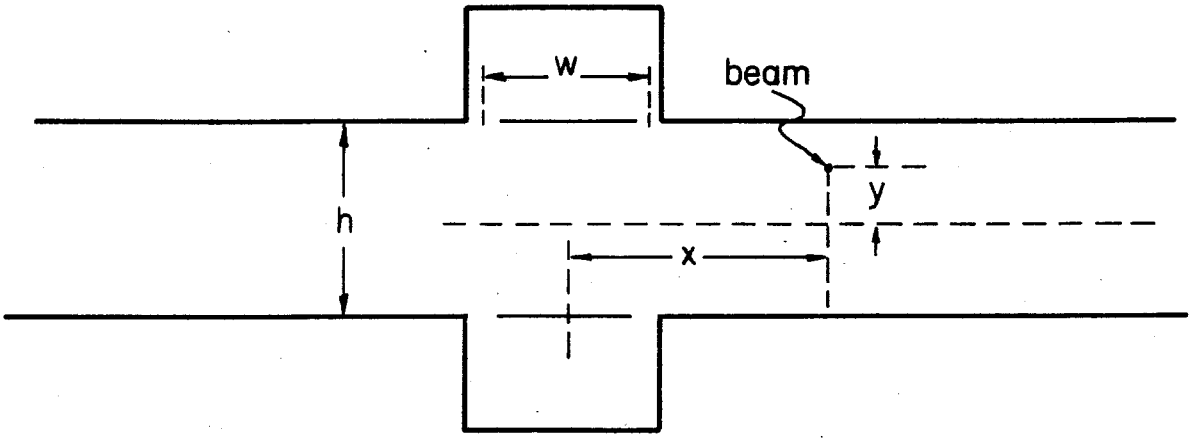

PICKUP - PAIR GEOMETRY

Figure 5-25

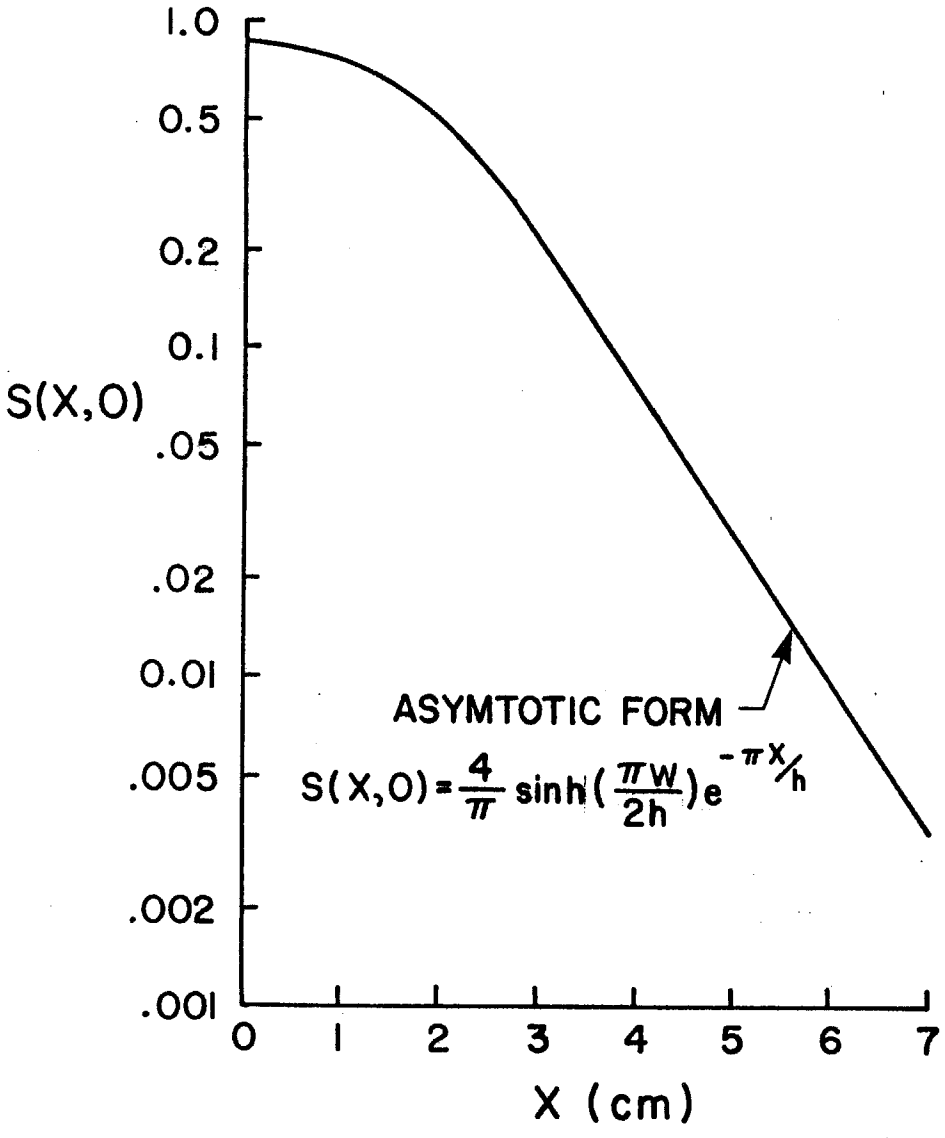

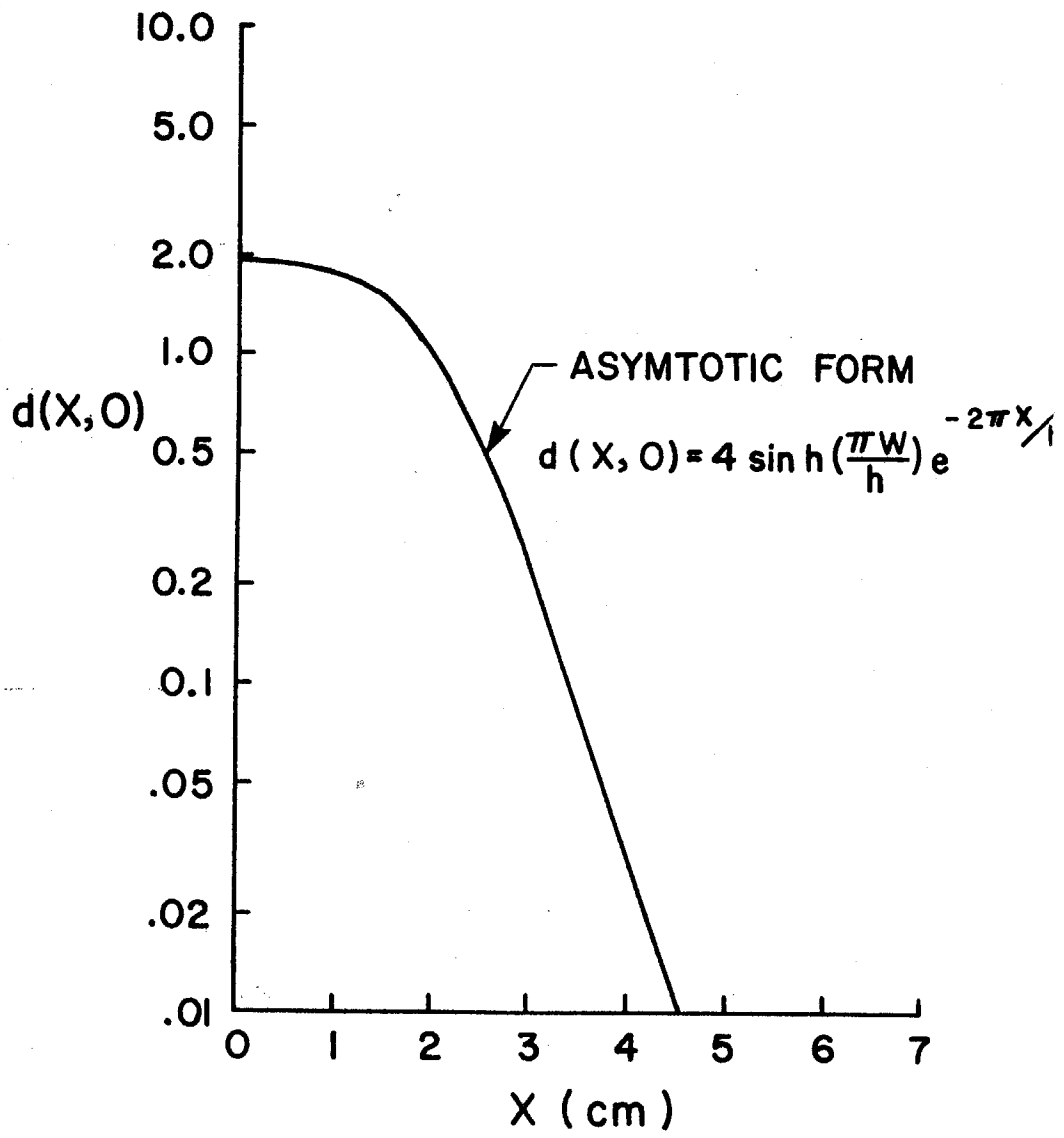

Plots of S(X,0) and d(X,0) us x for h=3cm and w=4cm

Figure 5-26

$$V_{out}(\omega) = d(x,y)\ \frac{y}{h}\sqrt{\frac{Z_{pu}Z_o}{2}}\ \sin\left(\frac{\ell\omega}{c}\right)\ e^{i\pi/2}\ i_b(\omega). \qquad (5.23)$$

$$\text{where } d(x,y) = \{e(x,y) - e(x,-y)\}\ \frac{h}{y},$$

and the difference mode transfer impedance at x = 0 is

$$Z_d(0,y) = d(0,y)\frac{y}{h}\ \sqrt{25\ Z_{pu}}, \qquad (5.24)$$

where $d(0,y) \approx 2\tanh(\pi w/2h) \approx \pi\ s(0,0)[1-1/3\ s^3(0,0)]$

and at large x, $d(x,0) \to 4\sinh(\pi w/h)e^{-2\pi x/h}$.

A plot of d(x,0) vs x is presented in Fig. 5-26(b).

Microwave power combiners add power of coherent signals, and the coupling impedance of n_p loop-coupler pairs is $\sqrt{n_p}$ times the impedance for a single pair, in both sum and difference modes. Figures 5-27 and 5-28 show a typical electrode assembly.

Based on calculations, as well as measurements with both wires and electron beams, the loop coupler characteristics shown in Table 5-VII are the values we use in this Design Report.

TABLE 5-VII LOOP COUPLER CHARACTERISTICS

Characteristic		1-2 GHz band	2-4 GHz band
characteristic impedance	Z_{pu}	100	75 Ω
height (gap) typical	h^{pu}	3.0	3.0 cm
effective width	w	4.0	2.5 cm
pairs per meter		15	25 per m
Sum Mode $s(0,0)$		0.843	0.664
transfer impedance	Z_s	42.2	28.8 Ω

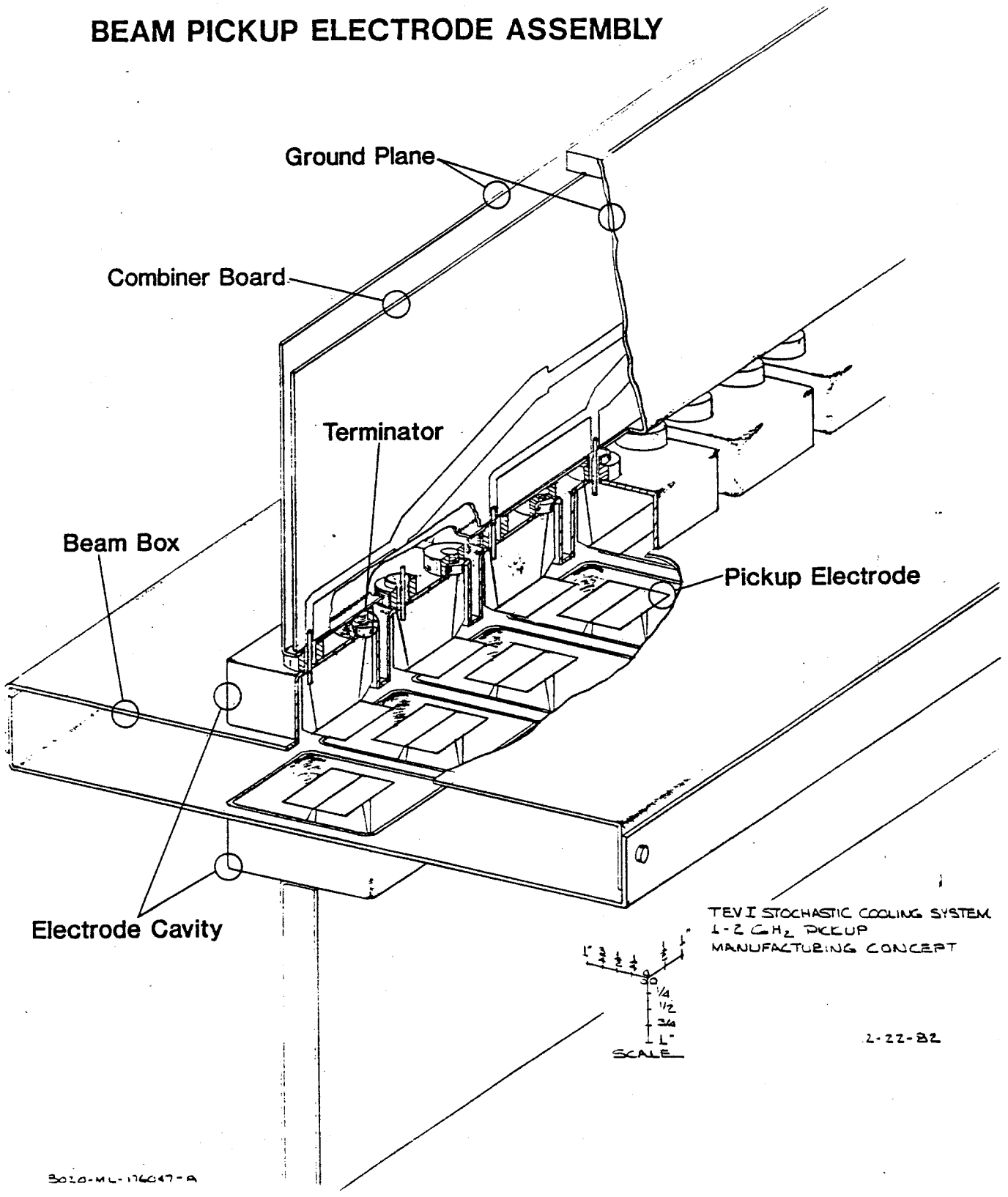
BEAM PICKUP ELECTRODE ASSEMBLY
Ground Plane
Combiner Board
Terminator
Beam Box
Pickup Electrode
Electrode Cavity
TEV I STOCHASTIC COOLING SYSTEM
1-2 GHz PICKUP
MANUFACTURING CONCEPT
2-22-82
SCALE
3010-MC-176647-A

Figure 5-27

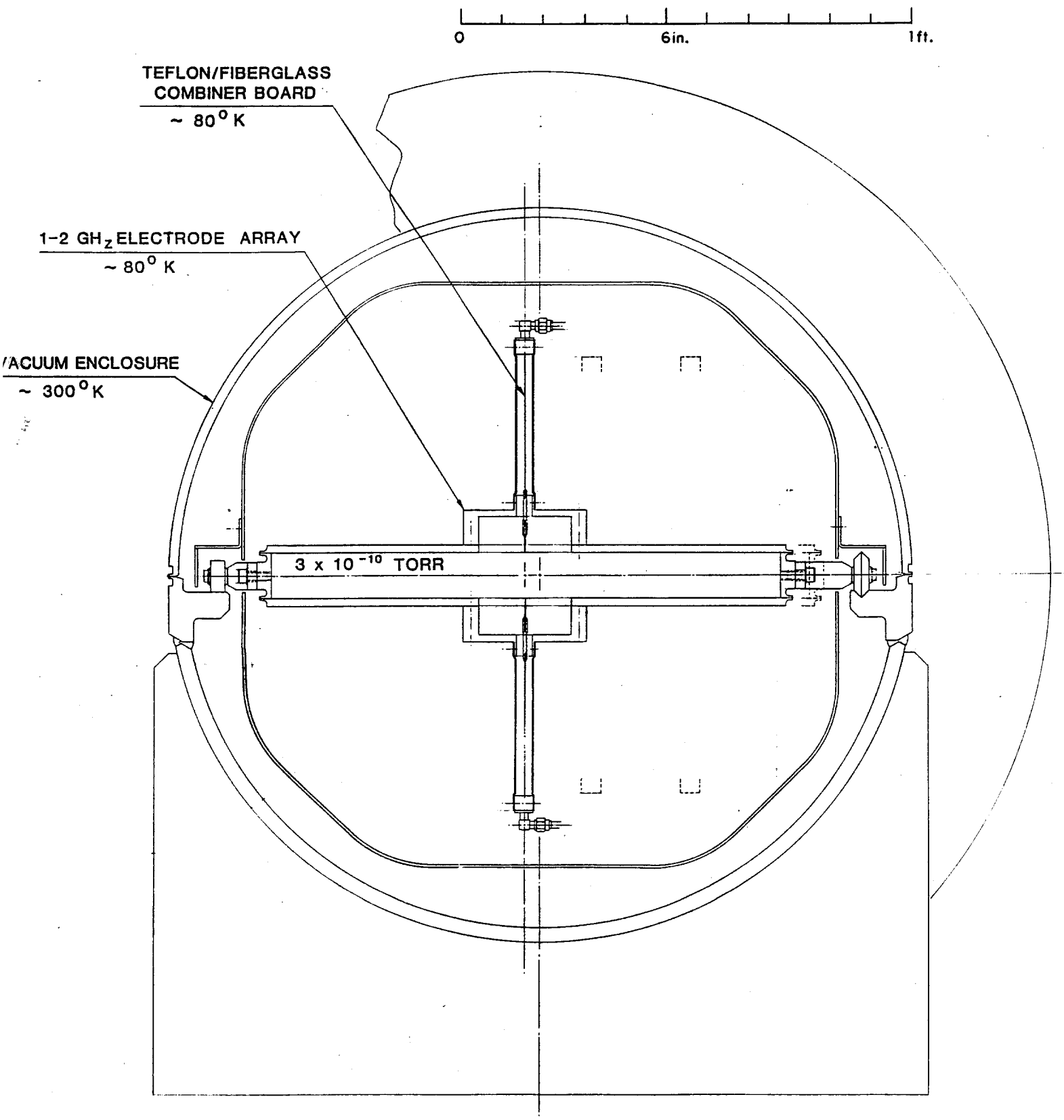

TYPICAL PICK-UP CROSS SECTION

Figure 5-28

Difference Mode			
d(0,y)		1.94	1.73
transfer impedance	Z_d	3230	2500 Ω/m

The electrode assemblies shown in Figs. 5-27 and 5-28 are approximately 1.2 meters long (for the 1-2 GHz band) and contain 16 pickup pairs. The signals are combined separately for top and bottom electrodes using a double-sided Teflon printed circuit board. The air-spaced ground plane yields a group velocity of about 0.98c. The electrodes are back-terminated in their characteristic impedance, and the whole assembly is cooled to liquid-nitrogen temperature to reduce the thermal noise power from the back termination, the skin effect losses in the circuit board, and teflon outgassing. In the 2-4 GHz band, it is quite possible that slot couplers will have a higher coupling impedance per unit length than loop couplers. A research and development program is underway in this area.

Tests on 16 pair 1-2 GHz electrode arrays connected in sum mode have been carried out at Argonne National Laboratory using a 20 MeV pulsed electron linear accelerator. Fast Fourier transforms of the electrode array output signal yield transfer-impedance measurements in the frequency domain. Transfer impedances at centerband of about 140 ohms have been measured in this manner (the calculated value is 168 ohms). The tests have also confirmed the $e^{-\pi x/h}$ spatial sensitivity, which is an important parameter in matching the electrode response to the expected antiproton spatial density in the Accumulator high-dispersion straight section. At large x, there is an indication that the beam excites resonances in the beam box which in turn are picked up by the electrodes. As the spatial sensitivity of the electrodes to these resonances is much flatter than the desired signal, they could dominate the electrode transfer impedance at large x. More beam tests are required to understand the magnitude of this effect, and to develop ways of attenuating these modes (e.g., use of ferrites in the beam box).

5.11.2 Preamplifiers. Commercial gallium-arsenide field-effect transistor (GaAsFet) amplifiers are available in the microwave frequency bands required for stochastic cooling. Although their thermal noise characteristics are relatively low (a 2.0 db noise figure amplifier, available in the 1-2 GHz band[13], has an equivalent noise temperature of 170 K) it would still contribute nearly 70% of the total thermal noise power. The design therefore includes preamplifiers cooled to liquid nitrogen temperatures. We expect equivalent noise temperatures of 75 K (NF = 1.0 db) and 120 K (NF = 1.5 db) for 1-2 GHz and 2-4 GHz amplifiers respectively. Minimization of thermal noise is not only important in relation to beam heating, but also in relation to the cost of extra traveling wave tube installed power required to amplify it.

Commercially available GaAsFet amplifiers designed to operate in the Mil spec temperature range (-55°C to 70°C) have been successfully operated as low as 77 K[14]. In this case a 1-2 GHz amplifier achieved an equivalent

noise temperature of 120 K (NF = 1.5db). GaAsFet amplifiers have been specially designed for operation at liquid-helium temperatures, and equivalent noise temperatures of 20 K (NF = 0.2 db) have been achieved in narrow band operation[15] (0.5 GHz bandwidth at 1.5 GHz).

We are presently pursuing parallel research and development efforts in this area. At Lawrence Berkeley Laboratory, a prototype GaAsFet amplifier has been built which has the following properties in the 1-2 GHz band:

Gain Average	33 db
Gain Flatness	±1.5 db
Phase Linearity	±15°
Noise Temperature Peak (NF=0.5)	40 K
Average (NF=0.35)	30 K
Input VSWR Peak	2.5:1
Average	1.75:1

Only slight improvements are seen when the amplifier is cooled to 14 K.

At Fermilab, measurements are being made on cooled commercially available amplifierss. This includes amplifiers with integrated bipolar biasing circuits which can only be cooled to -50°C, and amplifiers with separated biasing circuits, which can be cooled to 77°K. We have achieved average noise temperatures of 80 K and 110 K for amplifiers cooled to -50°C and 77 K respectively. Input VSWR has typically been better than 1.4:1.

Research and development is continuing in the 1-2 GHz band in both the above efforts. In addition, work is beginning in the 2-4 GHz band.

5.11.3 Notch Filters. Notch filters are needed in our design of the stochastic cooling system for several reasons. In one system, the stack tail momentum cooling system, notch filters are used both for reducing the microwave power at frequencies corresponding to particles in the core, and to assist in shaping the gain vs momentum (frequency) in the stack tail. In systems with poor signal to thermal noise ratio, notch filters are useful in reducing the extra traveling-wave tube installed power required to amplify it. If momentum cooling is implemented in the debuncher, a notch filter would be used to produce a phase inversion of the pickup sum signal at the harmonics of the central revolution frequency. The tolerance on the frequency deviation of the notch centers at each harmonic of the revolution frequency ω_0 in the frequency bandwidth is of the order of (for the Accumulator)

$$\left|\frac{\omega_n - n\omega_0}{n\omega_0}\right| < \eta\frac{\delta p}{p} \approx 10^{-5},$$

Where $\eta = 0.02$, p is 8.9 GeV/c and δp is about 2 MeV/c.

Filter designs include both shorted stubs, which use reflections from the shorted end of a long transmission line (nominally half the circumference of the Accumulator), and correlator types, which use the constructive and destructive interference of the same signal transmitted over two transmission lines (whose lengths differ by about the circumference of the Accumulator).

In our application, the large circumference of the Accumulator, in combination with the very high frequencies used in the electronics, imposes severe restrictions on the selection of transmission lines. In room-temperature transmission lines, the skin effect conductor resistance causes dispersion as well as attenuation. This is reduced by using larger diameter transmission lines. However, the maximum size of the transmission line is limited, since higher order modes are excited and affect the dispersion. In particular, in a 7.5-cm diameter 50-ohm transmission line, the TE_{11} mode propagates at frequencies above 2.0 GHz. These effects are only marginally better at 76.6 ohms, the impedance at which skin effect losses are minimized.

Our present notch filter is based on a correlator circuit using a 1.6 mm diameter 50 ohm superconducting transmission line. In such a line the major attenuation (power loss) is due to the loss tangent in the dielectric, and results in an attenuation of about 1.0 db per km in the 1-2 GHz band. Early measurements showed that shorted-stub filters typically had much higher dispersion than the same cable when used as a correlator filter. This due to the fact that power reflected by a single discontinuity in a correlator filter is absorbed by the isolated port on the input hybrid splitter, and can only reach the output hybrid if it is re-reflected by another discontinuity. Recent measurements have been made on a 330 m line in a cryostat as shown in Fig. 5-29. Dispersion and notch depth measurements in the 1-2 GHz band are shown in Fig. 5-30. This performance is believed to be adequate for the stack tail system. Shorted-stub filters do offer some advantages over correlator filters, however, as they allow greater flexibility in gain and phase shaping within each Schottky band. Present measurements indicate that the present superconducting line does indeed provide adequate performance in terms of dispersion and notch depth when used as a shorted stub. Research is still proceeding in this area. Research is also going on in the area of TWT correlator filters, to help control the TWT intermodulation (IM) distortion. This is discussed in the next section.

5.11.4 Traveling Wave Tubes (TWT's). The power amplifier stages in all our cooling systems are traveling wave tube amplifiers. Several commercial units are available in the 1-2 and 2-4 GHz bands with saturated output power ratings up to 200 watts. Traveling wave tubes are also available with power ratings above 1 kW.

Numerical studies show that in the stack tail momentum cooling system, the depth of the notches between the Schottky bands must be at least 40 db deep in order not to excessively heat the core. Even though notches of

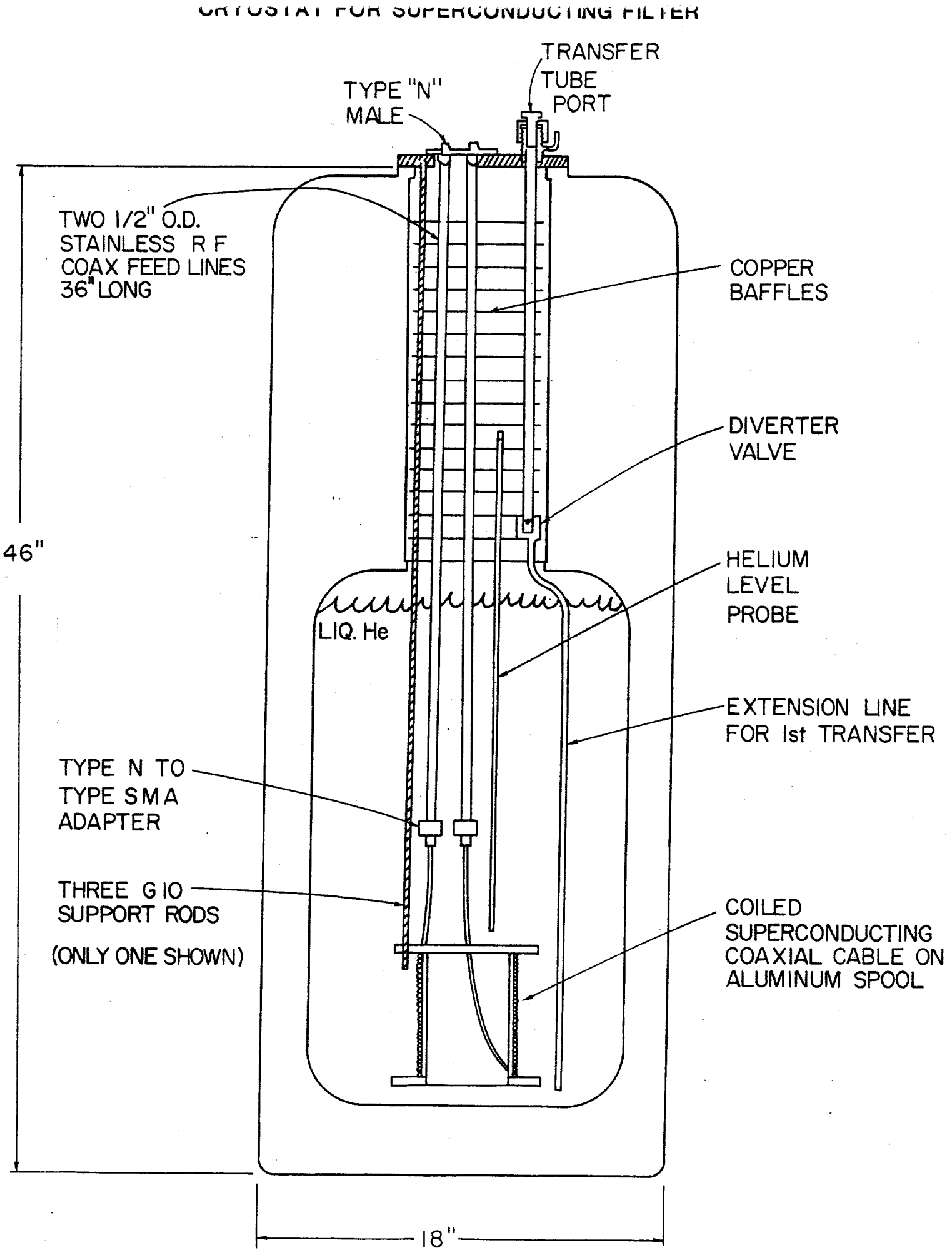
CRYOSTAT FOR SUPERCONDUCTING FILTER
TRANSFER TUBE PORT
TYPE "N" MALE
TWO 1/2" O.D. STAINLESS R F COAX FEED LINES 36" LONG
COPPER BAFFLES
DIVERTER VALVE
46"
HELIUM LEVEL PROBE
LIQ. He
EXTENSION LINE FOR 1st TRANSFER
TYPE N TO TYPE SMA ADAPTER
THREE G10 SUPPORT RODS
(ONLY ONE SHOWN)
COILED SUPERCONDUCTING COAXIAL CABLE ON ALUMINUM SPOOL
18"

Figure 5-29

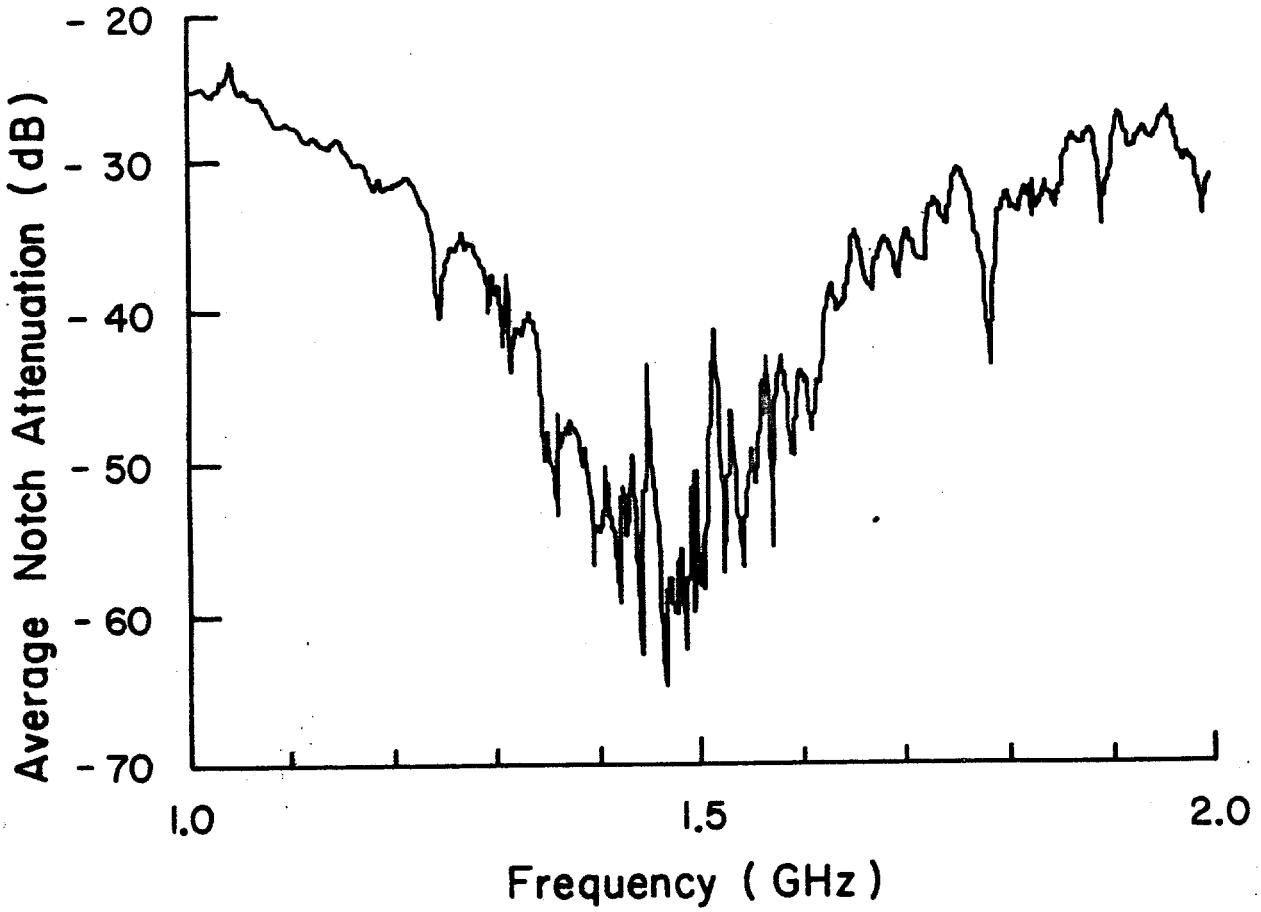
- 20
- 30
- 40
- 50
- 60
- 70
Average Notch Attenuation (dB)
1.0
1.5
2.0
Frequency (GHz)

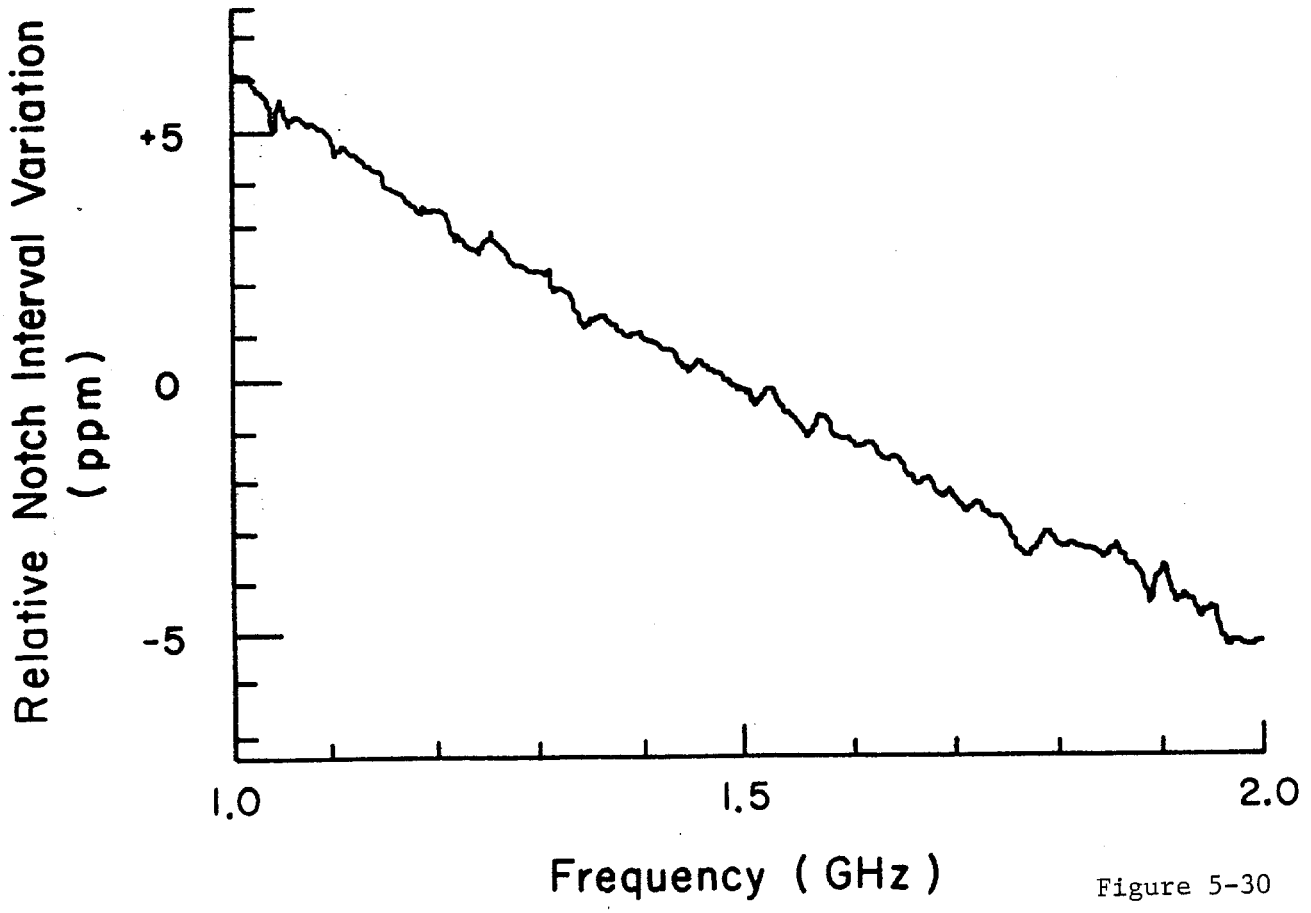
+5
0
-5
Relative Notch Interval Variation
(ppm)
1.0
1.5
2.0
Frequency (GHz)

Figure 5-30

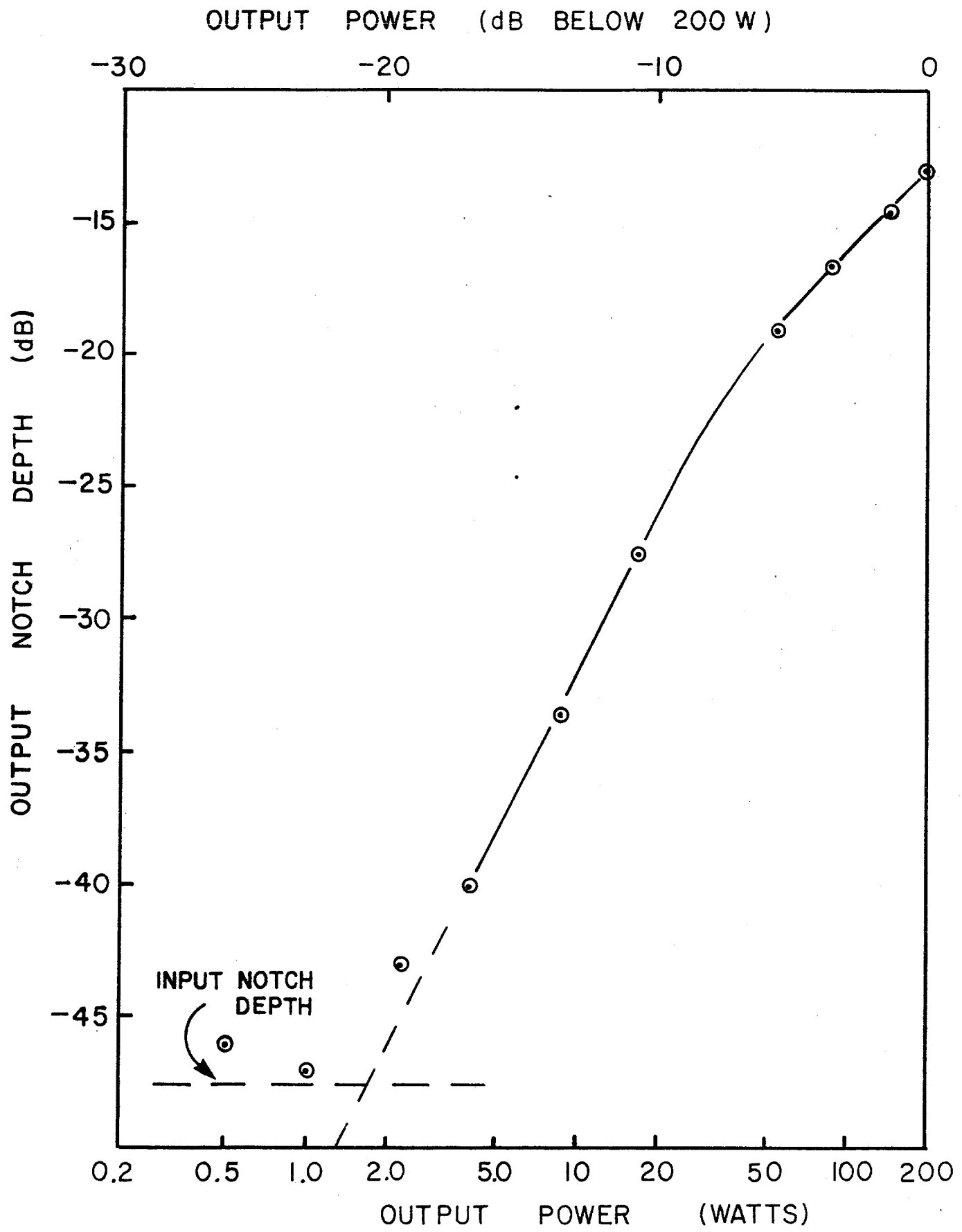
OUTPUT POWER (dB BELOW 200 W)
-30
-20
-10
0
-15
-20
-25
-30
-35
-40
-45
OUTPUT NOTCH DEPTH (dB)
INPUT NOTCH DEPTH
0.2
0.5
1.0
2.0
5.0
10
20
50
100
200
OUTPUT POWER (WATTS)

Figure 5-31

this depth can be obtained with the filters discussed above, the intermodulation distortion that occurs at higher power levels in TWT's can rapidly fill these in. Second-order intermodulation distortion can occur at the edges of the operating band of octave-bandwidth TWT's. Operation of the TWT's in a push-pull mode can reduce the second order IM products effectively, but, third-order IM distortion can occur at midband frequencies and is not reduced by operating the TWT's in push-pull mode. Measurements using a single TWT and a notched white-noise source show that the remaining notch depth at the TWT is only 13 dbc at full power (200 watts), but improves to about -30 dbc at 10 watts per TWT. This result is shown in Fig. 5-31. Since this measurement was made, tests on another design TWT with a higher bandwidth indicated a somewhat lower level of IM distortion at the same power levels. Specifically, the IM distortion improved to about -23 dbc from -20 dbc at 40 watts output power. The highly peaked Schottky spectrum produces a third-order intermodulation distortion which is naturally peaked in, rather than between, the Schottky bands, providing another 12 db of notch depth at core frequencies. To obtain 1600 watts of output power and notch depths of 40 db would require roughly 160 TWTs, each operating at about 10 watts.

The potential cost saving of being able to run the TWT's at 40 W rather than 10 has stimulated interest in using superconducting correlator filters on the output of the TWT's. In principle, the filter need only provide a notch depth of the order of 20 db, the remainder being provided by the TWT IM distortion of -20 dbc, and the IM form factor of the Schottky bands of 12 db. As a correlator filter using a superconducting transmission line is nearly lossless, we are investigating the possibility that such a filter could be used on the TWT outputs. Calculations show that the superconducting line could dissipate about 0.7 W/meter without quenching. In principle a superconducting correlator filter could carry several hundred watts of microwave power if the attenuation were 1 db per km. Such a power-correlator filter could be used on the output of a push-pull TWT pair to reduce the output power between the Schottky bands caused by IM distortion.

A research and development program has been directed toward building a power correlator filter capable of handling 80 watts of microwave power in the 1-2 GHz band (this corresponds to 40 watts per TWT, and 40 watts in the superconducting line). Tests thus far have only achieved 50% of this power level, and the present belief is that the thermal coupling between the Teflon and the outer conductor is less than optimal, causing an additional temperature rise. Pulsed-power tests with more than 100 watts being transmitted through the superconducting cable indicate that the attenuation is about as expected (around 1 db per km) even at these high power levels, hence the present limit is not due to anomalous attenuation at high power levels.

If further research in this area is unsuccessful in achieving reliable operation at 40 watts in the superconducting line, then an alternative circuit in which the superconducting line and the TWTs are combined in the

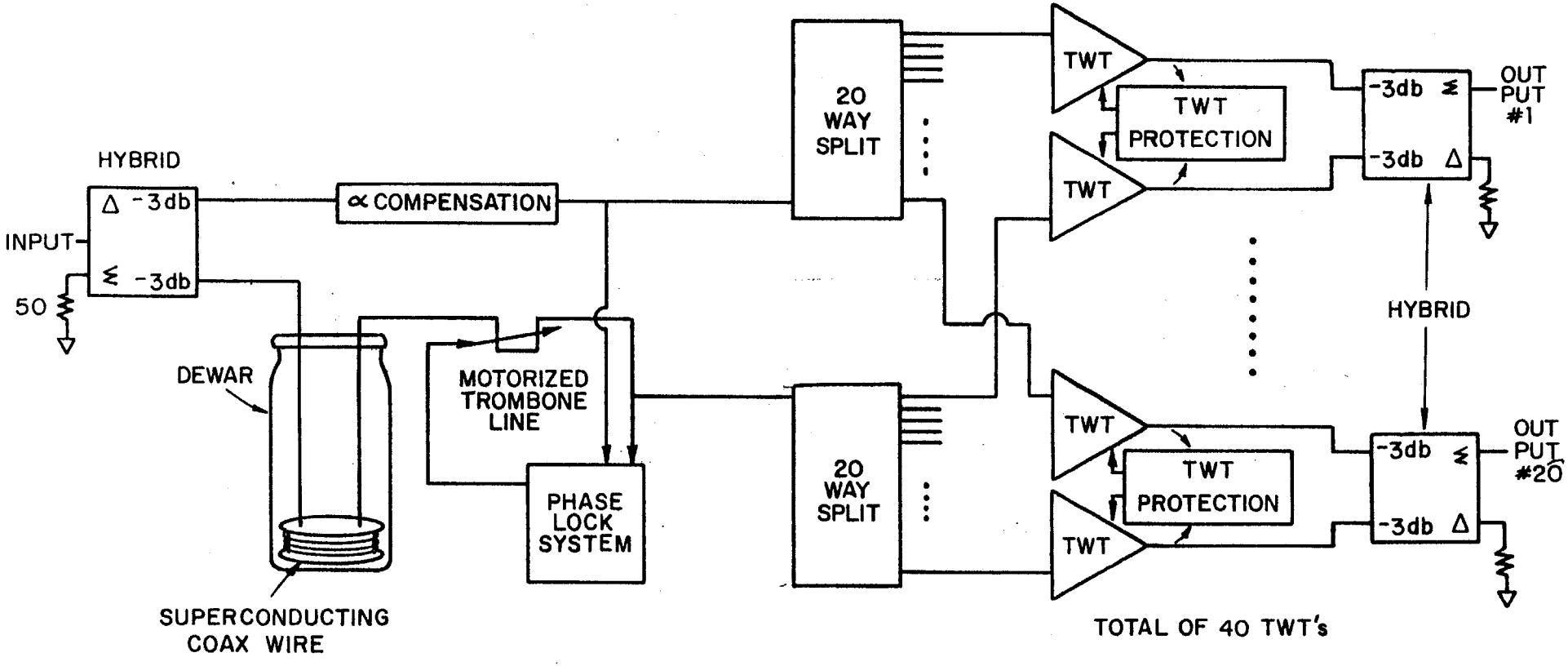

POWER CORRELATOR FILTER FOR STACKTAIL MOMENTUM COOLING

Figure 5-32

same correlator type loop circuit will be used. It is shown in Fig. 5-32. Such a circuit is more demanding on the TWT performance in the areas of gain and phase matching, phase linearity and IM distortion. It is believed that such a circuit could yield IM distortion reduction of the order of 6 db more than the same circuit without the filter. Hence present calculations show that IM distortion levels are marginal at 40 watts per TWT.

5.11.5 Kicker Electrode Assemblies. The kicker electrode assemblies are conceptually similar to the pickup electrode assemblies by virtue of the reciprocity theorem, which states that transfer impedances between pairs of terminals are unchanged when inputs and outputs are exchanged. The major differences are of a hardware nature: the combiner board is now a power splitter and some power dissipation and heating should be anticipated. The terminating resistor now must absorb microwave power, and means must be provided for heat removal. There is no thermal-noise problem as there was in the pickup case, so cryogenic cooling is only needed if adequate vacuum cannot be obtained otherwise, or if the terminating resistors cannot operate at 7 watts/resistor at room temperature. Tests on outgassing of materials are continuing in order to better understand their compatibility with the kicker electrode array design.

There is some concern that kicker electrodes will generate evanescent and propagating modes in the beam pipe. This is especially true of betatron cooling kickers, but can also be a problem in the momentum-cooling systems. Evanescent modes, even though highly damped, have phase velocities considerably different than the beam, and could lead to stochastic heating effects. The propagating modes, besides being able to heat the beam, can also propagate through the beam pipe back to pickup arrays and interfere with the pickup operation. The TE_{11} cutoff in a 35 mm diameter beam pipe is about 5 GHz, so such insertions would have to be placed in low-dispersion areas of the ring.

5.11.6 Other Considerations. Most of the components in the stochastic-cooling electronics have a limited bandwidth of about an octave, and this normally causes the frequency derivative of the phase delay to be frequency dependent. This leads to two parameters that need to be known for each element. The group delay (the slope of a straight-line fit to the phase delay vs frequency data in the operating band) and the phase intercept (the zero frequency intercept of the above straight line) need to be measured for each component and accounted for the final system. Deviations from the average group delay at particular frequencies, as well as gain nonuniformity may have to be corrected. Special circuits to cause gain shaping and constant phase offset will need to be designed and built. In brief, the group delay is adjusted using cables so that the information signal arrives at the kicker at the correct time. The phase intercept correction assures that it arrives with the correct phase angle. The gain correction assures that the signal power is properly apportioned to each Schottky band.

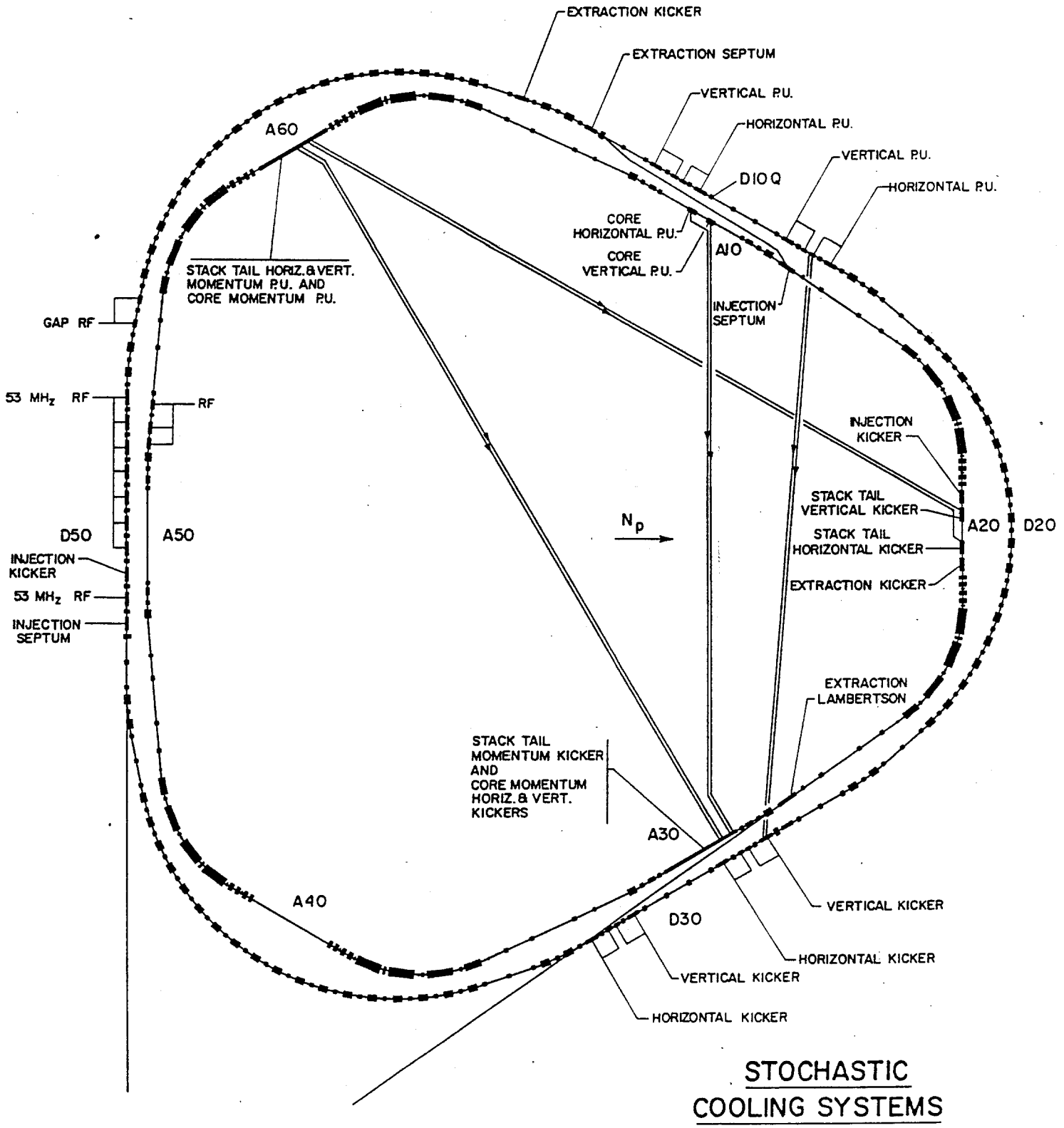
EXTRACTION KICKER
EXTRACTION SEPTUM
VERTICAL P.U.
HORIZONTAL P.U.
VERTICAL P.U.
HORIZONTAL P.U.
A60
D10Q
CORE HORIZONTAL P.U.
CORE VERTICAL P.U.
A10
INJECTION SEPTUM
STACK TAIL HORIZ.& VERT. MOMENTUM P.U. AND CORE MOMENTUM P.U.
GAP RF
53 MHz RF
RF
INJECTION KICKER
STACK TAIL VERTICAL KICKER
STACK TAIL HORIZONTAL KICKER
EXTRACTION KICKER
A20
D20
D50
A50
INJECTION KICKER
53 MHz RF
INJECTION SEPTUM
Np
EXTRACTION LAMBERTSON
STACK TAIL MOMENTUM KICKER AND CORE MOMENTUM HORIZ.& VERT. KICKERS
A30
A40
D30
VERTICAL KICKER
HORIZONTAL KICKER
VERTICAL KICKER
HORIZONTAL KICKER
STOCHASTIC COOLING SYSTEMS

Figure 5-33

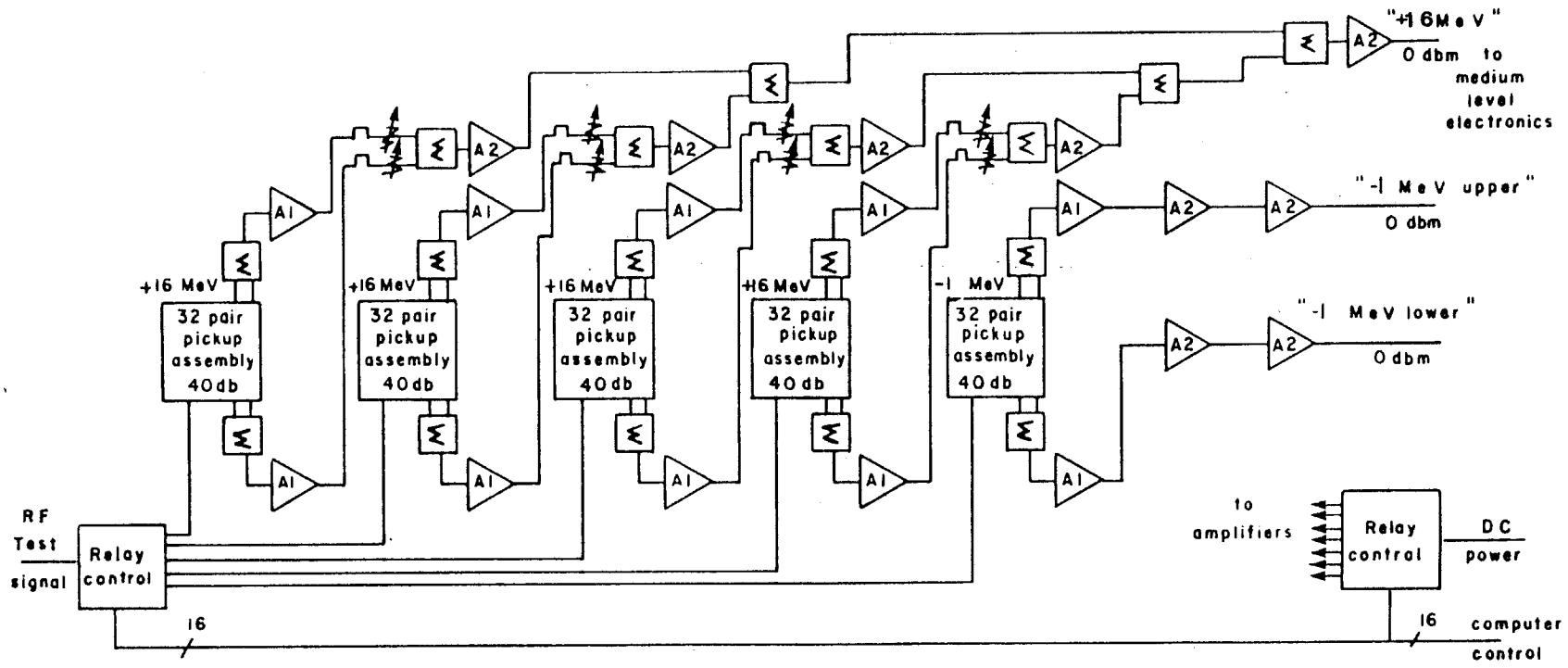

32 pair pickup assembly = 2.4m long module containing 32 pair of 1-2 GHz loop couplers cooled to 77°K. Upper and lower electrode signals are separately brought to cooled GaAsFet amplifiers through vacuum chamber wall. A 40 db coupler built into assembly allows insertion of test signal.

A1 = Low noise GaAsFet amplifier cooled to 77°K. Gain about 30 db. Equivalent noise temperature about 75°K.

A2 = Commercial bipolar 1-2 GHz amplifier, Avantek #UTC-20-104 or equivalent (gain = 23 db; equiv. noise temp. = 500°K).

= 2:1 power/inphase power combiner/splitter.

Manually adjusted liner delay pad.

Manually adjusted attenuator pad.

Figure 5-34a

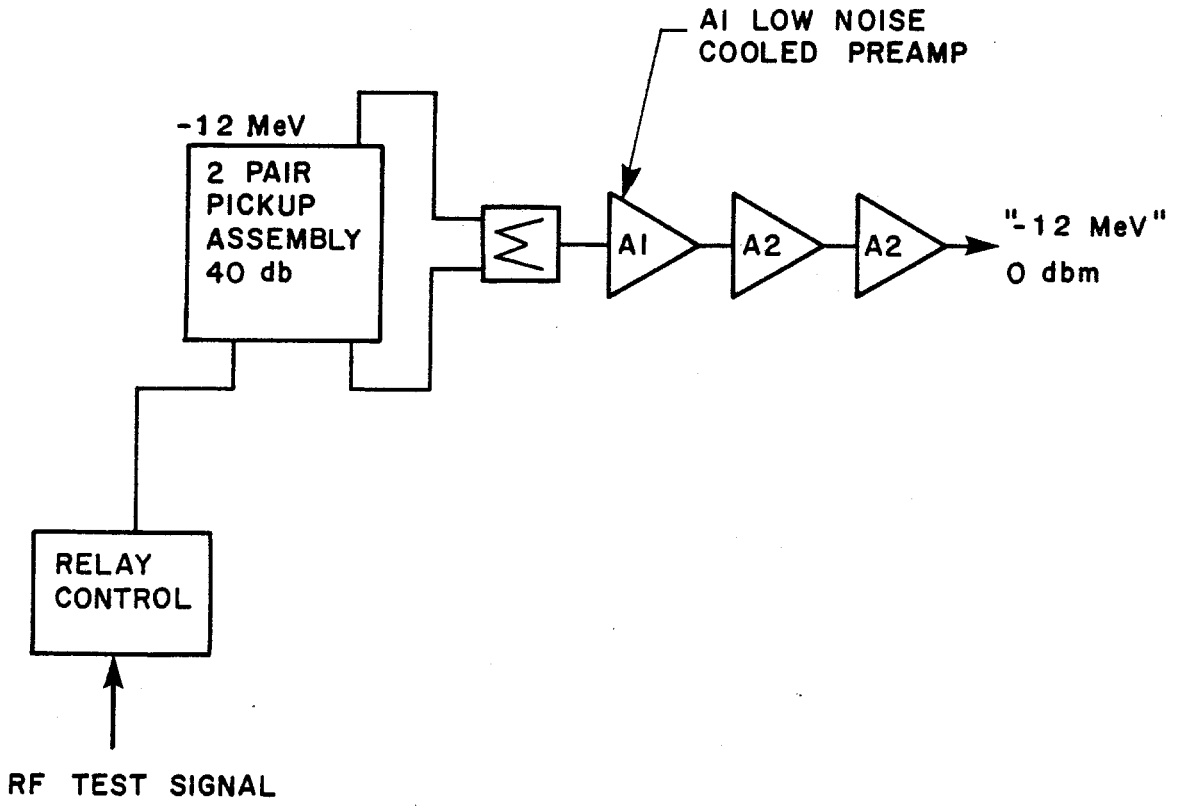

Stack Tail Momentum Low Level Electronics

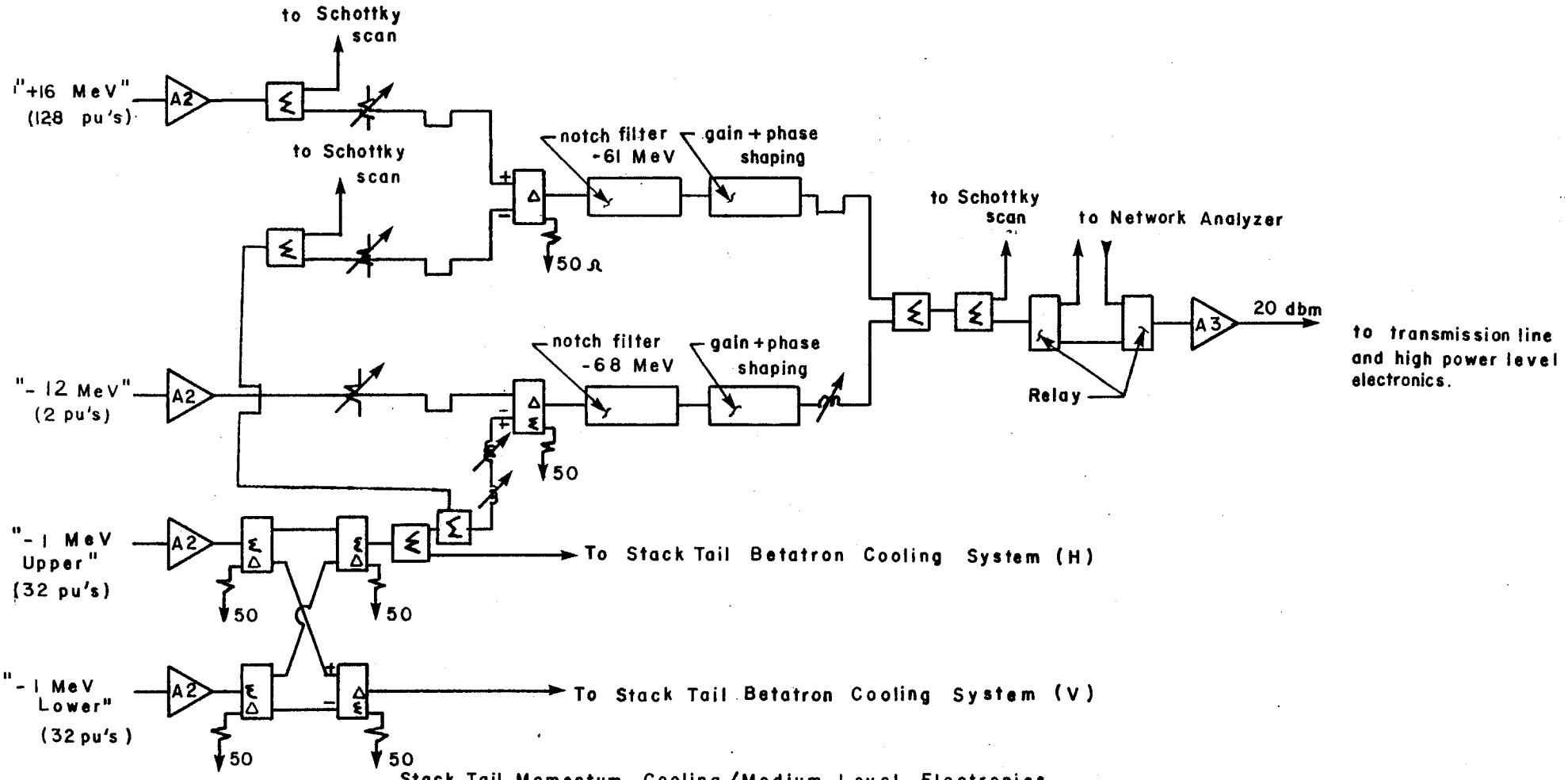
to Schottky scan
"+16 MeV" (128 pu's)
A2
to Schottky scan
notch filter -61 MeV
gain + phase shaping
50 Ω
to Schottky scan
to Network Analyzer
20 dbm
A3
to transmission line and high power level electronics.
notch filter -68 MeV
gain + phase shaping
"- 12 MeV" (2 pu's)
Relay
50
"- 1 MeV Upper" (32 pu's)
To Stack Tail Betatron Cooling System (H)
50
50
"- 1 MeV Lower" (32 pu's)
To Stack Tail Betatron Cooling System (V)
50
50
Stack Tail Momentum Cooling / Medium Level Electronics

Figure 5-35

The dispersion in the transmission lines carrying the signals across the ring also needs to be considered. In the 1-2 GHz stack tail systems, the largest diameter coaxial line which we can use is 1-5/8-in. diameter rigid line (air dielectric) as the TE_{11} mode propagates above 3.5 GHz. Calculations show that the expected dispersion is about 8° over the 1-2 GHz band for 150 m of line, based on the known skin effect losses. Preliminary measurements indicate that it may actually be somewhat larger, possibly due to excitation of evanescent modes at 2 GHz. In the 2-4 GHz range, the transmission line diameter would have to be limited to about 7/8", and the calculated dispersion would be about 18°. This line will probably be of the foam dielectric type, because the time-delay requirements are not overly restrictive.

5.11.7 Accumulator Stochastic Cooling System Layout. There are 6 specific cooling systems in the Accumulator. Their location is shown in Fig. 5-33. Their basic operating parameters are outlined in Table 5-VIII. All 3 stack tail systems operate in the 1-2 GHz band, while the 3 core systems operate in the 2-4 GHz band. All kicker assemblies have been located remotely from the pickup electrodes to minimize coupling and feedback.

The largest system is the stack-tail momentum-cooling system, requiring about 1600 W of microwave power. The pickup electrodes are located in the 9 m dispersion short straight section A60, and the kickers in the zero dispersion long straight section A30. A block diagram of the low-level electronics is shown in Fig. 5-34a and b. Groups of 16 pickup electrodes are summed on an internal edge-supported teflon printed circuit board into low noise preamps. Signals are separately amplified for the upper and lower electrodes to allow for gain and phase correction, as well as for forming both sum and difference signals. Signal processing is done in the medium level of electronics as shown in Fig. 5-35. This includes 3 notch filters (superconducting correlators) with notch minima set at +4, -2, and -3 MeV relative to the core. After gain and phase corrections, the signals are amplified to about +20 dbm and transmitted across the ring to the high level electronics (TWT's). At present we estimate that 40 TWT's are needed if we can operate them at 40 W each and maintain a 40 db notch depth at the core frequency (this number includes the Schottky form factor of about 12 db).

The stack-tail betatron cooling systems derive their pickup signals from the stack-tail momentum system as shown in Fig. 5-36. The kickers, however, are in straight Section A20, where the dispersion is about 9 m. The vertical and horizontal betatron systems require about 20 and 200 watts of output power respectively. As was pointed out earlier, the horizontal betatron signal is derived from beam in the asymptotic region of sum-mode pickups where the response is $e^{-\pi x/h}$, and hence there is a momentum Schottky signal as well as the normal betatron sidebands. It is expected that 1 TWT will be sufficient for the vertical and 2 for the horizontal system. It is possible that a notch filter could be used to reduce the momentum Schottky signal.

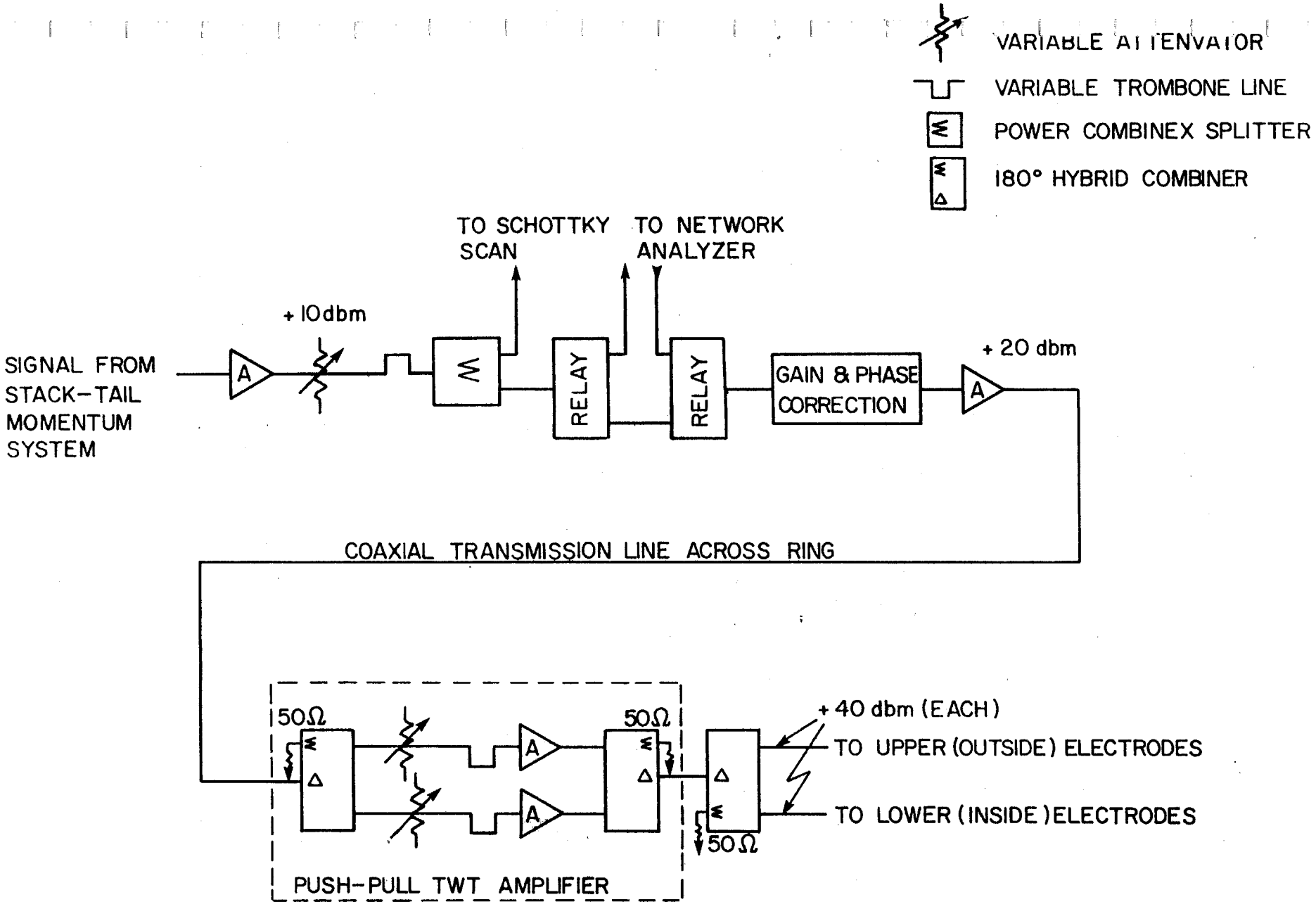

STACK-TAIL BETATRON COOLING SYSTEM (2 REQUIRED)

Figure 5-36

The core momentum system pickups are located in the high-dispersion straight Section A60 along with the stack-tail pickups. As indicated in Section 5.9.5 and Fig. 5-37, the core momentum pickups are double rows of pairs, each pair in sum mode. The difference signal of the two rows is then formed. These signals are processed as shown in Fig. 5-38 and also sent to kickers in the zero-dispersion straight section shared with the stack tail momentum kickers. This system requires about 30 W.

The core betatron system pickups are located in the zero-dispersion straight section A10. The signals are processed as per Fig. 5-38 and also sent to kickers in zero-dispersion straight section A30. Each system requires about 2 W.

TABLE 5-VIII ACCUMULATOR STOCHASTIC COOLING SYSTEMS

	Stack tail Momentum	Stack tail Betatron	Core Momentum	Core Betatron
Frequency band	1-2GHz	1-2GHz	2-4GHz	2-4GHz
Number of pickup pairs (loops)	128+32+8+2	(32)(H,V)	32 + 32	8(x2)
Pickup characteristic impedance	108 Ω	108,70 Ω	97 Ω	83 Ω
Pickup sensitivity s(0,0) or d(0,0)	0.85(s)	1.93(d)	0.59(ds)	1.59(d)
Back termination thermal noise temperature	80 K	80 K	80 K	293 K
Amplifier equivalent thermal noise temperature	25 K	25 K	200 K	293K
Amplifier gain (net)	150db	125db	110db	106db
Number of filters (superconducting correlators)	3	0	0	0
Output power		V+H		
-Schottky	1400W	10W+200W	30W	10W(x2)
-thermal	200W	10W+10W	0	0
-total	1600W	20W+210W	30W	10W(x2)
Number of TWT's (200 watt saturated power)	40	1+2	1	1(x2)
Number of kicker pairs (loops)	160	32(x2)	32	8(x2)
Kicker characteristic impedance	108[1] Ω	108[1],70[2] Ω	97[1] Ω	83[2] Ω
Kicker sensitivity s(0,0) or d(0,0)	0.85(s)	1.93(d)	0.59(s)	1.59(d)
Spare time delay with air dielectric line (β=.998)	205 nsec	23 nsec	230 nsec	110 nsec
Spare time delay with heliax (β=0.819)	197 nsec	-34 nsec	166 nsec	63 nsec

[1] even mode
[2] odd mode

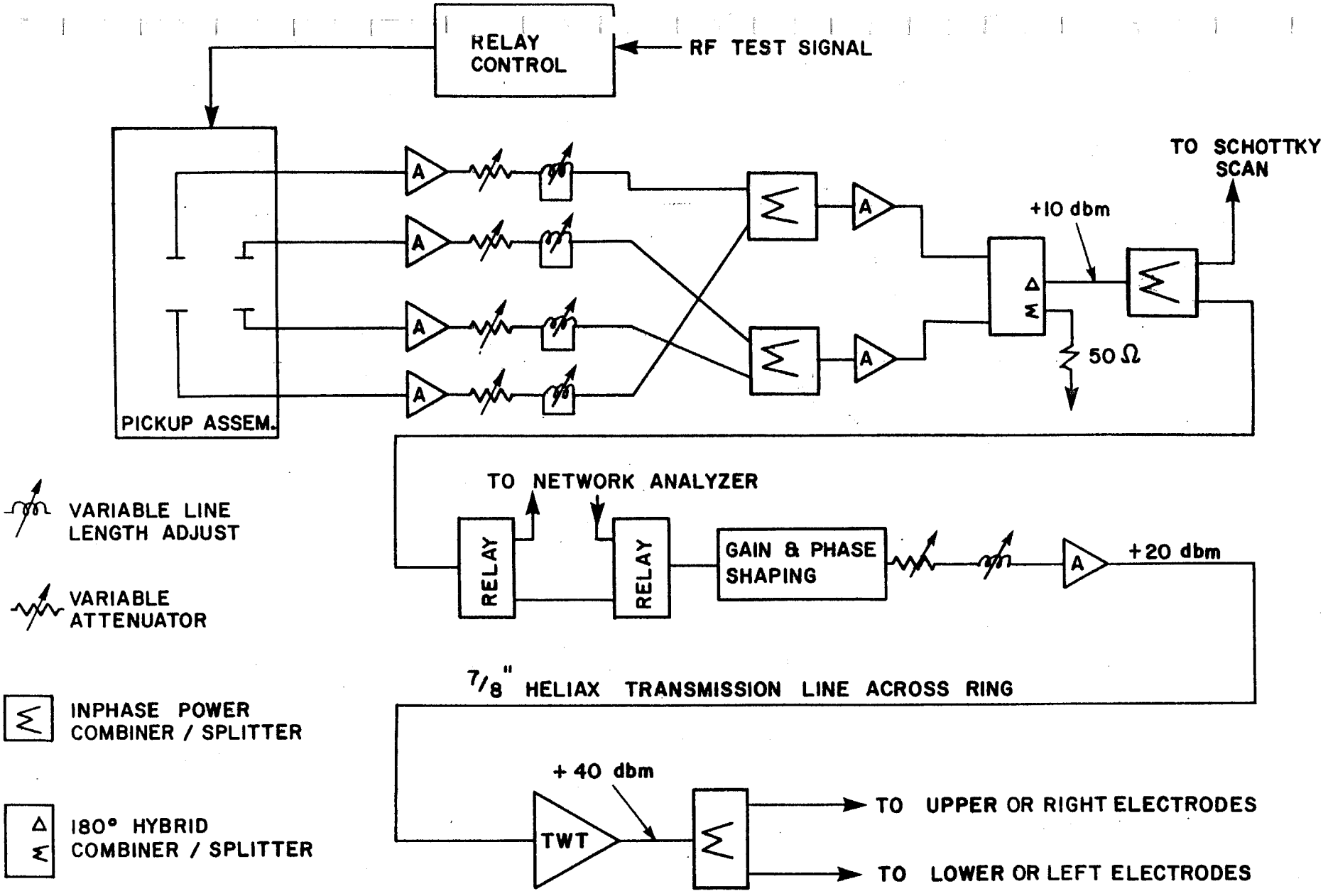

2-4 GHz Core Momentum Cooling System

Figure 5-37

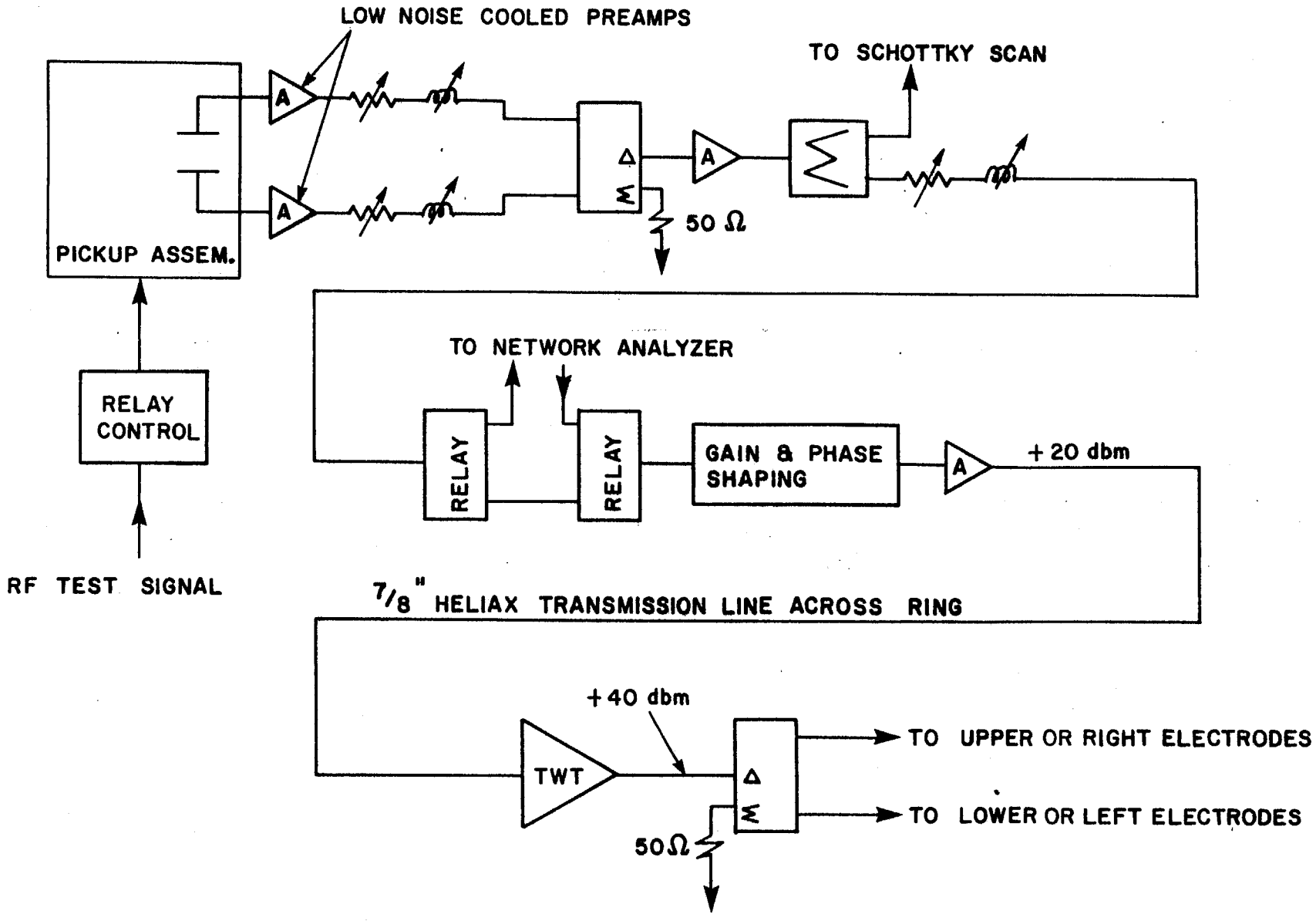

2-4 GHz Core Betatron Cooling System (2 Systems Required)

Figure 5-38

References

1. A.G. Ruggiero, "Vacuum Considerations for the Accumulator Ring," Fermilab $\bar{p}$ Note 194 (1982), unpublished.

2. D. Möhl, G. Petrucci, L. Thorndahl, and S. van der Meer, Physics Reports C, 58 (1980) 73-119.

3. S. van der Meer, "Stochastic Stacking in the Antiproton Accumulator," CERN/PS/AA/78-22 (1978); unpublished.

4. A.G. Ruggiero, "Stochastic Cooling - A Comparison with Bandwidth and Lattice Functions," Fermilab $\bar{p}$ note 171 (1981), unpublished.

5. A.G. Ruggiero, "Pickup Loop Analysis" $\bar{p}$ note 148 (1981), unpublished.

6. S. van der Meer, "A Different Formulation of the Longitudinal and Transverse Beam Response," CERN/PS/AA/80-4 (1980), unpublished.

7. A.G. Ruggiero, "Theory of Signal Suppression for Stochastic Cooling with Multiple Systems," Fermilab $\bar{p}$ note 193 (1982), unpublished.

8. F. Sacherer, "Stochastic Cooling Theory," CERN/ISR/TH/78-11 (1978), unpublished.

9. A.G. Ruggiero, "Revised Intrabeam Scattering Calculation," Fermilab $\bar{p}$ note 192 (1982), unpublished.

10. This discussion follows the discussion of C. Kim, "Design Options for the Fast Betatron Precooling Systems in the Debuncher or in the Injection Orbit," LBL Note BECON-25, unpublished.

11. Unslatter (CERN) unpublished; D. Neuffer, $\bar{p}$ note 199; A. Ruggiero, $\bar{p}$ Note 201.

12. F. Voelker (LBL) unpublished; J. Simpson (ANL) unpublished.

13. Avantek model ABG-2015 for example.

14. J. Shanley, Honeywell Inc., private communication (1982).

15. W. Weinreb et al; IEEE Trans. on Microwave Theory and Techniques 30, pg. 849 (1982).